CO-ORDINATE REGULATION OF CILIA AND THE CELL CYCLE IN CHLAMYDOMONAS REINHARDTII

by

Jeremy David Kirk Parker
B.Sc., University of Victoria, 2001

THESIS SUBMITTED IN PARTIAL FULFILLMENT OF
THE REQUIREMENTS FOR THE DEGREE OF

DOCTOR OF PHILOSOPHY

In the
Department of Biological Sciences

SIMON FRASER UNIVERSITY

Fall 2008

APPROVAL

Name: Jeremy David Kirk Parker

Degree: Doctor of Philosophy

Title of Thesis:

Co-ordinate regulation of cilia and cell cycle in *Chlamydomonas reinhardtii*

Examining Committee:

Chair: Dr. R. Mathewes, Professor

Dr. L. Quarmby, Professor, Senior Supervisor
Department of Molecular Biology and Biochemistry, S.F.U.

Dr. M. Moore, Professor
Department of Biological Sciences, S.F.U.

Dr. J. Mattsson, Associate Professor
Department of Biological Sciences, S.F.U.

Dr. N. Hawkins, Assistant Professor
Department of Molecular Biology and Biochemistry, S.F.U.

Dr. E. Verheyen, Professor
Department of Molecular Biology and Biochemistry, S.F.U.
Public Examiner

Dr. S. Dutcher, Professor
Department of Genetics, Washington University in St. Louis
External Examiner

14 October 2008
Date Approved

ABSTRACT

Cilia are multifunctional organelles implicated in many human diseases. Cilia project from the cell surface and thus are well-situated for roles both in motility and sensory reception. The green alga *Chlamydomonas reinhardtii* is a useful model system for studies of cilia due to its combination of genetics, molecular biology, and biochemistry. At the base of cilia are modified centrioles called basal bodies, which are connected with cilia via a transition zone. Ciliary assembly and disassembly must be co-ordinated with cell cycle progression because the basal bodies must be freed in order to organize the mitotic spindle. Ciliary disassembly can occur either by deflagellation, a drastic stress response, or resorption, a gradual process normally occurring before cell division. I hypothesized that there might be commonality between the two pathways for ciliary loss. I discovered that cells with mutations in ciliary assembly invoke deflagellation in some circumstances, and resorption in others. Deflagellation mutants also exhibited resorption defects, supporting my hypothesis. To further explore the relationship between deflagellation and cell cycle, Qasim Rasi and I examined katanin, a microtubule-severing protein implicated in deflagellation in *Chlamydomonas*, and in mitosis in mammalian cells. A reverse genetics approach revealed that the only cells that can survive knock-down of katanin are mutants which already lack cilia. This led us to form the hypothesis that the role of katanin in the cell cycle is related to its cilia-severing activity. In support of this idea, I observed that wild-type cells entering mitosis sever their cilia to free the basal bodies. Katanin-mediated deflagellation is defective in *fa2* mutants, and FA2 is a member of the Nek family of mitotic kinases. The Neks are a large family of kinases and through evolutionary analyses, Brian Bradley and I discovered that the family expanded early in eukaryotic evolution and it is likely that Neks co-ordinate the cycle of ciliary assembly and dissasemby with cell cycle progression. This study also identified the *Chlamydomonas* Nek CNK3 as an orthologue of the human disease gene Nek8, suggesting an avenue to further disease-related research.

To Bari, for putting up with me,

and

To Dave: it's not an MD, but it'll do.

ACKNOWLEDGEMENTS

I thank my supervisor, Lynne Quarmby; my co-authors, Qasim Rasi and Brian Bradley; my collaborators; Mark White, Arne Mooers, Jessica Feldman, Wallace Marshall, Nick Inglis, Michel Leroux, Dennis Diener, and Joel Rosenbaum; our lab tech, Shazina Khan; my students, Gurdial Dhillon, Leah Lim, Ashley Ringrose, Shannon Turvey, Aimee Jong, and others; my labmates, past and present, especially those picking up the pieces I've left behind; and Rosemary Redfield and Janet Yu, for telling me I belonged in grad school, and making sure I went.

TABLE OF CONTENTS

LIST OF FIGURES

LIST OF TABLES

LIST OF ABBREVIATIONS/ACRONYMS

EM	electron microscopy/micrograph
fa	*f*lagella *a*utotomy (deflagellation) mutant
fla	*fl*agellar *a*ssembly mutant (usually temperature-sensitive)
IBMX	3-Isobutyl-1-methylxanthine, a phosphodiesterase inhibitor
IFT	intraflagellar transport, a motility system within cilia/flagella
KAT1	*Chlamydomonas* katanin p60
LCA	last common ancestor
MAP	microtubule-associated protein
MTOC	microtubule organizing centre
Nek	NIMA-related kinase; NIMA is a fungal kinase essential for mitosis
PCP	planar cell polarity pathway, noncanonical Wnt pathway
PKD	polycystic kidney disease, results in progressive loss of kidney function
Rb/E2F	retinoblastoma/E2F pathway; controls entry to S phase of cell cycle
SOFA	site of flagellar assembly/autotomy; near the distal flagellar transition zone

CHAPTER 1
INTRODUCTION

1.1 Introduction to Cilia and Flagella

Cilia are slender, often motile, microtubule-based sensory organelles found in most eukaryotic species. Cilia vary morphologically, which led to their being named "cilia" in some species (typically when found to be relatively short and having a paddle-like motion, or no motility at all) and "flagella" in other species, including the green alga *Chlamydomonas* (typically when found to be relatively long and having an undulating motion). Due to possible confusion with bacterial flagella, use of the term "cilia" has become preferred, and throughout this work I will most often use "cilia" (singular cilium) as the generic term, but "flagella" (singular flagellum) and its derivatives when referring to *Chlamydomonas*.

Relatively few species have no cilia at all, including most Fungi and Plants, and the principle of parsimony indicates that species without cilia have independently lost these organelles, and their common ancestor must have been ciliated. The near-ubiquity of cilia is partially explained by noting the multiple functions of these organelles. In some lineages, such as humans and *Chlamydomonas*, cilia have both motility and sensory functions. In others, such as the nematode worm *Caenorhabditis elegans*, cilia play a purely sensory role. It is possible that in other organisms, cilia have only a role in motility. Far from being mere paddles or vestigial protrusions, cilia are dynamic structures with the potential to interact with, and respond to, their environment in

multiple ways. Only in the past decade has it become appreciated how many roles cilia play in human development and disease, thus giving studies of these organelles a new impetus.

In humans and other mammals, nearly all cell lineages have a single, non-motile, cilium called a primary cilium (one notable exception is the hematopoietic lineage) [Wheatley, 1995; Wheatley et al., 1996]. A number of factors led to these cilia being ignored by most scientists. First, the cilia found on most human cells are not motile; they are primary cilia, which have a simpler structure than motile cilia. Second, primary cilia are not essential for viability of tissue culture cell lines. Third, primary cilia are small (typically less than 6 μm long by 300nm thick; Wheatley [1995]) and inherently difficult to recognize, even by immunofluorescence microscopy. Fourth, diseases which have diverse symptoms but a common ciliary basis could not be recognized as such because no functions of primary cilia were appreciated until recently. This last point implies a chicken-or-the-egg-type scenario, which was resolved by the discovery that a mouse mutant for a gene required for ciliary assembly has defects in multiple tissues [Pazour et al., 2000; Taulman et al., 2001]. Since these discoveries, it has become appreciated that far from being vestigial, primary cilia play important roles in the development and maintenance of multiple tissues, and are entwined with such basic processes as cell polarity and the cell cycle [Quarmby and Parker, 2005]. Since cilia are elaborate, microtubule-based structures, I will first review some pertinent points about microtubules and their importance to understanding cells. Then I will discuss some functions of cilia in humans before finally reviewing cilia in my model organism of choice, *Chlamydomonas*.

1.2 The Microtubule Cytoskeleton

The microtubule cytoskeleton of a typical interphase cell consists of microtubules, a microtubule-organizing centre (MTOC) consisting of a centrosome with associated centrioles, and one or more cilia [Doxsey et al., 2005]. Microtubules are polarized, dynamic polymers of alpha-beta tubulin dimers [Kristofferson et al., 1986]. Microtubules are nucleated from gamma-tubulin ring complexes associated with the centrosome and thus have their minus ends at the centrosome while the plus ends, which preferentially incorporate new tubulin dimers, are in the cytoplasm [Joshi et al., 1992]. The centrosome consists of a "cloud" of proteinaceous pericentriolar material surrounding the centrioles, which are barrel-shaped structures composed largely of microtubules [Ou et al., 2003; Dutcher, 2003]. When a cilium is present, the microtubules of centrioles are contiguous with the microtubules that form the core of the cilium, called the axoneme; in this situation, centrioles are called basal bodies [Dutcher, 2003]. A diagram showing cross-sections of a primary cilium, a motile cilium (or flagellum), and a basal body (or centriole) is shown in Figure 1-1; also listed in this Figure are some basic properties of these structures.

The microtubule cytoskeleton functions both as a 'skeleton' and as a 'nervous system' for an interphase cell. That is, it provides both structural support and contributes to motility, and also acts as a scaffold for molecular motor-based cellular trafficking and signal integration [Doxsey et al., 2005]. Importantly, the centrosome, as its name implies, is situated near the centre of the cell, generally in a perinuclear location in most cell types [Vallee and Stehman, 2005]. This central location is important because several signalling pathways, which regulate the cell cycle, converge at the centrosome [Singla and Reiter,

2006]. Microtubules are not static structures, but even so they act as something akin to railroad tracks for intracellular trafficking. There are two major classes of microtubule-based molecular motors that carry molecular cargo: kinesins, which typically move towards microtubule plus ends (and thus typically away from the centrosome and towards the cell periphery) and dyneins, which move toward microtubule minus ends [Vale, 2003]. As an illustration of the effectiveness of such trafficking and its implications in signalling and cell cycle control, some viruses have been demonstrated to be transported via cytoplasmic dynein to the centrosome where viral effector proteins are able to exploit the host cell [Afonso et al., 2007]. Additionally, some modes of intracellular microtubule motility have been shown to be the result of microtubule dynamics, which typically require microtubule-associated proteins (MAPs) *in vivo* [Baas et al., 2005]. Microtubules with free minus ends (often as a result of severing by a MAP called katanin) are able to "treadmill", that is, they add new subunits at the plus end while losing subunits from the minus end, resulting in net movement towards the plus end [Baas et al., 2005].

In mitotic cells, the microtubule cytoskeleton is rearranged to form the mitotic spindle, which is responsible for chromosome segregation. The spindle forms when the centrosome splits, with each new centrosome consisting of one of the two centrioles from interphase, plus a new centriole that was assembled during S-phase [Tsou and Stearns, 2006]. The centriole pairs form two spindle poles, and each pole organizes microtubules with their minus ends at the spindle pole and their plus ends exploring the cell (where they will be stabilized by separate interactions with the cell cortex, the kinetochores of the chromosomes, and also overlapping microtubules emanating from the other spindle pole). To ensure consistent proper segregation of the DNA into two daughter cells, it is

important that the spindle be bipolar, with spindle poles on either side of the nucleus, and this requires correct centrosome splitting. The process of centrosome splitting is partially regulated by the mitotic kinase Nek2, a member of the NIMA-related family of kinases [Quarmby and Mahjoub, 2005]. Nek2 is an effector for the mitotic kinase Cdk2; Nek2 phosphorylation of C-Nap1, Rootletin, and beta-Catenin permits centrosome splitting [Bahe et al., 2005; Bahmanyar et al., 2007]. Split centrosomes push each other apart as part of spindle formation, which also involves a general reorganization of the microtubule network, including changes in microtubule dynamics, microtubule severing, and motor-based transport of intact microtubules [Rusan et al., 2002; Mogilner et al., 2006]. The spindle must also be correctly oriented with respect to the polarity of the daughter cells: spindle pole/centrosome inheritance is asymmetric in yeast [Bornens and Piel, 2002], flies [Yamashita et al., 2007] and human cells [Anderson and Stearns, 2007], and spindle orientation is important for asymmetric division and cell polarity in multiple tissues [Gönczy, 2008].

The preceding has described a traditional view of spindle assembly, but that view lacks an important consideration: if one (or more) centrioles has nucleated a cilium, it would be constrained in its movements (due to being anchored to the membrane) and this could prevent the mitotic spindle from achieving its proper orientation. (There are documented instances in which cells can form a spindle and go through mitosis with a cilium still attached to a centriole [e.g., Rieder et al., 1979] but these are thought to be the exception to the general rule.) Thus, the cilium must be disassembled or otherwise removed prior to cell division. As with centrosome splitting, it is likely that ciliary disassembly is regulated directly or indirectly by mitotic kinases, including possibly

Neks, which have been implicated in human ciliary disease [Quarmby and Parker, 2005; Otto et al., 2008].

1.3 Cilia and Human Disease

A handful of human diseases and syndromes have long been known to be due to dysfunctional motile cilia, but only recently has it been appreciated that a multitude of seemingly diverse syndromes have a common origin with dysfunctional primary cilia. The classic case of a disease caused by malfunctioning motile cilia is Kartagener's Syndrome [Afzelius, 1976]. In addition to male infertility and respiratory problems, half of patients have *situs inversis*, the reversal of the internal organs (so the heart is on the right, etc). For this disease, ciliary motility was an obvious culprit (at least for the first two symptoms, which are caused by immotile sperm and immotile ciliated respiratory epithelia) and causative genes in this disorder have indeed turned out to be motility-related [Storm van's Gravesande and Omran, 2005]. In the last decade, the range of symptoms confirmed to be due to dysfunctional primary, nonmotile, cilia has been greatly expanded, and ranges from polydactyly to hydrocephaly to hepatic biliary disease. This was instigated by the finding that a mouse model for autosomal recessive polycystic kidney disease (ARPKD), the *orpk* mouse, was defective in the gene orthologous to *Chlamydomonas IFT88* [Pazour et al., 2000; Taulman et al., 2001]. IFT88 is a subunit of intraflagellar transport particles. Intraflagellar transport, or IFT, is a microtubule motor-based transport system required for ciliary assembly [Cole et al., 1998]. In addition to the progressive loss of kidney function due to dedifferentiation of kidney collecting duct epithelial tissue, the hallmark of PKDs, the *orpk* mouse also has cystic biliary ducts, cystic pancreas, retinal degeneration, defective cochlear hair cell polarization, and bone

defects [reviewed by Lehman et al., 2008]. Furthermore, the proteins defective in human autosomal dominant PKD, polycystin-1 and polycystin-2, were discovered to partially co-localize to cilia, where they have mechanosensory and signalling functions [Pazour et al., 2002; Yoder et al,. 2002; Nauli et al., 2003].

Some sensory functions of cilia have been long appreciated; the best example of this is rod cells of the mammalian retina, in which the outer segment of the cell (containing multiple membranous layers of photoreceptors) is a modified cilium [Pazour and Witman, 2003]. Olfactory receptors localize to the cilia of sensory neurons. In these cases, the cilium acts as a sensory organelle because it is packed with receptors. In other cases, cilia have sensory functions because they mechanically sense fluid flow [Praetorius and Spring, 2001] or pressure [Malone et al., 2007]. In *C. elegans*, the role of cilia also includes thermosensation and osmoavoidance, suggesting the possibility that such roles could be conserved in mammals [Inglis et al., 2007]. Neuronal cilia may have several more functions [Whitfield 2004], including sateity in mice [Davenport et al., 2007].

Primary cilia also have non-sensory functions. Important signalling receptors localize to cilia, including the somatostatin receptor, the PDGF-alpha receptor, and others [Christensen et al., 2007]. Cilia have several properties that make them effective scaffolds for localization of receptors. They have an inbuilt trafficking system, they have a high ratio of surface area to volume, they project out from the cell (and its boundary layer, [Marshall and Nonaka, 2006]) into the intercellular milieu, and at their base is the centrosome, a hub of intracellular signalling [Doxsey et al., 2005]. Mammalian cilia are involved in the development and maintenance of multiple tissues and organs via the Wnt and Hedgehog signalling pathways. For example, the ciliary protein Inversin functions as

part of a switch between canonical Wnt signalling and non-canonical Wnt signalling (also known as the planar cell polarity (PCP) pathway)[Simons et al., 2005]. The PCP pathway is required for hair cell organization in the inner ear and mutation in some ciliary genes leads to deafness [Jones et al., 2008]. Several components of Hedgehog signalling have been found to localize to cilia in vertebrates, including Smoothened, Patched, and the Gli2/3 proteins [reviewed by Eggenschwiler and Anderson, 2007], while mice mutant in genes required for ciliary assembly often die *in utero* with defects similar to known Hedgehog signalling mutants [Huangfu et al., 2003]. The development of conditional or tissue-specific targeted gene knock-outs in mice is continuing to identify more ciliary functions [Lehman et al., 2008].

As mentioned above, members of the Nek family of kinases have been implicated in ciliary diseases, or ciliopathies, in both mice and humans. Nek1 and Nek8 are the proteins affected in two mouse models of PKD [Upadhya et al., 2000; Liu et al., 2002], while Nek8 has also been implicated as a causative gene in human nephronophthisis, a severe juvenile cystic kidney disease [Otto et al., 2008]. Both mouse mutants have defects in many tissues, supporting the hypothesis that cilia and Neks play roles in development and maintenance of multiple tissues.

Now that the widespread nature of ciliopathies is recognized, it has become more important to study the basic cell biology of cilia. Proteomic and genomic studies have identified proteins required for ciliary assembly and function in different organisms, including humans, *C.elegans*, and *Chlamydomonas* [reviewed by Inglis et al., 2006]. Much work remains to put this large body of information into coherent pathways.

Chlamydomonas is perhaps the most simple model organism for the study of cilia, for reasons that will now be considered.

1.4 *Chlamydomonas* as a Model System for the Study of Cilia

Chlamydomonas reinhardtii is a green alga; that is, it is a unicellular member of the Kingdom Plantae; but the evolutionary conservation of cilia means that many processes and molecules relevant to human cilia structure/function are conserved in *Chlamydomonas*. Because the lineage which led to *Chlamydomonas* diverged from the lineage which led to land plants relatively soon after the plant and animal lineages had themselves diverged [Yoon et al., 2004], *Chlamydomonas* has retained characteristics of both actual ancient plants and ancient precursors to animals, but like all other extant organisms, it is also a product of millions of years of subsequent selection. As a free-living, freshwater-dwelling, auxotrophic, sexual, unicellular organism, *Chlamydomonas* faces numerous challenges. Essentially, cells must be able to escape predation and find conditions amenable for photosynthesis, for which the motility and sensory functions of cilia are required [reviewed by Kirk, 1998]. As single cells, sensory inputs for the various stimuli must either be localized to the cilia or tightly coupled to the cilia, as there are no other cells that can act as intermediaries. Single *Chlamydomonas* cells are motile and able to phototax [Witman, 1993], chemotax [Sjoblad and Frederikse, 1981], gravitotax [Roberts, 2006], avoid predation [Weithoff, 2004], and can be grown either phototrophically or heterotrophically [Sager and Granick, 1954]. General advantages to using *Chlamydomonas* as a model system include a sequenced genome [Merchant et al., 2007], haploid tetrad genetics [Dutcher, 1995], the ability to cheaply grow biochemical quantities of cells [Harris, 1989], nuclear transformation/mutagenesis [Kindle, 1990],

suitability for EM studies [e.g. Cavalier-Smith, 1974], and an exploitable microRNA pathway [Molnár et al., 2007]. Cilia-specific advantages of *Chlamydomonas* include ease of screening mutagenized populations for motility phenotypes, ease of biochemical purification and fractionation of cilia, and ability to use cell models (detergent-extracted cells) for *in vitro* motility assays [reviewed by Silflow and Lefebvre, 2001].

1.5 Structure and Motility of *Chlamydomonas* Cilia

A diagram showing some essential features of *Chlamydomonas* cilia is presented in Figure 1-2. Most cilia have a stereotypical structure, with nine microtubule doublets forming the core of the axoneme, which is surrounded by plasma membrane [Gibbons, 1961]. Cross-sections of cilia seen by EM reveal the conservation of the arrangement of the nine outer doublets: regardless of length, abundance, or species, the cross section looks the same for the majority of cilia/flagella [reviewed by Gibbons, 1981]. Motile cilia additionally have two microtubules in the centre of the axoneme, which are called the central pair microtubules and are functionally significant for motility [Omoto and Witman, 1981]. Another prominent feature of motile cilia is the dynein arms, which are projections arising from the outer doublet microtubules [Gibbons and Gibbons, 1973]. The dyneins walk along the adjacent microtubule doublets, which would result in a sliding motion of the outer doublets were they not constrained by various structural linkages (as directly shown in *in vitro* studies, [Baccetti *et al*., 1985; Okagaki and Kamiya, 1986]). Since the doublets are tightly bound together in intact flagella, the dynein motility results in a bend in the cilium. More recent work has helped clarify the role of the central pair in the regulation and propagation of flagellar bends [Wargo and Smith, 2003; Mitchell and Nakatsugawa, 2004]. As mentioned above, ciliary motility can

range from the relatively simple sweeping motion of trachial epithelia to the multiple propagating waves along sperm flagella, and in some cases these motilities can both be carried out by the very same cilium. This is at least partially achieved via fine control over calcium levels; several axonemal proteins can bind calcium, and changes in intraciliary calcium correlate with changes in waveform [Kamiya and Witman, 1984; Segal and Luck, 1985].

As mentioned above, cilia arise as from the basal bodies, and as such there is a transition zone between the basal body and the cilium proper (diagrammed in Figures 1-2; see also Cavalier-Smith [1974]; Sanders and Salisbury [1989]; Johnson and Porter [1968]; O'Toole et al. [2003]; panels from some of these references are reproduced in Figure 1-3). Additionally, because the basal body is in the cytoplasm while the membranous cilium extrudes from the cell, there are transition fibres that anchor the basal body to the membrane [Gilula and Satir, 1972; O'Toole et al., 2003]. As both the ciliary membrane and matrix have compositions distinct from the rest of the cell [Pazour et al., 2005], it has been proposed that the transition fibres form a so-called "pore complex" which regulates protein entry to the cilium in a way analogous to nuclear pore complexes [Deane *et al.*, 2001; Wemmer and Marshall, 2007]. The distal end of the cilium also deviates from the canonical structure of the rest, as the outer doublets become singlets near the distal tip; also, the ends of the axonemal microtubules are connected to capping structures [Dentler and Rosenbaum, 1977]. Some proteins localize to the tip of the cilium, forming a tip complex proposed to regulate assembly of new axonemal components and reorganization of IFT particles as they switch from anterograde to retrograde movement [Pedersen et al., 2003; 2005].

1.6 Intraflagellar Transport

Intraflagellar transport is a microtubule motor-based motility within cilia [Kozminski et al., 1993]. This process is depicted in Figure 1-2. Large protein complexes (IFT complexes) are transported bidirectionally via kinesins and dyneins walking along the outer doublet microtubules [Cole et al., 1998]. Intraflagellar transport was first discovered in *Chlamydomonas*, in which the movement of IFT complexes can be visualized by light microscopy [Kozminski et al., 1993]. IFT has been demonstrated to be required for transport of ciliary precursors into and out of the cilium [Qin et al, 2004] and is required for ciliary assembly and maintenance [Kozminski et al., 1995; Marshall and Rosenbaum, 2001]. The need for IFT is apparent from a consideration of the structures we have discussed so far. Microtubules grow predominantly at their plus ends [Dentler et al., 1974], and plus ends of the axonemal microtubules are encased in a compartment separate from most of the cell. Furthermore, the minus ends of axonemal microtubules are ultimately capped by the amorphous disc of the proximal basal body [O'Toole et al., 2005]. The problem is compounded as the axoneme lengthens, because the plus ends get further away. A transport system to carry components along the axoneme to the distal end is an obvious solution, and one that probably co-evolved with cilia themselves early on in eukaryotic evolution, as demonstrated by the conservation of IFT proteins in distantly-related organisms [Inglis et al., 2006]. Indeed, the exception proves the rule: in *Drosophila* spermatocytes, IFT is not required to build flagella because they are assembled within the main body of the cell [Han et al., 2003].

The molecular details of IFT do not concern us here; it is enough to note that anterograde IFT requires a heterotrimeric kinesin-2 while retrograde IFT requires

cytoplasmic dynein with its typical entourage of light chains [Cole, 2003]. IFT is required in both the anterograde and retrograde directions for flagellar assembly and maintenance: mutants of accessory proteins of cytoplasmic dynein have no flagella, or very short flagella [Pazour et al., 1998]. This is proposed to be due to the inability of anterograde components to be recycled back to the base of the cilium. Consistent with this hypothesis, the short cilia are found packed with IFT particles as seen by EM [Pazour et al., 1998]. IFT particles themselves are composed of a core of scaffold proteins [Cole, 2003]. Most IFT proteins do not have well-defined non-scaffolding roles as yet, with exceptions including IFT20 which mediates trafficking of some ciliary membrane proteins from the Golgi to the cilium [Follit et al., 2006], and IFT46, which transports outer dynein arms [Hou et al., 2007]. Proteins associated with IFT particles may be roughly divided between those required for ciliary assembly itself, and those required for ciliary targeting or trafficking of various flagellar components, receptors or channels. The "core" IFT genes were discovered in *Chlamydomonas* via biochemical fractionation and peptide sequencing [Cole et al., 1998]. Several genes encoding IFT proteins have since been shown to be mutated in the temperature-sensitive flagellar assembly mutant collection of *Chlamydomonas* [Huang et al, 1977; Walther et al., 1994; Mueller et al., 2005]; and other IFT-related genes were discovered by genetic or genomic approaches in *C. elegans* [Li et al., 2004; Blaque et al., 2005].

In addition to being essential for ciliary assembly, IFT is also specifically required for the movement of proteins that undergo motility within cilia. This has been shown in multiple organisms, and the molecules involved include calcium channels [Qin et al., 2005], proteins activated by flagellar adhesion in *Chlamydomonas* gametes [Wang et al.,

2006], and the Hedgehog receptor Smoothened [Kovacs et al., 2008]. It is likely that many more sensory/signalling molecules undergo IFT. In some cases (e.g. *Chlamydomonas* mating) IFT conducts a sensory signal from the cilia to the cell body [Wang et al., 2006], simply because the cilia is where the signal must be localized. In other cases, it is possible that cilia/IFT is required for signalling to reduce noise (by concentrating receptors in a compartment of high surface area to volume ratio); to more effectively sample the extracellular milieu, potentially even sensing a gradient; and/or as a way to downregulate receptors which have bound ligand, using transport to the cell body rather than endocytosis. Still, the most fundamental function of IFT is ciliary assembly, so it may also be expected that IFT could play a role in ciliary length regulation.

1.7 Flagellar Maintenance/Length Control

Ciliary assembly has been most intensively studied in *Chlamydomonas*, because it is simple to cause cells to lose their flagella (deflagellate) without killing the cells, and thus the cells can be observed as they re-grow their flagella [reviewed by Quarmby, 2004]. Cells that have been deflagellated induce a gene expression program in which tubulins and the many other genes required to make flagella are transcribed, and the resulting proteins help make a full-length flagellum in ~1 hour [Lefebvre et al., 1980; Stolc et al., 2005]. If protein synthesis is blocked, then sufficient precursors are available within the cell to make half-length flagella [Coyne and Rosenbaum, 1970]. In a classic experiment, *Chlamydomonas* cells, which lost one flagellum via deflagellation, were observed to resorb the remaining flagellum concurrent with regenerating the missing flagellum; when the two flagella reached the same length, the resorbing flagellum often switched to

regeneration, and then both flagella grew until they reached normal length [Rosenbaum et al., 1968]. Elegant experiments using a combination of genetics and radiolabelled proteins provided strong evidence that new flagellar components are added at the distal ends of flagella [Johnson and Rosenbaum, 1992].

These details were appreciated for a long time before the molecular mechanism of flagellar assembly, IFT, was discovered. The kinesin-2 mutated in the *fla10-1* strain [Walther et al., 1994] is responsible for anterograde IFT [Kozminski et al., 1995]; at the restrictive temperature, the cilia of *fla10* cells become depleted of IFT proteins and the cells lose their flagella entirely within a few hours [Cole et al., 1998]. This work led to the proposal of a model for ciliary length control [Marshall and Rosenbaum, 2001]. Briefly, this model, the balance point model, holds that the steady-state ciliary length is determined by the relative action of the competing processes of length-dependent assembly and length-independent disassembly. Thus, long flagella (*lf*) mutants would have either reduced disassembly or increased assembly rates (or both), while the converse would be true of short flagella (*shf*) mutants [Marshall, 2004]. Conversely, if a protein is suspected to play a role in regulation of either assembly or disassembly, then a length phenotype may result. A collection of temperature-sensitive flagellar assembly mutants, the *fla* mutants [Huang et al., 1977], had their rates of IFT quantitatively examined (at the permissive temperature) and were found to have a variety of defects; these IFT defects are not, however, reflected as length defects [Iomini et al., 2001]. Conversely, examination of IFT rates in long flagella mutants revealed little change in velocity or frequency of IFT particles compared to wild-type cells [Dentler, 2005]. These results

suggest that the balance point model, as originally formulated, cannot explain ciliary length control.

1.8 Flagellar Disassembly

Deflagellation is a stress response that is the most dramatic form of flagellar disassembly, and results in the severing of the axonemal microtubules above the transition zone [Figure 1-3A; Lewin and Lee, 1982; Sanders and Salisbury, 1989]. In contrast, resorption is coupled to the cell cycle and is a relatively slow process in which the length of flagella gradually decreases [Cavalier-Smith, 1974]. Each disassembly process can be induced experimentally.

Deflagellation is not a random breakage event: there exist *Chlamydomonas* mutants that are unable to deflagellate [Lewin and Lee, 1982], there is a physiologically-defined calcium signalling pathway leading to deflagellation [Quarmby and Hartzell, 1994], and deflagellation occurs at a specific point distal to the ciliary transition zone [Lewin and Lee, 1982; Sanders and Salisbury, 1989]. A forward genetic screen for deflagellation mutants uncovered multiple alleles at three loci: *FA1*, *FA2*, and *ADF1* [Finst et al., 1998]. *adf1* mutants are defective in the calcium signalling pathway; when wild-type cells are treated with dilute organic acids, the cytoplasm acidifies and this is followed by a calcium influx that does not occur in *adf1* mutant cells [Quarmby and Hartzell, 1994]. Although the *adf1* mutation is mapped to a 500kb region of the genome, the causative mutation is not yet known [J. Parker, J. Kirschner, L. Quarmby, unpublished data]. The direct sensor for calcium is not known, although the EF-hand proteins calmodulin and centrin are both components of flagella and basal bodies [Gitelman and Witman, 1980; Sanders and Salisbury, 1989]. The *Chlamydomonas*

flagellar proteome [Pazour et al., 2005] identified several more calcium-binding proteins that could also play a role in deflagellation. FA1 is a protein that contains coiled-coil domains and multiple leucine-rich repeats, and localizes to the region of the basal bodies [Finst et al., 2000]. In addition, FA1 has putative Calcium/Calmodulin-binding motifs and thus is a candidate for transduction of the calcium signal. FA2 is a NIMA-related kinase that localizes both to the basal bodies and to a region of the transition zone proximal to the site of severing, the so-called SOFA (Site Of Flagellar Autotomy) [Mahjoub et al., 2002; 2004]. The role of FA2 in deflagellation is not known, but it may participate in the assembly, activation, and/or proper positioning of a severing complex. *fa1* and *fa2* mutants are both unable to deflagellate in response to any known stimulus: if cells are permeabilized and calcium added, wild-types and *adf1* mutants will deflagellate, but both *fa* mutants fail to deflagellate [Finst et al., 1998]. A fourth protein, katanin, has been functionally implicated in deflagellation [Lohret et al., 1998] but a katanin mutant was not recovered in a large-scale screen for deflagellation mutants [Finst et al., 1998]. A pan-specific antibody versus katanin recognizes *Chlamydomonas* basal bodies by immunogold EM, and this antibody blocks deflagellation when added to permeabilized cells [Lohret et al., 1999]. Also, isolated axonemes are a substrate in vitro for purified katanin (*Chlamydomonas* KAT1 protein), demonstrating that KAT1 is able to sever the doublet microtubules of axonemes [Lohret et al., 1998]. Centrin forms the distal striated fibres that connect the basal bodies at their distal ends [Salisbury et al., 1988; Koblenz et al., 2003], as well as the stellate fibres in the interior of the transition zone [O'Toole et al., 2003]. These fibres contract upon deflagellation, and a *Chlamydomonas* strain with a point mutation in centrin, the *vfl2* mutant, is reported to be less effective at deflagellation

[Sanders and Salisbury, 1989]. Overall, a satisfying model based on current data for acid-induced deflagellation, is that acidification of the cytosol stimulates calcium release via ADF1, leading to activation of FA1 (directly, by binding calmodulin or centrin) and possibly FA2 (indirectly, perhaps via FA1). Alternatively, FA2 could be required for localization of FA1 or KAT1, KAT1 is then stimulated to directly sever the axonemal microtubules. Concomitant centrin contraction may help pinch off the flagellum, but this had been shown to be neither necessary nor sufficient for deflagellation [Sanders and Salisbury, 1989; Quarmby, 2004].

The other form of flagellar disassembly, resorption, differs from deflagellation in several aspects, most obviously in that it is slow and conservative. Whereas complete deflagellation of a culture can be induced by acidification of the media within seconds, resorption is much slower, although the time it takes varies considerably depending on the circumstances. Resorption naturally occurs in cells prior to mitosis and in the quadriflagellate cells resulting from mating [Cavalier-Smith, 1974]. In premitotic cells, resorption has been reported to take ~30 minutes; resorption after gamete fusion also takes ~30 minutes [Cavalier-Smith, 1974; Marshall and Rosenbaum, 2001]. Resorption can also be induced by various pharmacological agents, including IBMX, caffeine, N-8, and other agents interfering with phosphodiesterases or cyclic nucleotide-dependent kinases [Tuxhorn et al., 1998], or simply by lowering the calcium concentration and increasing the sodium concentration of the medium [Lefebvre et al., 1978]. Drug- or buffer-induced resorption is typically much slower and less complete than premitotic resorption; various agents result in only a 50% decrease in length and often take several hours to be effective [Lefebvre et al., 1978; Tuxhorn et al., 1998]. Flagella are known to

be dynamic and undergo constant turnover [Marshall and Rosenbaum, 2001], so the pharmacological studies are consistent with interfering with flagellar assembly while allowing constitutive disassembly. Electron micrographs of resorbing cilia often show disorganization of the distal end [Cavalier-Smith, 1974; Gaffal, 1988; Dentler, 2005]. It is likely that resorption can occur by more than one mechanism, and the faster mechanism involved in premitotic disassembly may involve more than mere lack of assembly. No resorption-defective mutants are known in *Chlamydomonas*, presumably because they would be either cilia-less (due to assembly/length control issues) or lethal (due to inability to free the basal bodies to act as spindle pole organizers).

1.9 *Chlamydomonas* Cell Cycle

General features of the vegetative and sexual life cycles of *Chlamydomonas* are diagrammed in Figure 1-4. During normal mitosis in *Chlamydomonas,* the basal bodies are released from the flagella in order to act at the spindle poles [Coss, 1974]. Recall that basal bodies are anchored to cell membranes via the ciliary transition zone (Figure 1-2; Section 1.6) and thus if basal bodies were not released from the flagella, a normal bipolar spindle could form only if the flagella could move within the cell membrane. However, *Chlamydomonas* has a rigid cell wall that is retained during mitosis. Flagella pass through the cell wall via tunnels at the anterior end of the cell, but the tunnels cannot move to accommodate flagella or therefore basal bodies during spindle formation. Thus, the cell wall precludes the possibility of maintaining flagella attached to the basal bodies during mitosis, as occurs in some algal species [Bloodgood, 1974]. The requirement of premitotic ciliary loss in walled cells has been termed the 'flagellation constraint' [Kirk 1998, and references therein]. Logically, since *Chlamydomonas* cells require cilia for

optimal growth (by maintaining themselves at the optimal illumination levels for photosynthesis), cells cannot have cilia during mitosis, and cellular growth cannot occur at night, then cells should divide at night, and they do [Craigie and Cavalier-Smith, 1982].

Cells that have grown very large during the day do not divide only once (and thus produce two still-large daughter cells), but rather they undergo N rounds of G2/M to produce 2^N equal-sized daughter cells [depicted in Figure 1-4; Craigie and Cavalier-Smith, 1982]. Mutations in *Chlamydomonas* genes that affect cell cycle progression may manifest as perturbations in cell size, since a mutation that slows cell cycle progression would result in cells that reach a larger size before dividing [reviewed by Umen, 2005]. If the pathway that determines how many rounds of division the mother cell should undergo is intact, then the daughter cells of our putative mutant would be normal-sized. However, in an asynchronous population, the defect would be apparent as a cell size distribution skewed towards larger cells than in a wild-type culture. A cell size phenotype could also result from a mutation that leads the mother cell to incorrectly gauge its size, and so divides at the wrong size and/or the wrong number of times [Umen and Goodenough, 2001]. Additionally, size defect can result from unequal cell division. Mutant strains lacking functional basal bodies have cell size defects due to unequal partitioning of the mother cell between its daughters: basal bodies are required for organization of the rootlet microtubule and centrin systems, which are in turn required for correct placement of the cytokinetic furrow relative to the nucleus [Ehler et al., 1995].

The molecular details of cell cycle regulation in *Chlamydomonas* have received little attention, but there is an Rb/E2F pathway [Umen and Goodenough, 2001], and

identifiable homologues of many other known cell cycle regulators [Bisova et al., 2005]. It is likely that cell cycle regulation in this organism is complex as it must be able to cope with not only the usual challenges any "typical" cell might face, but also involves regulation by light, cell size, and flagella status. A complex circadian clock system helps co-ordinate growth with daylight [Mittag et al., 2005], and cell size/growth issues were touched on above. Since cilia must not be present during mitosis, they must be disassembled and then reassembled in co-ordination with cell cycle progression, and in co-ordination with the other microtubule/centriole-related changes that must occur during the transition into mitosis. Thus, mitotic kinases that regulate the other changes are candidates to regulate the changes in ciliation. Accordingly, the deflagellation protein FA2 is a member of the Nek family of cell cycle kinases [Mahjoub et al., 2002], while a Cdk-like protein partially controls ciliary assembly/length [Tam et al., 2007] and an Aurora-like kinase has been implicated in all forms of ciliary disassembly [Pan et al., 2004]. *fa2* mutant cells were found to have a cell size defect, suggesting that FA2 plays a role in cell cycle progression [Mahjoub et al., 2002]. As the only known function of FA2 is deflagellation, this suggests that either deflagellation may play a role in the cell cycle, or that FA2 has two independent functions, one ciliary and one related to cell cycle.

Several EM studies of premitotic *Chlamydomonas* cilia have been reported. Dogma in the field is that cilia are gradually disassembled from their tips, until the basal bodies are freed entirely [Cavalier-Smith 1974; Gaffal, 1988]. This implies that even the transition zone, which is anchored to the membrane by multiple contacts [O'Toole et al., 2003], must be disassembled. In contrast, one study clearly showed evidence for a deflagellation-like severing event, as mostly-intact axonemes were seen in mitotic cells

[Johnson and Porter, 1968] (Figure 1-3c). Supporting this, in a third study there are signs of separation between the basal body and transition zone [Gaffal, 1988]. Piasecki and Silflow [2007] reported seeing flagella still attached to mitotic cells, and in these cells, the basal bodies were detached from the flagella, and the cells had normal spindles These differing results may be due to preparation or other experimental variations; or they could reflect real differences in premitotic resorption that occur in response to growth conditions.

1.10 Questions

In this present work, I set out to answer several questions regarding the mechanisms and regulation of flagellar resorption, especially before mitotic entry, in *Chlamydomonas reinhardtii*. In Chapter 2, I examine the *fla* mutants, which are temperature-sensitive flagellar assembly mutants reported to resorb at the restrictive temperature. I found that these mutants instead deflagellate at the restrictive temperature. By altering the calcium concentration of the medium, or by use of a *fa* mutant background, I found I could prevent deflagellation and instead force the cells to resorb. Furthermore, I found that *fa,fla* double mutants resorb slowly, and acid shock can induce resorption in deflagellation mutants. These data suggest that resorption and deflagellation may share common mechanisms or regulatory elements. Next, in Chapter 3, I collaborated with Brian Bradley and we found evidence for the potential involvement for the Nek family of mitotic kinases in co-ordinating ciliary assembly and disassembly. Based on the fact that the deflagellation protein FA2 is a Nek, as well as the involvement of mouse Neks in ciliopathies, we hypothesized that organisms requiring ciliary assembly and disassembly to be co-ordinated with cell cycle progression would have more Neks than organisms

lacking cilia. Using the recently available tools of sequenced genomes and Bayesian inference, we performed a large-scale phylogeny of the Nek kinase family and found support for our hypothesis. Organisms lacking cilia, or having cilia only on terminally differentiated cells, have relatively few Neks. Furthermore, the relationships between Nek family members indicate that this family expanded early in eukaryotic evolution. In Chapter 4, we chose to examine more closely the role of katanin in *Chlamydomonas*. Based on my previous result from Chapter 2, I hypothesized that the microtubule-severing role of katanin in deflagellation may also be required for pre-mitotic resorption of flagella. Supporting this, Qasim Rasi and I found that strains expressing less KAT1 can be obtained via RNA interference methods in flagella-less mutants, but not in wild-type cells. We also show that wild-type *Chlamydomonas* cells must indeed sever their flagella, and that this severing may occur between the transition zone and the basal bodies. This thesis therefore sheds light on basic mechanisms of flagellar dynamics in *Chlamydomonas*, and also suggests roles for *Chlamydomonas* Neks in the regulation of these processes.

1.11 Figures

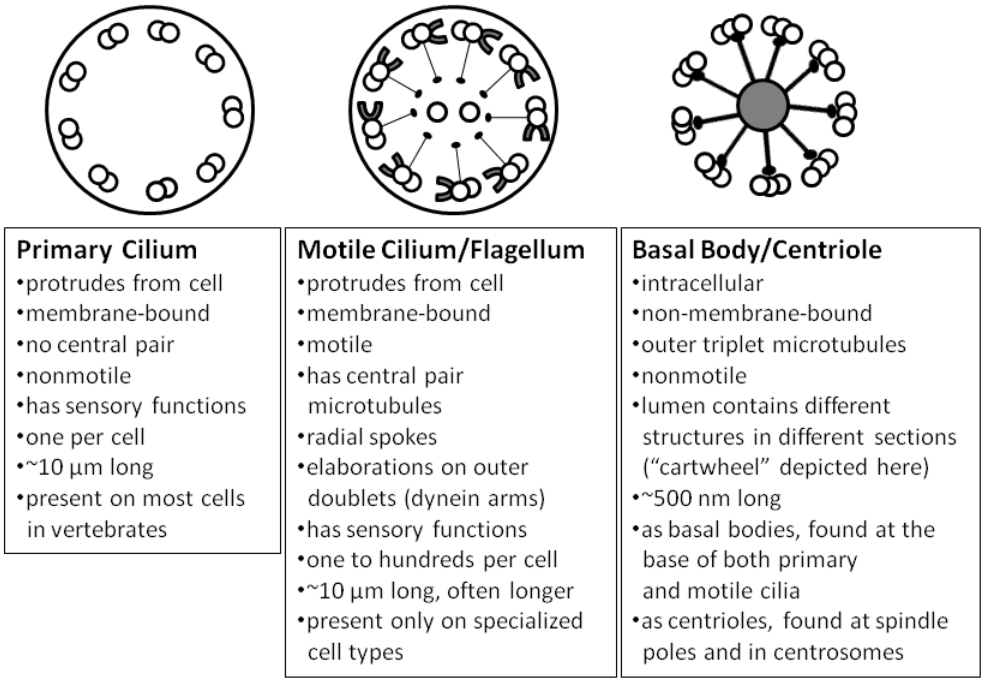

Figure 1-1. Diagram showing typical, simplified, cross-sections of a primary cilium, a motile cilium, and a basal body; and a list of basic attributes of each structure.

Based on data from multiple sources, especially O'Toole et al. [2003], Wheatley [1995], and Rosenbaum and Witman [2002] and references therein; also see text.

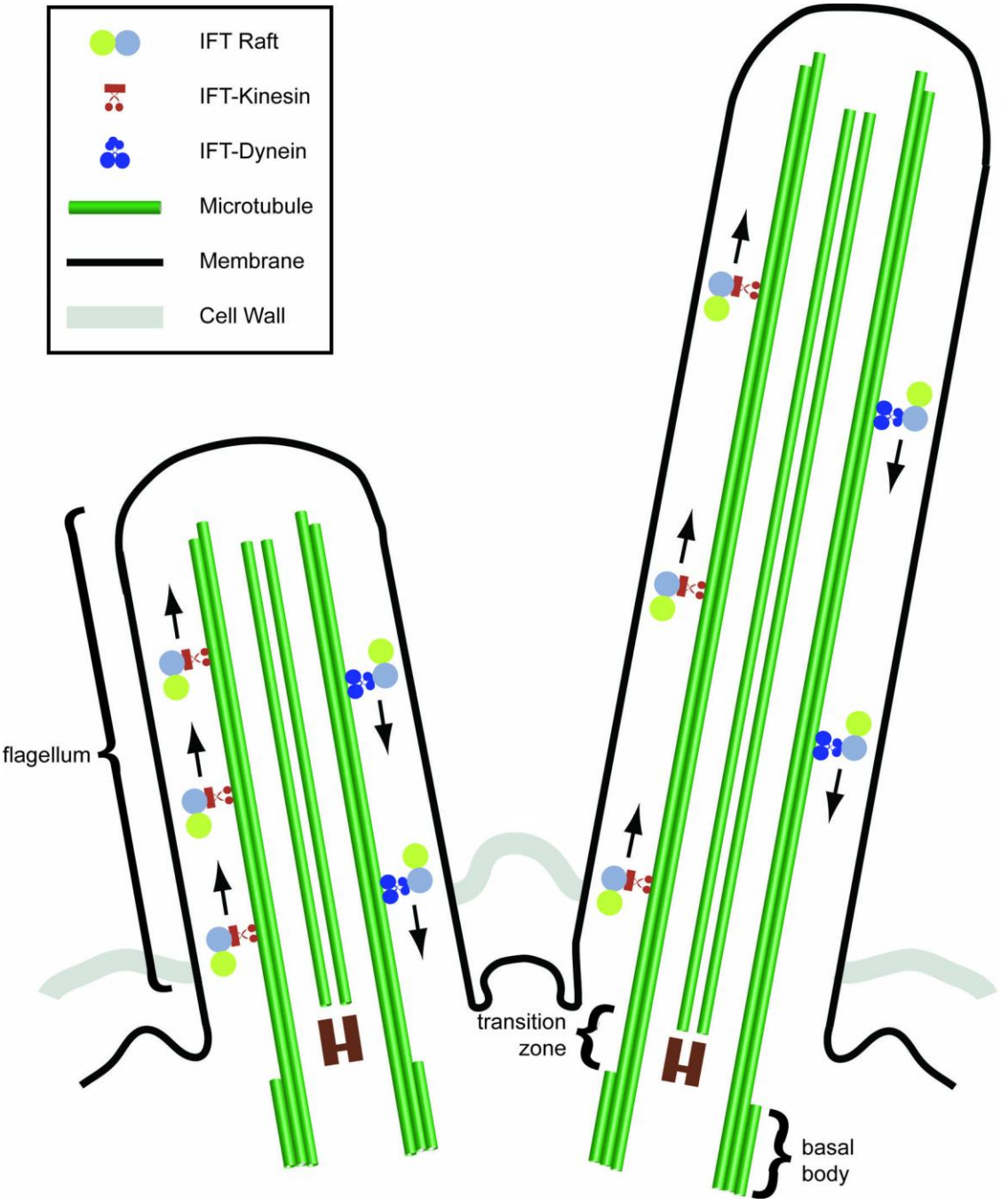

Figure 1-2. Diagram of *Chlamydomonas* flagella, transition zones, and basal bodies.

The diagram shows IFT rafts and their associated motors, central pair microtubules, outer doublet microtubules, the basal bodies, and the flagellar transition zone. Note that flagella have membranes and protrude through the cell wall. This particular cell has unequal length flagella and thus the longer flagellum on the right would be shortening while the shorter flagellum on the left would be growing (see Section 1-7).

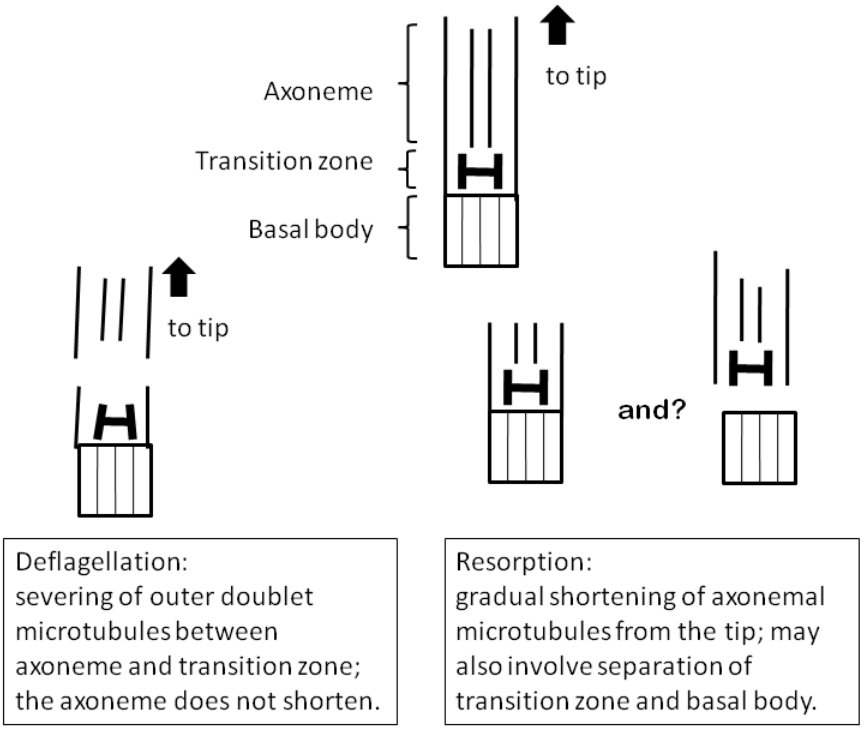

Figure 1-3. Diagrams of disassembling *Chlamydomonas* flagella.

Top: intact flagellum, showing part of the axoneme, the transition zone, and the basal body. The flagellar membrane is not depicted for simplicity.

Bottom left, a flagellum after deflagellation. The outer doublets have been severed distal to the transition zone, proximal to the origin of the central pair microtubules. Based on data from Lewin & Lee, 1985, and Sanders & Salisbury, 1989.

Bottom right, diagrams of flagellar resorption. The axonemal microtubules, including the outer doublets and the central pair, gradually shorten from the tip and may be disorganized. In some images, a shortened flagellum is seen attached to a transition zone, but no basal body is present, thus the basal body may sometimes separate from the transition zone (extreme right figure). Based on data from Cavalier-Smith, 1974, and Johnson and Porter, 1968.

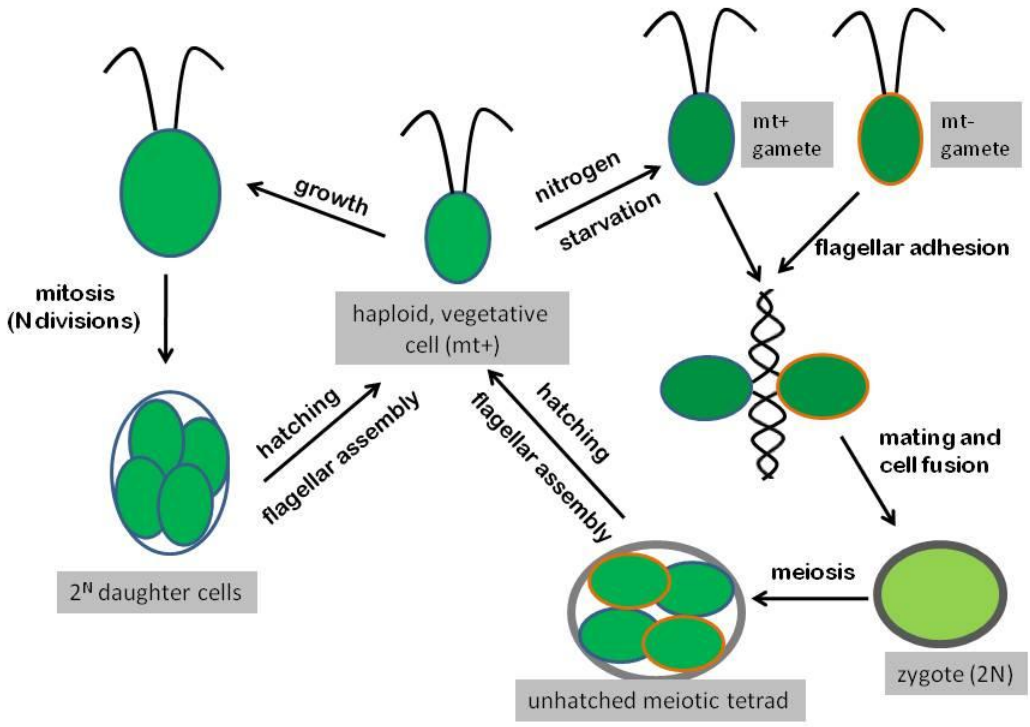

Figure 1-4. Diagram of the *Chlamydomonas* vegetative and sexual life cycles.

Haploid cells typically reproduce asexually, and go through one-to-four rounds of mitosis depending on the size of the mother cell pre-mitosis. Daughter cells hatch from the mother cell wall after flagellar assembly permits cell motility. Cells rid themselves of their flagella prior to mitosis (see text).

Gametogenesis is induced by nitrogen starvation. Haploid gametes of the two mating types, designated mt+ and mt-, express adhesion proteins on their flagella that allow gametes to bind to gametes of the opposite mating type. The gametes fuse to ultimately form a 2N zygote surrounded by a thicker protective wall. The zygote is resistant to environmental insult and requires exposure to light in order to mature and begin meiosis. As with the vegetative cycle, newly-divided cells must assemble flagella to efficiently escape the zygotic cell wall.

Figure based on the work of Sager and Granick [1953], Cavalier-Smith [1974], Bergman et al. [1975], as well as Harris [1989] and references therein.

1.12 References

Afonso PV, Zamborlini A, Saïb A, Mahieux R. Centrosome and retroviruses: the dangerous liaisons. Retrovirology. 2007 Apr 14;4:27.

Afzelius BA. A human syndrome caused by immotile cilia. Science. 1976 Jul 23;193(4250):317-9.

Anderson CT, Stearns T. The primary cilium: what once did nothing, now does everything. J Musculoskelet Neuronal Interact. 2007 Oct-Dec;7(4):299.

Baas PW, Karabay A, Qiang L. Microtubules cut and run. Trends Cell Biol. 2005 Oct;15(10):518-24.

Bahe S, Stierhof YD, Wilkinson CJ, Leiss F, Nigg EA. Rootletin forms centriole-associated filaments and functions in centrosome cohesion. J Cell Biol. 2005 Oct 10;171(1):27-33.

Bahmanyar S, Kaplan DD, Deluca JG, Giddings TH Jr, O'Toole ET, Winey M, Salmon ED, Casey PJ, Nelson WJ, Barth AI. beta-Catenin is a Nek2 substrate involved in centrosome separation. Genes Dev. 2008 Jan 1;22(1):91-105.

Baccetti B, Porter KR, Ulrich M. High voltage electron microscopy of sperm axoneme. J Submicrosc Cytol. 1985 Apr;17(2):171-6.

Bergman K, Goodenough UW, Goodenough DA, Jawitz J, Martin H. Gametic differentiation in *Chlamydomonas reinhardtii*. II. Flagellar membranes and the agglutination reaction. J Cell Biol. 1975 Dec;67(3):606-22.

Bisova K, Krylov DM, Umen JG. Genome-wide annotation and expression profiling of cell cycle regulatory genes in *Chlamydomonas reinhardtii*. Plant Physiol. 2005 Feb;137(2):475-91.

Blacque OE, Perens EA, Boroevich KA, Inglis PN, Li C, Warner A, Khattra J, Holt RA, Ou G, Mah AK, McKay SJ, Huang P, Swoboda P, Jones SJ, Marra MA, Baillie DL, Moerman DG, Shaham S, Leroux MR. Functional genomics of the cilium, a sensory organelle. Curr Biol. 2005 May 24;15(10):935-41.

Bloodgood RA. Resorption of organelles containing microtubules. Cytobios. 1974 Mar-Apr;9(35):142-61.

Bornens M, Piel M. Centrosome inheritance: birthright or the privilege of maturity? Curr Biol. 2002 Jan 22;12(2):R71-3.

Cavalier-Smith T. Basal body and flagellar development during the vegetative cell cycle and the sexual cycle of *Chlamydomonas reinhardtii*. J Cell Sci. 1974 Dec;16(3):529-56.

Christensen ST, Pedersen LB, Schneider L, Satir P. Sensory cilia and integration of signal transduction in human health and disease. Traffic. 2007 Feb;8(2):97-109.

Cole DG, Diener DR, Himelblau AL, Beech PL, Fuster JC, Rosenbaum JL. *Chlamydomonas* kinesin-II-dependent intraflagellar transport (IFT): IFT particles contain proteins required for ciliary assembly in *Caenorhabditis elegans* sensory neurons. J Cell Biol. 1998 May 18;141(4):993-1008.

Cole DG. The intraflagellar transport machinery of *Chlamydomonas reinhardtii*. Traffic. 2003 Jul;4(7):435-42.

Coss RA. Mitosis in *Chlamydomonas reinhardtii* basal bodies and the mitotic apparatus. J Cell Biol. 1974 Oct;63(1):325-9

Coyne B, Rosenbaum JL. Flagellar elongation and shortening in *Chlamydomonas*. II. Re-utilization of flagellar proteins. J Cell Biol. 1970 Dec;47(3):777-81.

Craigie RA, Cavalier-Smith T. Cell Volume and the Control of the *Chlamydomonas* Cell Cycle. J. Cell Sci. 1982 54: 173-191.

Davenport JR, Watts AJ, Roper VC, Croyle MJ, van Groen T, Wyss JM, Nagy TR, Kesterson RA, Yoder BK. Disruption of intraflagellar transport in adult mice leads to obesity and slow-onset cystic kidney disease. Curr Biol. 2007 Sep 18;17(18):1586-94.

Deane JA, Cole DG, Seeley ES, Diener DR, Rosenbaum JL. Localization of intraflagellar transport protein IFT52 identifies basal body transitional fibers as the docking site for IFT particles. Curr Biol. 2001 Oct 16;11(20):1586-90.

Dentler W. Intraflagellar transport (IFT) during assembly and disassembly of *Chlamydomonas* flagella. J Cell Biol. 2005 Aug 15;170(4):649-59.

Dentler WL, Granett S, Witman GB, Rosenbaum JL. Directionality of brain microtubule assembly in vitro. Proc Natl Acad Sci U S A. 1974 May;71(5):1710-4.

Dentler WL, Rosenbaum JL. Flagellar elongation and shortening in *Chlamydomonas*. III. structures attached to the tips of flagellar microtubules and their relationship to the directionality of flagellar microtubule assembly. J Cell Biol. 1977 Sep;74(3):747-59.

Doxsey S, Zimmerman W, Mikule K. Centrosome control of the cell cycle. Trends Cell Biol. 2005 Jun;15(6):303-11.

Dutcher SK. Mating and tetrad analysis in *Chlamydomonas reinhardtii*. Methods Cell Biol. 1995;47:531-40.

Dutcher SK. Elucidation of basal body and centriole functions in *Chlamydomonas reinhardtii*. Traffic. 2003 Jul;4(7):443-51

Eggenschwiler JT, Anderson KV. Cilia and developmental signaling. Annu Rev Cell Dev Biol. 2007;23:345-73.

Ehler LL, Holmes JA, Dutcher SK. Loss of spatial control of the mitotic spindle apparatus in a *Chlamydomonas reinhardtii* mutant strain lacking basal bodies. Genetics. 1995 Nov;141(3):945-60

Finst RJ, Kim PJ, Griffis ER, Quarmby LM. Fa1p is a 171 kDa protein essential for axonemal microtubule severing in *Chlamydomonas*. J Cell Sci. 2000 Jun;113 (Pt 11):1963-71.

Finst RJ, Kim PJ, Quarmby LM. Genetics of the deflagellation pathway in *Chlamydomonas*. Genetics. 1998 Jun;149(2):927-36.

Follit JA, Tuft RA, Fogarty KE, Pazour GJ. The intraflagellar transport protein IFT20 is associated with the Golgi complex and is required for cilia assembly. Mol Biol Cell. 2006 Sep;17(9):3781-92.

Gaffal KP The basal body-root complex of *Chlamydomonas reinhardtii* during mitosis. Protoplasma 1988 143(2):118-29.

Gibbons BH, Gibbons IR. The effect of partial extraction of dynein arms on the movement of reactivated sea-urchin sperm. J Cell Sci. 1973 Sep;13(2):337-57.

Gibbons IR. Structural asymmetry in cilia and flagella. Nature. 1961 Jun 17;190:1128-9.

Gibbons IR. Cilia and flagella of eukaryotes. J Cell Biol. 1981 Dec;91(3 Pt 2):107s-124s.

Gitelman SE, Witman GB. Purification of calmodulin from *Chlamydomonas*: calmodulin occurs in cell bodies and flagella. J Cell Biol. 1980 Dec;87(3 Pt 1):764-70.

Gönczy P. Mechanisms of asymmetric cell division: flies and worms pave the way. Nat Rev Mol Cell Biol. 2008 May;9(5):355-66.

Han YG, Kwok BH, Kernan MJ. Intraflagellar transport is required in Drosophila to differentiate sensory cilia but not sperm. Curr Biol. 2003 Sep 30;13(19):1679-86.

Harris, E. The *Chlamydomonas* Sourcebook: A Comprehensive Guide to Biology and Laboratory Use. Academic Press, 1989.

Hou Y, Qin H, Follit JA, Pazour GJ, Rosenbaum JL, Witman GB. Functional analysis of an individual IFT protein: IFT46 is required for transport of outer dynein arms into flagella. J Cell Biol. 2007 Feb 26;176(5):653-65.

Huang B, Rifkin MR, Luck DJ. Temperature-sensitive mutations affecting flagellar assembly and function in *Chlamydomonas reinhardtii*. J Cell Biol. 1977 Jan;72(1):67-85.

Huangfu D, Liu A, Rakeman AS, Murcia NS, Niswander L, Anderson KV. Hedgehog signalling in the mouse requires intraflagellar transport proteins. Nature. 2003 Nov 6;426(6962):83-7.

Inglis PN, Boroevich KA, Leroux MR. Piecing together a ciliome. Trends Genet. 2006 Sep;22(9):491-500.

Inglis PN, Ou G, Leroux MR, Scholey JM. The sensory cilia of *Caenorhabditis elegans*. WormBook. 2007 Mar 8:1-22.

Iomini C, Babaev-Khaimov V, Sassaroli M, Piperno G. Protein particles in *Chlamydomonas* flagella undergo a transport cycle consisting of four phases. J Cell Biol. 2001 Apr 2;153(1):13-24.

Johnson KA, Rosenbaum JL. Polarity of flagellar assembly in *Chlamydomonas*. J Cell Biol. 1992 Dec;119(6):1605-11.

Johnson UG, Porter KR. Fine structure of cell division in *Chlamydomonas* reinhardi. Basal bodies and microtubules. J Cell Biol. 1968 Aug;38(2):403-25.

Jones C, Roper VC, Foucher I, Qian D, Banizs B, Petit C, Yoder BK, Chen P. Ciliary proteins link basal body polarization to planar cell polarity regulation. Nat Genet. 2008 Jan;40(1):69-77.

Joshi HC, Palacios MJ, McNamara L, Cleveland DW. Gamma-tubulin is a centrosomal protein required for cell cycle-dependent microtubule nucleation. Nature. 1992 Mar 5;356(6364):80-3.

Kamiya R, Witman GB. Submicromolar levels of calcium control the balance of beating between the two flagella in demembranated models of *Chlamydomonas*. J Cell Biol. 1984 Jan;98(1):97-107.

Kindle KL. High-frequency nuclear transformation of *Chlamydomonas reinhardtii*. Proc Natl Acad Sci U S A. 1990 Feb;87(3):1228-32.

Kirk DL. *Volvox*: Molecular-Genetic Origins of Multicellularity and Cellular Differentiation. Cambridge University Press, 1998

Koblenz B, Schoppmeier J, Grunow A, Lechtreck KF. Centrin deficiency in *Chlamydomonas* causes defects in basal body replication, segregation and maturation. J Cell Sci. 2003 Jul 1;116(Pt 13):2635-46.

Kovacs JJ, Whalen EJ, Liu R, Xiao K, Kim J, Chen M, Wang J, Chen W, Lefkowitz RJ. Beta-arrestin-mediated localization of smoothened to the primary cilium. Science. 2008 Jun 27;320(5884):1777-81

Kozminski KG, Beech PL, Rosenbaum JL. The *Chlamydomonas* kinesin-like protein FLA10 is involved in motility associated with the flagellar membrane. J Cell Biol. 1995 Dec;131(6 Pt 1):1517-27.

Kozminski KG, Johnson KA, Forscher P, Rosenbaum JL. A motility in the eukaryotic flagellum unrelated to flagellar beating. Proc Natl Acad Sci U S A. 1993 Jun 15;90(12):5519-23.

Kristofferson D, Mitchison T, Kirschner M. Direct observation of steady-state microtubule dynamics. J Cell Biol. 1986 Mar;102(3):1007-19.

Lefebvre PA, Nordstrom SA, Moulder JE, Rosenbaum JL. Flagellar elongation and shortening in *Chlamydomonas*. IV. Effects of flagellar detachment, regeneration, and resorption on the induction of flagellar protein synthesis. J Cell Biol. 1978 Jul;78(1):8-27.

Lefebvre PA, Silflow CD, Wieben ED, Rosenbaum JL. Increased levels of mRNAs for tubulin and other flagellar proteins after amputation or shortening of *Chlamydomonas* flagella. Cell. 1980 Jun;20(2):469-77.

Lehman JM, Michaud EJ, Schoeb TR, Aydin-Son Y, Miller M, Yoder BK. The Oak Ridge Polycystic Kidney mouse: Modeling ciliopathies of mice and men. Dev Dyn. 2008 Aug;237(8):1960-71.

Li JB, Gerdes JM, Haycraft CJ, Fan Y, Teslovich TM, May-Simera H, Li H, Blacque OE, Li L, Leitch CC, Lewis RA, Green JS, Parfrey PS, Leroux MR, Davidson WS, Beales PL, Guay-Woodford LM, Yoder BK, Stormo GD, Katsanis N, Dutcher SK. Comparative genomics identifies a flagellar and basal body proteome that includes the BBS5 human disease gene. Cell. 2004 May 14;117(4):541-52.

Liu S, Lu W, Obara T, Kuida S, Lehoczky J, Dewar K, Drummond IA, Beier DR. A defect in a novel Nek-family kinase causes cystic kidney disease in the mouse and in zebrafish. Development. 2002 Dec;129(24):5839-46.

Lohret TA, McNally FJ, Quarmby LM. A role for katanin-mediated axonemal severing during *Chlamydomonas* deflagellation. Mol Biol Cell. 1998 May;9(5):1195-207.

Lohret TA, Zhao L, Quarmby LM. Cloning of *Chlamydomonas* p60 katanin and localization to the site of outer doublet severing during deflagellation. Cell Motil Cytoskeleton. 1999;43(3):221-31.

Mahjoub MR, Montpetit B, Zhao L, Finst RJ, Goh B, Kim AC, Quarmby LM. The FA2 gene of *Chlamydomonas* encodes a NIMA family kinase with roles in cell cycle progression and microtubule severing during deflagellation. J Cell Sci. 2002 Apr 15;115(Pt 8):1759-68.

Mahjoub MR, Qasim Rasi M, Quarmby LM. A NIMA-related kinase, Fa2p, localizes to a novel site in the proximal cilia of *Chlamydomonas* and mouse kidney cells. Mol Biol Cell. 2004 Nov;15(11):5172-86.

Malone AM, Anderson CT, Tummala P, Kwon RY, Johnston TR, Stearns T, Jacobs CR. Primary cilia mediate mechanosensing in bone cells by a calcium-independent mechanism. Proc Natl Acad Sci U S A. 2007 Aug 14;104(33):13325-30.

Marshall WF, Nonaka S. Cilia: tuning in to the cell's antenna. Curr Biol. 2006 Aug 8;16(15):R604-14.

Marshall WF, Rosenbaum JL. Intraflagellar transport balances continuous turnover of outer doublet microtubules: implications for flagellar length control. J Cell Biol. 2001 Oct 29;155(3):405-14.

Marshall WF. Cellular length control systems. Annu Rev Cell Dev Biol. 2004;20:677-93

Merchant SS, Prochnik SE, Vallon O, Harris EH, Karpowicz SJ, Witman GB, Terry A, Salamov A, Fritz-Laylin LK, Maréchal-Drouard L, Marshall WF, et al. The *Chlamydomonas* genome reveals the evolution of key animal and plant functions. Science. 2007 Oct 12;318(5848):245-50.

Mitchell DR, Nakatsugawa M. Bend propagation drives central pair rotation in *Chlamydomonas reinhardtii* flagella. J Cell Biol. 2004 Aug 30;166(5):709-15.

Mittag M, Kiaulehn S, Johnson CH. The circadian clock in *Chlamydomonas reinhardtii*. What is it for? What is it similar to? Plant Physiol. 2005 Feb;137(2):399-409.

Mogilner A, Wollman R, Civelekoglu-Scholey G, Scholey J. Modeling mitosis. Trends Cell Biol. 2006 Feb;16(2):88-96.

Molnár A, Schwach F, Studholme DJ, Thuenemann EC, Baulcombe DC. miRNAs control gene expression in the single-cell alga *Chlamydomonas reinhardtii*. Nature. 2007 Jun 28;447(7148):1126-9.

Mueller J, Perrone CA, Bower R, Cole DG, Porter ME. The FLA3 KAP subunit is required for localization of kinesin-2 to the site of flagellar assembly and processive anterograde intraflagellar transport. Mol Biol Cell. 2005 Mar;16(3):1341-54.

Nauli SM, Alenghat FJ, Luo Y, Williams E, Vassilev P, Li X, Elia AE, Lu W, Brown EM, Quinn SJ, Ingber DE, Zhou J. Polycystins 1 and 2 mediate mechanosensation in the primary cilium of kidney cells. Nat Genet. 2003 Feb;33(2):129-37.

Okagaki T, Kamiya R. Microtubule sliding in mutant *Chlamydomonas* axonemes devoid of outer or inner dynein arms. J Cell Biol. 1986 Nov;103(5):1895-902.

Omoto CK, Witman GB. Functionally significant central-pair rotation in a primitive eukaryotic flagellum. Nature. 1981 Apr 23;290(5808):708-10.

O'Toole ET, Giddings TH, McIntosh JR, Dutcher SK. Three-dimensional organization of basal bodies from wild-type and delta-tubulin deletion strains of *Chlamydomonas reinhardtii*. Mol Biol Cell. 2003 Jul;14(7):2999-3012.

Otto EA, Trapp ML, Schultheiss UT, Helou J, Quarmby LM, Hildebrandt F. NEK8 mutations affect ciliary and centrosomal localization and may cause nephronophthisis. J Am Soc Nephrol. 2008 Mar;19(3):587-92.

Ou YY, Zhang M, Chi S, Matyas JR, Rattner JB. Higher order structure of the PCM adjacent to the centriole. Cell Motil Cytoskeleton. 2003 Jun;55(2):125-33.

Pan J, Wang Q, Snell WJ. An aurora kinase is essential for flagellar disassembly in *Chlamydomonas*. Dev Cell. 2004 Mar;6(3):445-51.

Pazour GJ, Agrin N, Leszyk J, Witman GB. Proteomic analysis of a eukaryotic cilium. J Cell Biol. 2005 Jul 4;170(1):103-13.

Pazour GJ, Dickert BL, Vucica Y, Seeley ES, Rosenbaum JL, Witman GB, Cole DG. *Chlamydomonas* IFT88 and its mouse homologue, polycystic kidney disease gene tg737, are required for assembly of cilia and flagella. J Cell Biol. 2000 Oct 30;151(3):709-18.

Pazour GJ, San Agustin JT, Follit JA, Rosenbaum JL, Witman GB. Polycystin-2 localizes to kidney cilia and the ciliary level is elevated in orpk mice with polycystic kidney disease. Curr Biol. 2002 Jun 4;12(11):R378-80.

Pazour GJ, Wilkerson CG, Witman GB. A dynein light chain is essential for the retrograde particle movement of intraflagellar transport (IFT). J Cell Biol. 1998 May 18;141(4):979-92.

Pazour GJ, Witman GB. The vertebrate primary cilium is a sensory organelle. Curr Opin Cell Biol. 2003 Feb;15(1):105-10.

Pedersen LB, Geimer S, Sloboda RD, Rosenbaum JL. The Microtubule plus end-tracking protein EB1 is localized to the flagellar tip and basal bodies in *Chlamydomonas reinhardtii*. Curr Biol. 2003 Nov 11;13(22):1969-74.

Pedersen LB, Miller MS, Geimer S, Leitch JM, Rosenbaum JL, Cole DG. *Chlamydomonas* IFT172 is encoded by FLA11, interacts with CrEB1, and regulates IFT at the flagellar tip. Curr Biol. 2005 Feb 8;15(3):262-6.

Piasecki BP, Lavoie M, Tam LW, Lefebvre PA, Silflow CD. The Uni2 Phosphoprotein is a Cell Cycle regulated Component of the Basal Body Maturation Pathway in *Chlamydomonas reinhardtii*. Mol Biol Cell. 2008 Jan;19(1):262-73.

Praetorius HA, Spring KR. Bending the MDCK cell primary cilium increases intracellular calcium. J Membr Biol. 2001 Nov 1;184(1):71-9.

Qin H, Burnette DT, Bae YK, Forscher P, Barr MM, Rosenbaum JL. Intraflagellar transport is required for the vectorial movement of TRPV channels in the ciliary membrane. Curr Biol. 2005 Sep 20;15(18):1695-9.

Qin H, Diener DR, Geimer S, Cole DG, Rosenbaum JL. Intraflagellar transport (IFT) cargo: IFT transports flagellar precursors to the tip and turnover products to the cell body. J Cell Biol. 2004 Jan 19;164(2):255-66.

Quarmby LM, Mahjoub MR. Caught Nek-ing: cilia and centrioles. J Cell Sci. 2005 Nov 15;118(Pt 22):5161-9.

Quarmby LM, Parker JD. Cilia and the cell cycle? J Cell Biol. 2005 Jun 6;169(5):707-10.

Quarmby LM. Cellular deflagellation. Int Rev Cytol. 2004; 233:47-91.

Rieder CL, Jensen CG, Jensen LC. The resorption of primary cilia during mitosis in a vertebrate (PtK1) cell line. J Ultrastruct Res. 1979 Aug;68(2):173-85.

Roberts AM. Mechanisms of gravitaxis in *Chlamydomonas*. Biol Bull. 2006 Apr;210(2):78-80.

Rosenbaum JL, Moulder JE, Ringo DL. Flagellar elongation and shortening in *Chlamydomonas*. The use of cycloheximide and colchicine to study the synthesis and assembly of flagellar proteins. J Cell Biol. 1969 May;41(2):600-19.

Rusan NM, Tulu US, Fagerstrom C, Wadsworth P. Reorganization of the microtubule array in prophase/prometaphase requires cytoplasmic dynein-dependent microtubule transport. J Cell Biol. 2002 Sep 16;158(6):997-1003.

Sager R, Granick S. Nutritional studies with *Chlamydomonas* reinhardi. Ann N Y Acad Sci. 1953 Oct 14;56(5):831-8.

Salisbury JL, Baron AT, Sanders MA. The centrin-based cytoskeleton of *Chlamydomonas reinhardtii*: distribution in interphase and mitotic cells. J Cell Biol. 1988 Aug;107(2):635-41.

Segal RA, Luck DJ. Phosphorylation in isolated Chlamydomonas axonemes: a phosphoprotein may mediate the Ca2+-dependent photophobic response. J Cell Biol. 1985 Nov;101(5 Pt 1):1702-12.

Silflow CD, Lefebvre PA. Assembly and motility of eukaryotic cilia and flagella. Lessons from *Chlamydomonas reinhardtii*. Plant Physiol. 2001 Dec;127(4):1500-7

Simons M, Gloy J, Ganner A, Bullerkotte A, Bashkurov M, Krönig C, Schermer B, Benzing T, Cabello OA, Jenny A, Mlodzik M, Polok B, Driever W, Obara T, Walz G. Inversin, the gene product mutated in nephronophthisis type II, functions as a molecular switch between Wnt signaling pathways. Nat Genet. 2005 May;37(5):537-43.

Singla V, Reiter JF. The primary cilium as the cell's antenna: signaling at a sensory organelle. Science. 2006 Aug 4;313(5787):629-33.

Sjoblad RD, Frederikse PH. Chemotactic responses of *Chlamydomonas reinhardtii*. Mol Cell Biol. 1981 Dec;1(12):1057-60.

Stolc V, Samanta MP, Tongprasit W, Marshall WF. Genome-wide transcriptional analysis of flagellar regeneration in *Chlamydomonas reinhardtii* identifies orthologs of ciliary disease genes. Proc Natl Acad Sci U S A. 2005 Mar 8;102(10):3703-7.

Storm van's Gravesande K, Omran H. Primary ciliary dyskinesia: clinical presentation, diagnosis and genetics. Ann Med. 2005;37(6):439-49.

Tam LW, Wilson NF, Lefebvre PA. A CDK-related kinase regulates the length and assembly of flagella in *Chlamydomonas*.J Cell Biol. 2007 Mar 12;176(6):819-29.

Taulman PD, Haycraft CJ, Balkovetz DF, Yoder BK. Polaris, a protein involved in left-right axis patterning, localizes to basal bodies and cilia. Mol Biol Cell. 2001 Mar;12(3):589-99.

Tsou MF, Stearns T. Controlling centrosome number: licenses and blocks. Curr Opin Cell Biol. 2006 Feb;18(1):74-8.

Tuxhorn J, Daise T, Dentler WL. Regulation of flagellar length in *Chlamydomonas*. Cell Motil Cytoskeleton. 1998;40(2):133-46.

Umen JG, Goodenough UW. Control of cell division by a retinoblastoma protein homolog in *Chlamydomonas*. Genes Dev. 2001 Jul 1;15(13):1652-61.

Umen JG. The elusive sizer. Curr Opin Cell Biol. 2005 Aug;17(4):435-41.

Upadhya P, Birkenmeier EH, Birkenmeier CS, Barker JE. Mutations in a NIMA-related kinase gene, Nek1, cause pleiotropic effects including a progressive polycystic kidney disease in mice. Proc Natl Acad Sci U S A. 2000 Jan 4;97(1):217-21

Vale RD. The molecular motor toolbox for intracellular transport. Cell. 2003 Feb 21;112(4):467-80.

Vallee RB, Stehman SA. How dynein helps the cell find its center: a servomechanical model. Trends Cell Biol. 2005 Jun;15(6):288-94.

Walther Z, Vashishtha M, Hall JL. The *Chlamydomonas* FLA10 gene encodes a novel kinesin-homologous protein. J Cell Biol. 1994 Jul;126(1):175-88.

Wang Q, Pan J, Snell WJ. Intraflagellar transport particles participate directly in cilium-generated signaling in *Chlamydomonas*. Cell. 2006 May 5;125(3):549-62.

Wargo MJ, Smith EF. Asymmetry of the central apparatus defines the location of active microtubule sliding in *Chlamydomonas* flagella. Proc Natl Acad Sci U S A. 2003 Jan 7;100(1):137-42

Weithoff G. Vertical niche separation of two consumers (Rotatoria) in an extreme habitat. Oecologia. 2004 May;139(4):594-603.

Wemmer KA, Marshall WF. Flagellar length control in *Chlamydomonas*--paradigm for organelle size regulation. Int Rev Cytol. 2007;260:175-212.

Wheatley DN. Primary cilia in normal and pathological tissues. Pathobiology 995;63: 222-238.

Wheatley DN, Wang AM, Strugnell GE. Expression of primary cilia in mammalian cells. Cell Biol Int. 1996 Jan;20(1):73-81.

Whitfield JF. The neuronal primary cilium--an extrasynaptic signaling device. Cell Signal. 2004 Jul;16(7):763-7.

Witman GB, Carlson K, Berliner J, Rosenbaum JL. *Chlamydomonas* flagella. I. Isolation and electrophoretic analysis of microtubules, matrix, membranes, and mastigonemes. J Cell Biol. 1972 Sep;54(3):507-39.

Witman GB. *Chlamydomonas* phototaxis. Trends Cell Biol. 1993 Nov;3(11):403-8.

Yamashita YM, Mahowald AP, Perlin JR, Fuller MT. Asymmetric inheritance of mother versus daughter centrosome in stem cell division. Science. 2007 Jan 26;315(5811):518-21.

Yoder BK, Hou X, Guay-Woodford LM. The polycystic kidney disease proteins, polycystin-1, polycystin-2, polaris, and cystin, are co-localized in renal cilia. J Am Soc Nephrol. 2002 Oct;13(10):2508-16.

Yoon, H.S., Hackett, J.D., Cinglia, C., Pinto, G., and Bhattacharya, D. (2004). A molecular timeline for the origin of photosynthetic eukaryotes.

CHAPTER 2
CHLAMYDOMONAS FLA MUTANTS REVEAL A LINK BETWEEN DEFLAGELLATION AND INTRAFLAGELLAR TRANSPORT

Jeremy D.K. Parker and Lynne M. Quarmby

This Chapter published in BMC Cell Biology, August 2003.

2.1 Abstract

Background

Cilia and flagella are often lost in anticipation of mitosis or in response to stress. There are two ways that a cell can lose its flagella: resorption or deflagellation. Deflagellation involves active severing of the axoneme at the base of the flagellum; this process is defective in *Chlamydomonas fa* mutants. In contrast, resorption has been thought to occur passively as a consequence of constitutive disassembly at the tip in the absence of continued assembly, which requires intraflagellar transport (IFT). *Chlamydomonas fla* mutants are unable to build and maintain flagella due to defects in IFT.

Results

fla10 cells, which are defective in kinesin-II, the anterograde IFT motor, resorb their flagella at the restrictive temperature (33^{o}C), as previously reported. We find that in standard media containing ~300μM calcium, *fla10* cells lose flagella by deflagellation at 33^{o}C. This temperature-induced deflagellation of a *fla* mutant is not predicted by the passive disassembly of the IFT-based model for flagellar length control. Other *fla* mutants behave similarly, losing their flagella by deflagellation instead of resorption, if adequate calcium is available. These data suggest a new model whereby flagellar resorption involves active disassembly at the base of the flagellum via a mechanism with components in common with the severing machinery of deflagellation. As predicted by

this model, we discovered that deflagellation stimuli induce resorption if deflagellation is blocked either by mutation in a *FA* gene or by lack of calcium. Further support for this model comes from our discovery that *fla10-fa* double mutants resorb their flagella more slowly than *fla10* mutants.

Conclusions

Deflagellation of the *fla10* mutant at the restrictive temperature is indicative of an active disassembly signal, which can manifest as either resorption or deflagellation. We propose that when IFT is halted by either an inactivating mutation or a cellular signal, active flagellar disassembly is initiated. This active disassembly is distinct from the constitutive disassembly which plays a role in flagellar length control.

2.2 Introduction

Intraflagellar transport (IFT) was first characterized in the unicellular green alga *Chlamydomonas* [1] and has since been shown to be required for flagellar assembly in a variety of systems [2, 3]. IFT is the bidirectional movement of large protein complexes (IFT particles) along the flagellar axoneme, and has anterograde and retrograde components mediated by the plus and minus-end directed microtubule motors kinesin-II and cytoplasmic dynein, respectively [reviewed in 4, 5]. In *Chlamydomonas*, null mutations in genes necessary for activity of either kinesin-II or cytoplasmic dynein result in bald (flagella-less) cells or cells with very short, abnormal flagella [6, 7]. Retrograde IFT is not proposed to be directly involved in disassembly, but rather is necessary to recycle IFT particles [7, 8].

A model for flagellar length control has been proposed wherein anterograde IFT is required for transport of axonemal precursors to the distal tip of the flagellum; these precursors are necessary both for *de novo* flagellar assembly and to offset the constitutive disassembly that occurs at the tips of flagella [8]. This model suggests that the steady-

state length of a flagellum is determined kinetically by the relative contributions of assembly, mediated by anterograde IFT, and disassembly at the tip, which is IFT-independent [9]. Thus, the phenotype of *Chlamydomonas* long flagella mutants could be a result of either an upregulation of anterograde IFT, or due to a decrease in the rate of disassembly at the tip [8, 9, 10].

A *Chlamydomonas* temperature-sensitive mutant for flagellar assembly, *fla10*, has been characterized as having a lesion in a subunit of kinesin-II [11]. *fla10* cells have wild-type flagella at the permissive temperature (20^{o}C), but are bald at the restrictive temperature (33^{o}C) [12]. In agreement with the length control model, *fla10* cells incubated at an intermediate temperature have intermediate-length flagella [8]. It has been accepted that the flagella of *fla10* cells resorb at the restrictive temperature due to continued disassembly in the absence of anterograde IFT [e.g., 13].

Several other temperature-sensitive flagellar assembly mutants (*fla* mutants) are available in *Chlamydomonas* [12, 14, 15]. Unlike *fla10*, the genes for these mutants have not yet been identified. However, like *fla10*, these *fla* mutants have been shown to have defects in IFT, even at the permissive temperature [15, 16]. The majority of the *fla* mutants have been reported to undergo flagellar resorption at 33^{o}C [12, 15, 16], presumably due to defects at different points in the IFT cycle disrupting flagellar assembly. Most *fla* mutants are unable to regenerate flagella at 33^{o}C, with the exception of *fla2* [12]. *fla2* is also exceptional in that it has been observed to deflagellate, rather than resorb, at the restrictive temperature [2, 12, 14].

Deflagellation, like IFT, is a conserved process in eukaryotic cilia and flagella [reviewed in 17]. Deflagellation/deciliation is the regulated severing of the axoneme, and

has been shown to occur in response to a number of stimuli, including pH shock, 42^{o}C heat shock, and treatment with dibucaine or alcian blue. Calcium plays a central role in signalling deflagellation: calcium influx mediates acid shock-induced deflagellation [18], and axonemal severing can be induced *in vitro* in response to calcium [19]. Our lab has cloned two essential components of the deflagellation pathway, the flagellar autotomy genes *fa1* and *fa2* [20, 21]. *fa* mutants do not undergo deflagellation in response to any known stimulus. We have also demonstrated that the microtubule-severing ATPase katanin is likely to mediate axonemal severing during deflagellation [19, 22]. We have localized both katanin and Fa1p to the site of deflagellation, the flagellar transition zone between the basal body and the flagellum proper [20, M. Mahjoub and LMQ, unpublished observations].

In many ciliated cells, including vertebrate cells and *Chlamydomonas*, flagella/cilia are shed or resorbed prior to mitosis [23, 24, 25, 26]. It has been proposed that mammalian primary cilia are important to maintain cells in a differentiated state; the best-characterized example is the role of kidney epithelial cilia in models of polycystic kidney disease [reviewed in 27]. Therefore, as has already been demonstrated for flagellar assembly [3, 27], genes required for flagellar resorption or deflagellation may be implicated in disease and/or development.

It is unknown what determines whether a given cell type deflagellates or resorbs prior to mitosis. Indeed, even in the same organism, flagellar loss may occur via different mechanisms at different stages of the life cycle [23]. Flagellar resorption and deflagellation have been thought to occur by dramatically different mechanisms and at different locations: resorption via disassembly at the tip [8, 13] and deflagellation by

severing at the base [28]. However, a role for severing activity at the base during resorption has been suggested by elegant EM studies performed on cells resorbing their flagella prior to mitosis [29]. We now provide further evidence that flagellar resorption involves severing activity at the base, and that active disassembly by resorption is distinct from the passive constitutive disassembly involved in flagellar length control.

Our examinations of the phenotypes of *fla10* and *fla2*, reported here, lead us to the conclusion that flagellar resorption of *fla* mutants results from active disassembly, rather than passive disassembly in the absence of IFT. We show that in common culture medium for *Chlamydomonas*, the predominant mode of flagellar loss at 33^{o}C for *fla10* is deflagellation. Blocking the ability to deflagellate, either by lowering the extracellular calcium concentration or by genetically blocking the deflagellation pathway, causes *fla10* cells to resorb their flagella at the restrictive temperature. Likewise, we demonstrate that *fla2* cells undergo flagellar loss via deflagellation, and that resorption occurs in low calcium or by genetically introducing a *fa* mutation. Furthermore, *fla10-fa1* and *fla10-fa2* double mutant populations are defective for resorption, as many cells retain flagella past the time when *fla10* mutants are bald. Finally, we find that flagellar resorption can be induced in cells unable to deflagellate in response to deflagellation stimuli. Our findings indicate that the deflagellation and resorption pathways are not separate, but that each can result from a disassembly signal, which culminates at the flagellar transition zone. We propose that IFT and flagellar disassembly share common regulatory elements.

2.3 Methods

Strains

Chlamydomonas reinhardtii mutants *fla2* (CC-1390) and *fla10-1* (CC-1919) were provided by the *Chlamydomonas* Genetics Center. Wild-type strain B214 was provided by Dr. G. Pazour (University of Massachusetts). The *fa1-1* mutant was isolated by R.A. Lewin [42]; the *fa2-1* and *adf1-5* mutants were isolated in our lab [38]. Genetic crosses to obtain the double mutants *fla10-fa1-1*, *fla10-fa2-1*, *fla2-fa1-1,* and *fla2-fa2-1* were performed by standard techniques [30]. All cells were maintained on TAP (Tris-Acetate-Phosphate) media [30] under constant illumination at 20^{o}C.

Since *Chlamydomonas* cells transiently resorb their flagella after resuspension in HEPES buffer (10mM HEPES-KOH, pH 7.2) (with or without added calcium), cultures were incubated overnight in HEPES prior to HEPES experiments. No chelators were used in the preparation of low-calcium HEPES buffer as trace amounts of calcium are required for cell viability over the length of the experiments.

Timecourses and flagella length measurements

Cells were resuspended at 3x10^{6} cells/mL in buffer or media, pre-warmed to the temperature of the incubation, at time zero. We find that the flagellar loss phenotypes of *fla10* are very temperature-sensitive, and a 1^{o}C temperature difference can have a large effect on the kinetics of the experiment; this likely accounts for varying reports on the time required for *fla10* cultures to become bald. Thus, the same culture of cells was used for both +/- calcium at each temperature. Samples were fixed in 2% gluteraldehyde for flagellar length measurements and free flagella determinations. Cells were examined under DIC on an Olympus IX70 microscope (Carsen Group Inc., Ontario, Canada) and lengths of both flagella on at least 70 cells were measured using software provided with

the DeltaVision system (Applied Precision, Seattle, Washington). All experiments were repeated on at least three independent cultures.

2.4 Results and Discussion

***fla10* and *fla2* deflagellate at the restrictive temperature**

Cultures of *fla2* cells in TAP medium contain free flagella after incubation at the restrictive temperature of 33°C. Due to their small size, and tendency to stick to each other and to attached flagella, free flagella are difficult to accurately identify; however, as *fla2* cells can regenerate and re-deflagellate at 33°C, the appearance of abundant free flagella is quite obvious. Our initial observations of the *fla10* temperature-sensitive phenotype led us directly to the conclusion that this mutant also deflagellates, as many free flagella are seen in the presence of calcium at 33°C in both *fla10* and *fla2* cultures (Figure 2-1).

As *fla10* has only been previously characterized as resorbing flagella at 33°C, and given our knowledge of the role played by calcium in the deflagellation pathway, we reasoned that deflagellation would be prevented if *fla10* cells were incubated at 33°C in buffer lacking added calcium. We found this indeed to be the case; there is no indication of deflagellation by *fla10* cells at 33°C in the absence of calcium, yet cultures are still mostly bald after ~6 hours (Figures 2-1, 2-2). We extended our observations by demonstrating that *fla2* cells also do not deflagellate at 33°C in the absence of calcium (Figure 2-1). Adding calcium to minimal buffer to a concentration approximately that of TAP media (340μM) [30] restored the deflagellation phenotype of both *fla* mutants. As a further control, blocking the deflagellation response by creating double mutants of either *fla10* or *fla2* with either of *fa1* or *fa2* also prevented the appearance of free flagella after

six hours (Figure 2-1 and data not shown). Wild-type cells do not deflagellate under these conditions. Furthermore, several other *fla* mutants do deflagellate at 33^{o}C, including *fla1, fla3, fla8, fla15,* and *fla17* (data not shown).

Having examined the culture media under various conditions, we turned our attention to the cells themselves. The average flagellar lengths of *fla10* and *fla2* cells, but not wild-type cells, decrease at 33^{o}C (Figure 2-2). We have shown that the *fla* mutants deflagellate at 33^{o}C in the presence of added calcium, yet the differences in the average flagellar length plots are difficult to discern whether or not calcium was added, especially for *fla10* (diamonds in Figure 2-2A, B). This similarity of the average flagellar length plots holds whether or not zero-length flagella are included in the average length calculations (Figure 2-2C, D).

To better illustrate the effects of calcium at the restrictive temperature on the *fla* mutants, we have chosen a novel means of presenting flagellar length data. By plotting the length of the longer flagellum versus the length of the shorter flagellum for *fla10*, *fla2*, and wild-type cells (Figures 2-3, 2-4, and 2-5, respectively), we can more clearly observe the states of individual cells during timecourses at the restrictive temperature. Points representing bald cells fall at the origin, while points representing uniflagellate cells are found on the x-axis. Additionally, we have plotted the percent of biflagellate, uniflagellate, and bald cells in the population for each timepoint as insets in the scatter plots. This presentation allows one to quickly assess the flagellation state of a population, and changes in that state over time.

Figure 2-3 presents timecourses for *fla10* flagellar lengths at 33^{o}C, in the absence or presence of added calcium. In both populations, cells begin with flagella of

approximately equal lengths, and the distribution of flagellar lengths falls from ~8-11μm. After one hour at the restrictive temperature, flagellar lengths of most cells in calcium remain unchanged, although a few cells now have flagella of unequal lengths. In contrast, the flagella of cells in calcium-free buffer have shortened to 5-10μm (average length of 7.5μm, Figure 2-2C).

After three hours at 33°C, cells in each population have shorter flagella, and there is an increase in the numbers of uniflagellate and bald cells in both populations. At this time in nominally calcium-free buffer, several cells with flagella shorter than 4μm are observed. These short flagella indicate that resorption is occurring. Conversely, in the presence of calcium, no flagella <4μm are seen, suggesting that cells deflagellate before flagellar resorption is complete. *fla10* cells incubated at 20°C did not undergo significant flagellar loss or shortening, and after 6 hours at 20°C, populations resembled zero-hour timepoints (bottom panels in Figure 2-3).

Figure 2-4 is a timecourse for the *fla2* mutant, which was previously reported to deflagellate at the restrictive temperature [2, 12, 14]. After 6 hours in HEPES at 33°C, but not at 20°C, over one-quarter of the *fla2* cells are bald. Fewer cells with flagella >9μm are seen after 6 hours at 33°C compared with earlier timepoints and 20°C controls. At the three hour timepoint in the presence of calcium, there is a dramatic increase in bald cells in the *fla2* population (Figure 2-4, inset). In contrast to *fla10*, *fla2* cells are able to regenerate flagella at the restrictive temperature [12, 14, and data not shown]. This regeneration accounts for the increase in the number of cells with short flagella in the *fla2* population at later timepoints. After overnight incubation at 33°C, *fla2* cultures are often entirely bald.

Figure 2-5 shows the flagellar lengths of wild-type cells after a shift to 33°C. In contrast to the *fla* mutants, wild-type flagella do not undergo appreciable changes in length at 33°C. In principle, the resorption phenotype of *fla10* at 33°C could be solely due to constitutive disassembly in the absence of anterograde IFT, and the deflagellation phenotype a secondary consequence due to the stress of elevated temperature. However, wild-type cells do not deflagellate at 33°C (Figures 2-1, 2-5), although they will deflagellate at 42°C (data not shown).

fla10-fa double mutants are slow to resorb flagella

The deflagellation phenotype of *fla10* and *fla2* at 33°C in calcium is blocked by either *fa* mutation (Figure 2-1 and data not shown). We wished to examine double mutant cell populations, and because *fla2* is able to regenerate flagella at the restrictive temperature, we focused on *fla10-fa* mutants. We find that both *fla10-fa1* and *fla10-fa2* double mutants resorb flagella more slowly than *fla10* at 33°C (Figure 2-6). This held true whether or not calcium was present in the medium, and, as for the *fla10* single mutant, similar flagellar loss kinetics were observed regardless of calcium (Figure 3 and data not shown). This result is reminiscent of the partial block of *fla10* flagellar resorption by six different extragenic suppressors [31]; it is unknown whether any of these suppressors are *fa* genes.

fla10 mutant populations are >90% bald after 6 hours at 33°C (Figures 2-3, 2-6), whereas only ~1/3 of *fla10-fa* cells are bald at this time (Figure 2-6). Moreover, at later timepoints when *fla10* cells are all bald, many double mutant cells still retain flagella. Strikingly, at all timepoints, the double mutant populations are enriched in cells with unequal length flagella as well as uniflagellate cells. Resorbing populations of *fla10* cells

also have a few uniflagellate cells, but cells with unequal length flagella are not often observed (Figure 2-3). Thus, the appearance of cells with flagella of unequal length in double mutant populations correlates with an overall decrease in the resorption rate.

The prevalence of uniflagellate cells, as well as flagella of unequal lengths, is at odds with the classical picture of *Chlamydomonas* long-zero flagellar dynamics [8, 32]. This model predicts that cells with flagella of unequal length should be rarely seen: the combination of length-control kinetics, and the fact that the two flagella share a common pool of precursors, means that any length imbalance between the flagella of a single cell will be corrected [8]. However, long-zero experiments are typically carried out in conditions permissive for flagellar regeneration, which is not the case for *fla10* mutants at the restrictive temperature. In agreement with this, *fla2* cultures contain fewer uniflagellate cells than *fla10* cultures at the restrictive temperature, and this is likely due to the ability of *fla2*, but not *fla10*, to reassemble flagella at the restrictive temperature.

The observation of unequal shortening of flagella in a resorbing population (Figure 2-6) parallels the observation that one flagellum is prone to deflagellate before the other (Figures 2-3, 2-4, 2-6 and data not shown). Loss of one flagellum at a time is not observed in response to a strong deflagellation signal, but is observed after treatment with weaker stimuli such as a mild acid shock (data not shown) or threshold concentrations of alcian blue [33]. The two flagella of *Chlamydomonas* are not equivalent; the *cis* flagellum is defined as the one closest to the eyespot. Rather than the random loss of either flagellum, we hypothesize that the *cis* and *trans* flagella are differentially sensitive to disassembly signals, as they are to motility-related calcium signals [34]. This hypothesis predicts that disassembly will be initiated earlier and/or

proceed more rapidly in one flagellum, which could explain the abundance of unequal length flagella observed in Figure 6.

Resorption is mediated at the transition zone

On the basis of a survey of the modes of flagellar loss in unicellular algae and fungi, Bloodgood divided flagellar loss into several categories [23]. Examples were cited of the same organism (or even the same cell) undergoing flagellar loss sometimes by resorption and sometimes by deflagellation [23]. Rather than supposing that organisms undergo flagellar loss by different mechanisms at different stages of their life cycles, we contend that the mechanism of flagellar loss is conserved, and that subtle variations in signaling leads to the appearance of either deflagellation or various forms of resorption. This conserved mechanism would involve severing of the axoneme at the base of the flagellum.

We now summarize specific experimental data suggesting that resorption is mediated at the transition zone, the site of deflagellation, rather than by constitutive disassembly at flagellar tips. First, *fla10* and *fla2* mutant cells disassemble their flagella at the restrictive temperature via deflagellation in the presence of calcium, and via resorption in the absence of added calcium. Second, *fa* mutants, which are unable to deflagellate, are slow to resorb; this effect would not be predicted if resorption were entirely due to dynamics at flagellar tips. The slow resorption phenotype of *fa1* is especially informative, as this mutant is slow to assemble flagella (JDKP, Ben Montpetit, LMQ, unpublished observations), in which case the length-control theory predicts that *fa1* should be fast to resorb. Third, the slow resorption of *fla10-fa* double mutant cells produces uniflagellate cells in the absence of deflagellation, a consequence not predicted

by the dynamic length control model but in accordance with the results of mild deflagellation treatments. Fourth, while *Chlamydomonas* cells resorb their flagella prior to mitosis [24], EM studies have provided evidence that flagella are detached from basal bodies, but not lost from cells, during pre-mitotic resorption [29]. This seeming contradiction may be explained by our proposal that resorption requires microtubule severing activity at the flagellar transition zone.

There are also some theoretical considerations. Not only the tips of the outer doublet microtubules, but rather the whole axoneme, has been shown to undergo turnover in sea urchin embryos [35]. If this turnover occurs in all eukaryotic flagella, then flagellar tip dynamics alone [8] or lattice translocation models [36] could potentially account for this turnover. However, we believe a regulated ratcheting of the axoneme at the transition zone, coupled with dynamic activity at the tip, provides the most satisfying explanation for the occurrence of axonemal turnover even while a flagellum remains functional. Additionally, there is the consideration that flagellar length in *Chlamydomonas* is cell-cycle dependent, and flagella undergo a period of slow resorption prior to a period of fast resorption preceding cell division [8]. We hypothesize that the slow phase of resorption is mediated by the length-control mechanism, while the fast phase of resorption is mediated by severing of axonemal microtubules in the transition zone.

The flagellar disassembly pathway

The deflagellation phenotype of *fla10* is significant, as it implies an active signalling event is at work. We predicted that if the deflagellation severing complex is responsible for resorption, then providing a deflagellation stimulus to a cell unable to deflagellate

should induce resorption. Indeed, this is consistent with temperature-sensitive resorption of *fla10* in the absence of added calcium, and with temperature-induced resorption of *fla10-fa* double mutants with or without added calcium. To investigate whether this effect is more general, or only due to some special nature of the *fla* phenotype, we examined the effect of pH shock on mutants unable to respond by deflagellation. As previously shown, acid treatment of *fa1*, *fa2*, or *adf1* mutants does not lead to deflagellation as it does for wild-type cells [37, 38]. However, as predicted by our model, these mutants do indeed resorb their flagella within one hour after a 30s acid shock (Figure 2-7). This resorption is not necessarily complete, and is complicated by the tendency of the acid-treated *fa* cells to coil their flagella starting from the distal ends. These coiled flagella get smaller over time, and before disappearing entirely they become dense, stumpy structures. Sanders and Salisbury noted that the *Chlamydomonas* centrin mutant, *vfl-2*, will sometimes resorb rather than deflagellate in response to the deflagellation agent, dibucaine [39]. We have further extended these results by performing deflagellation experiments on wild-type cells in low-calcium buffer. Acid shock, dibucaine treatment, and 42^{o}C heat shock all induce flagellar resorption of wild-type cells in low calcium buffer (data not shown).

We conclude that resorption and deflagellation both may result from a "flagellar disassembly" signal. If the fast phase of flagellar resorption results from disassembly mediated by the severing complex at the transition zone, as we have argued, then a new picture of deflagellation emerges: calcium-mediated hyperactivation of the severing complex following a disassembly signal leads to deflagellation. This model exposes our lack of understanding of the endogenous signaling pathways that lead to flagellar

disassembly. Flagellar disassembly occurring prior to mitosis or meiosis in *Chlamydomonas* must occur via resorption, even in medium containing calcium, as cultures typically contain few free flagella. If agents such as intracellular acidification, dibucaine, and heat shock induce deflagellation by hyperactivation of an endogenous disassembly pathway by causing an increase in intracellular calcium, then why should similar treatments in low calcium cause resorption? Two nonexclusive possibilities present themselves: either the severing apparatus has progressively greater activity at higher calcium thresholds, and has partial activity sufficient to mediate resorption without full calcium activation; or there is a calcium-independent signaling pathway which is induced by treatments such as intracellular acidification.

A candidate for providing such a signal is the IFT pathway. Recent work has suggested that IFT has signaling functions [40], and it has been suggested that these signalling functions are perhaps more important for flagellar assembly than the physical transport of flagellar components [5]. Halting IFT in the presence of calcium induces deflagellation, as we have shown with the IFT mutant *fla10*, in which IFT halts quickly after shift to the restrictive temperature [41]. *fla10* and *fla2* are not the only IFT mutants which deflagellate; we have observed deflagellation at the restrictive temperature for several other *fla* mutants (data not shown). As most *fla* mutants have defects at some point in the IFT cycle at the permissive temperature [16], it is likely that IFT is disrupted in these mutants at the restrictive temperature. As first mentioned anecdotally by Kozminski et al. [41], halting IFT seems to lead to deflagellation.

As IFT is so intimately involved in flagellar assembly, it should not come as a surprise that it may play a role in flagellar disassembly. It is intuitive that a cell should

not attempt to continue building a flagellum at a time when it is actively disassembling a flagellum, and this logic suggests that signalling events that regulate IFT should be related to flagellar disassembly signals. Deflagellation of *fla10* at the restrictive temperature, when anterograde IFT is halted, raises the possibility that functional IFT counteracts a constitutive disassembly signal. This could be adaptive. For example, for cells with damaged flagella, deflagellation would be the favoured disassembly response, due to its speed and ability of *Chlamydomonas* to upregulate genes required for flagellar assembly post-deflagellation. If deflagellation is blocked, flagellar disassembly will instead occur via resorption.

2.5 Conclusion

We find that temperature-sensitive flagellar loss in the *Chlamydomonas* IFT mutants *fla10* and *fla2* is not due to passive resorption at flagellar tips, which plays a crucial role in flagellar length control, but rather due to activation of a disassembly pathway (Figure 8). We also find that flagellar disassembly can occur either by deflagellation or resorption in response to the same stimuli, and that deflagellation is preferred if sufficient calcium is available. Mutants unable to deflagellate are also slow to resorb flagella. We propose that resorption is actively mediated in the transition zone at the base of the flagellum, and that cellular signals that regulate IFT may also regulate flagellar disassembly.

2.6 Acknowledgements

We thank Doug Cole for directing our interest towards *fla2*; Arden Ma for initial analysis of the *fla2* deflagellation phenotype in our lab; Elizabeth Harris and the *Chlamydomonas* Genetics Center for strains; our colleagues at SFU for illuminating discussions; and an anonymous reviewer for several helpful remarks. JDKP thanks Rosemary Redfield for inspiration. This work was funded by the Natural Sciences and Engineering Research Council (NSERC, RGPIN 227132).

2.7 Figures

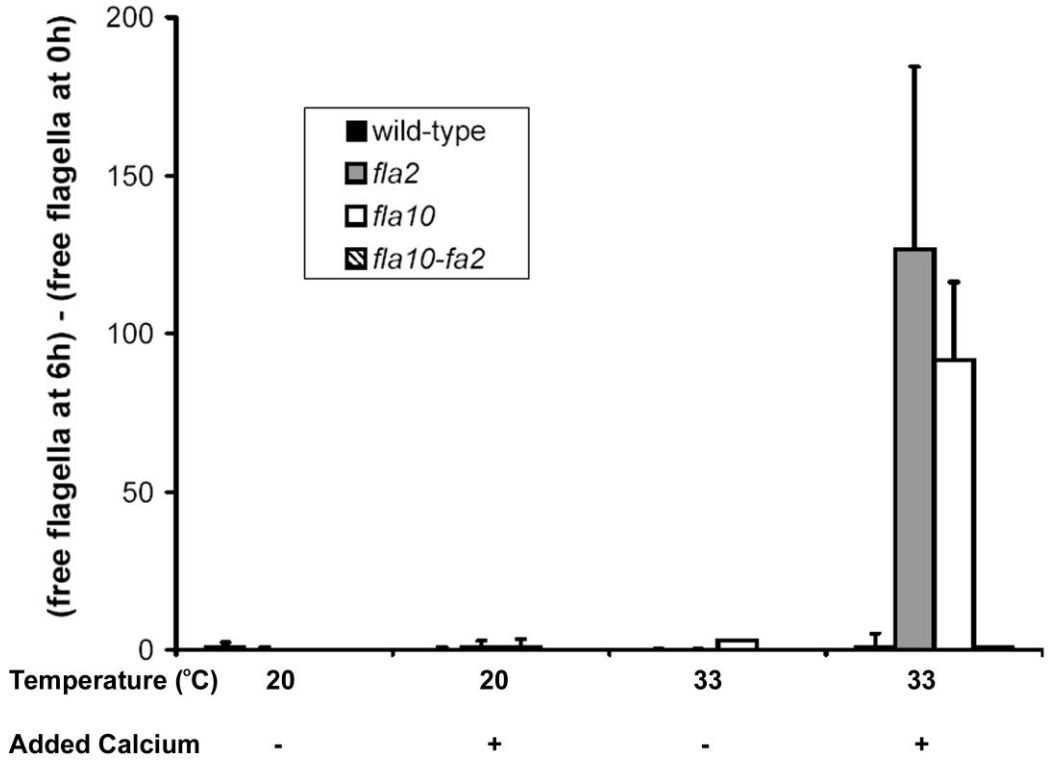

Figure 2-1. Free flagella in *Chlamydomonas* media are indicative of deflagellation.

Determination of free flagella under various conditions. Free flagella observed per 100 cells were counted after 0 and 6 hours at 20°C or 33°C, in either the presence (TAP medium or HEPES+Ca) or absence (HEPES buffer) of calcium, and the difference 6h-0h was calculated. Each data point is the average of at least three experiments on independent cultures.

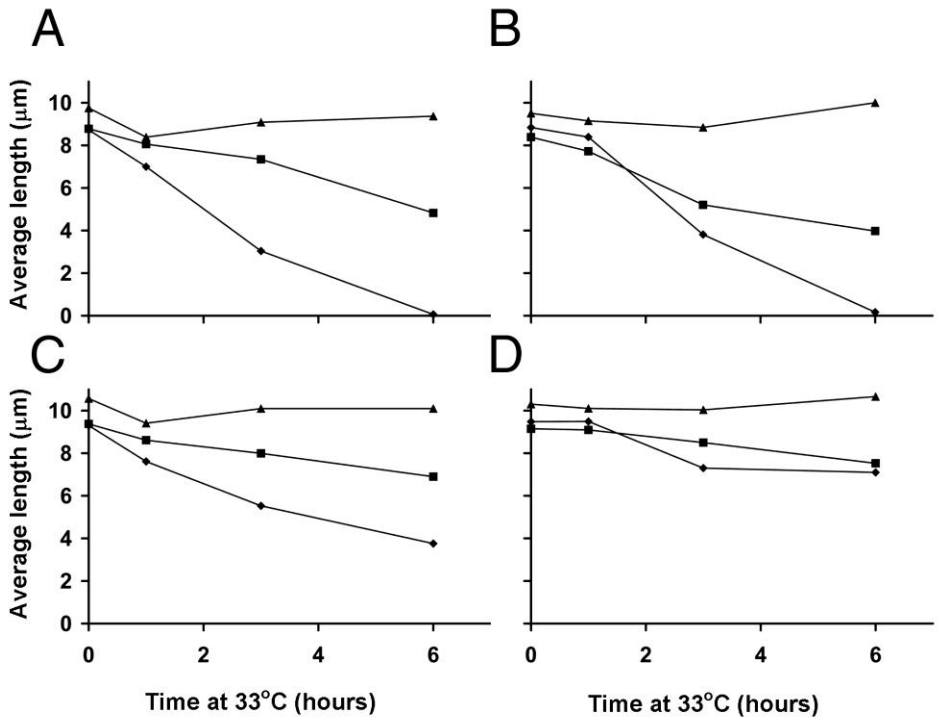

Figure 2-2. *fla10* and *fla2* average flagellar lengths decrease during incubation at 33°C.

Cells were resuspended in pre-warmed buffer at t = 0h. At least 70 cells were examined per timepoint. ▲ wild-type, ■ *fla2*, ♦ *fla10*.

(A) Incubation in HEPES, including contribution of bald and uniflagellate cells.

(B) Incubation in HEPES+Ca, including contribution of bald and uniflagellate cells.

(C) The same samples as (A), but averages exclude contributions of zero-length flagella.

(D) The same samples as (B), but averages exclude contribution of zero-length flagella.

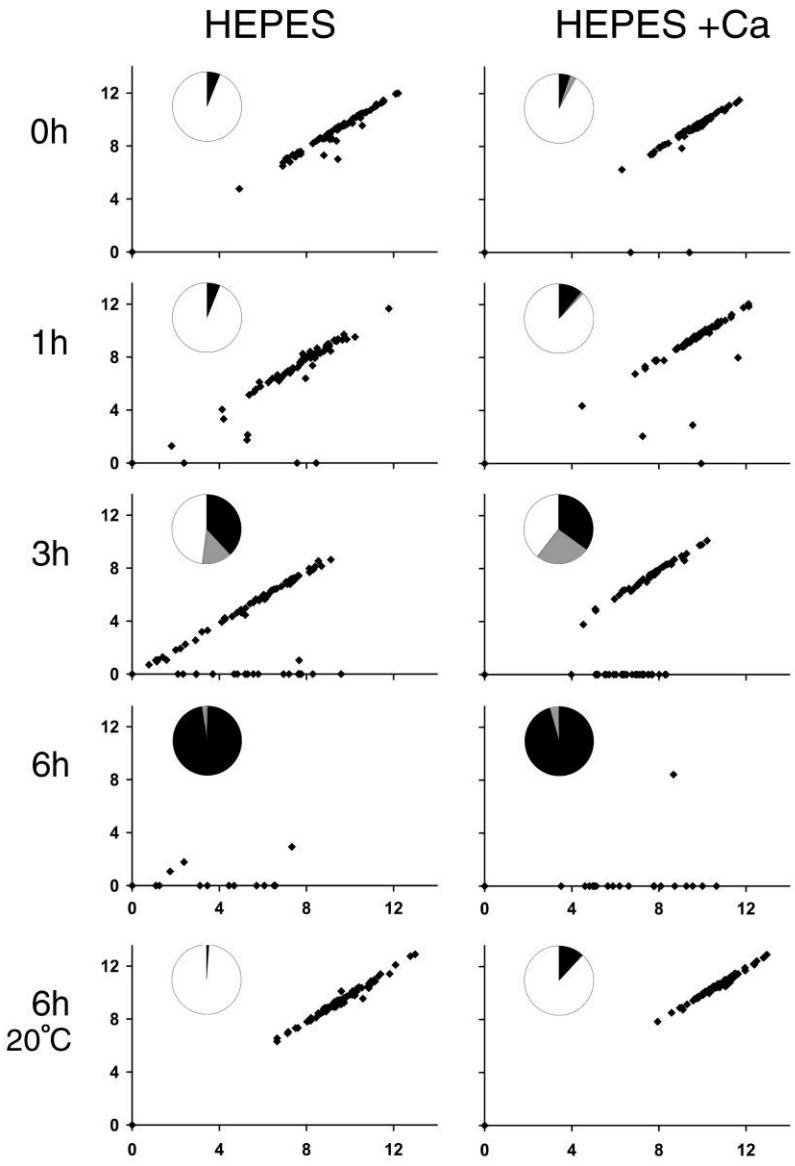

Figure 2-3. Scatter plots of *fla10* timecourses in HEPES and HEPES+Ca.

Data shown is the same as *fla10* data in Figure 2-2. Each flagellum from at least 70 cells was measured, and the lengths plotted as the length of the longer flagellum (in μm) on the X-axis and the length of the shorter flagellum (in μm) on the Y-axis, such that each point in a graph corresponds to a single cell (except where two points overlap, such as at the origin). Insets show the percent of biflagellate (white), uniflagellate (grey), and bald (black) cells in each sample.

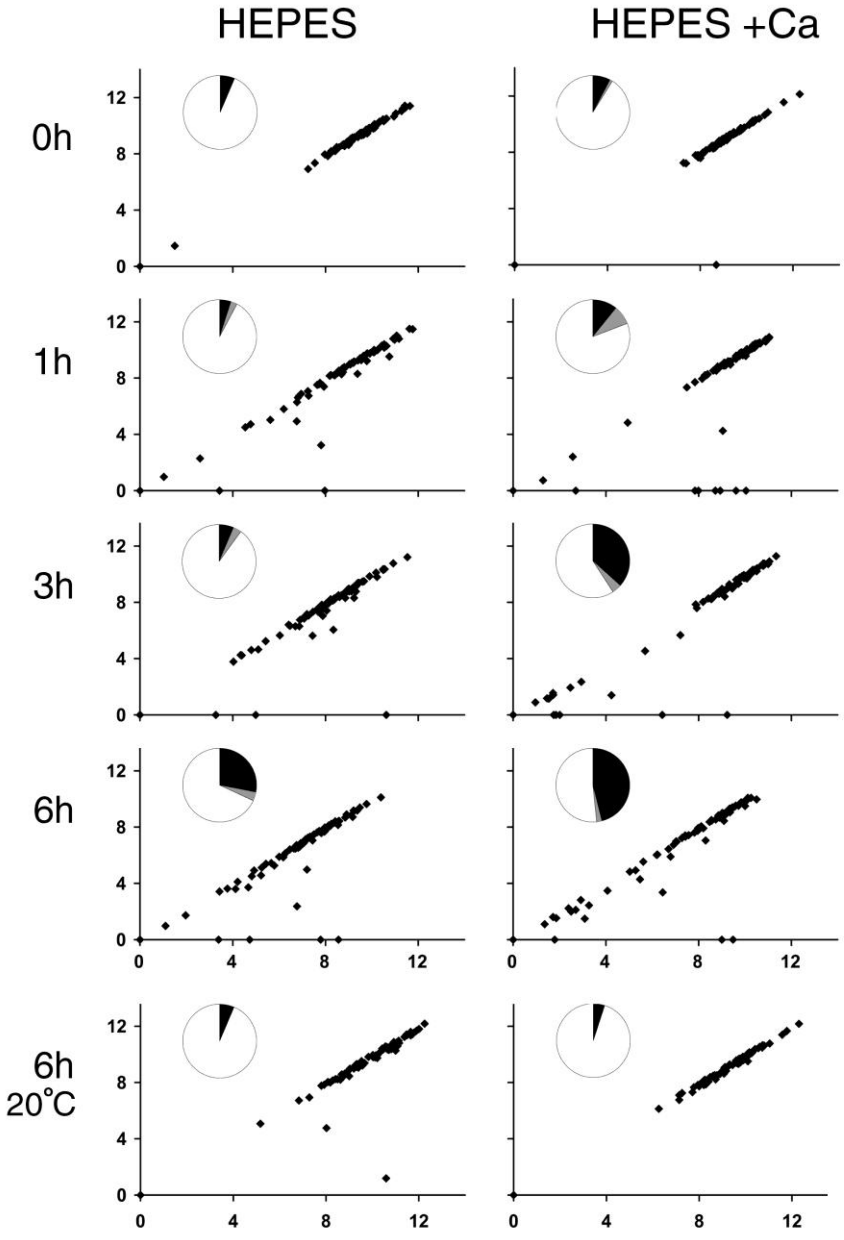

Figure 2-4. Scatter plots of *fla2* timecourses in HEPES and HEPES+Ca.

See Figure 3 legend for further details.

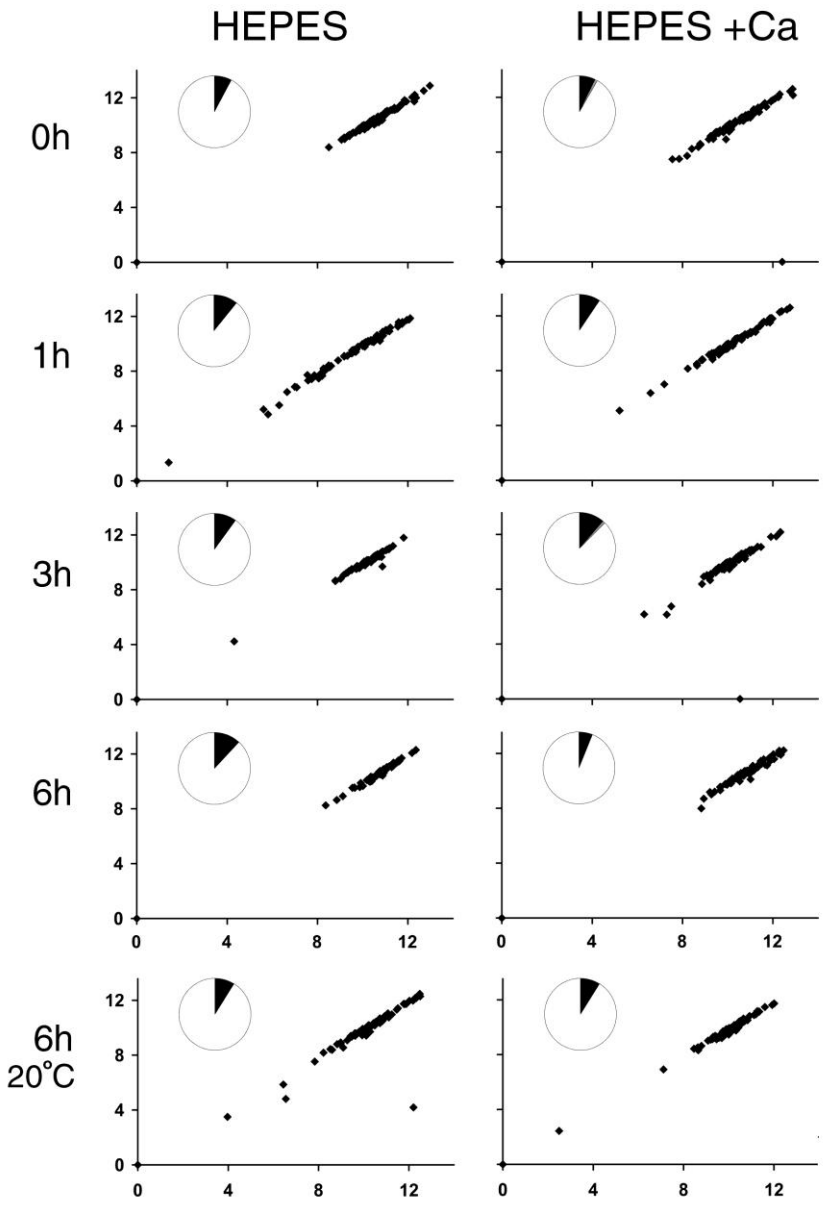

Figure 2-5. Scatter plots of wild-type timecourses in HEPES and HEPES+Ca.
See Figure 3 legend for further details.

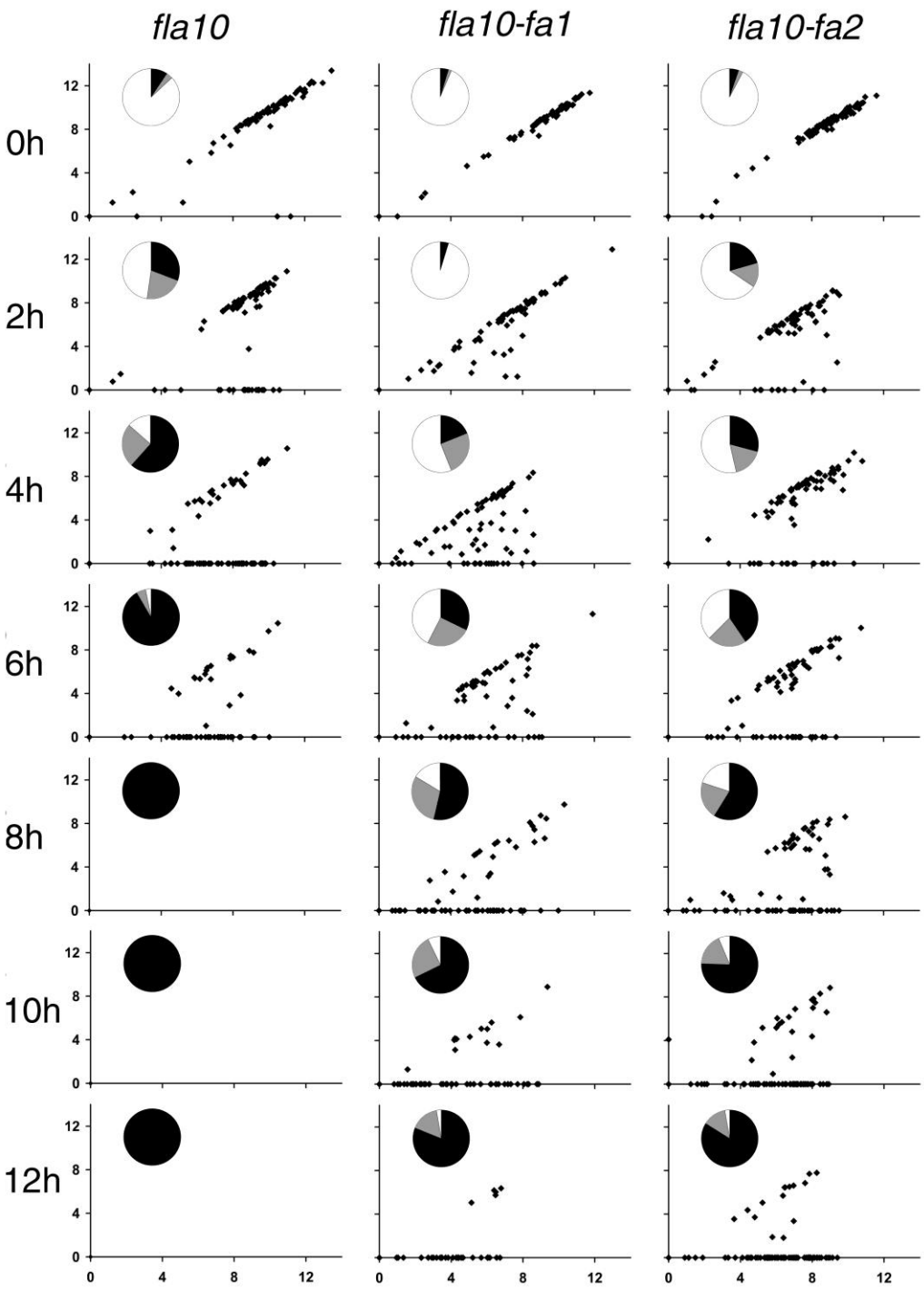

Figure 2-6. Double mutants of *fla10* with *fa1* or *fa2* are slower to disassemble flagella at the restrictive temperature than *fla10* single mutants.

Scatter plots of 33°C timecourses for *fla10*, *fla10-fa1* and *fla10-fa2*; plots prepared as described in the legend to Figure 3. TAP cultures were resuspended in pre-warmed TAP media at t = 0h. No free flagella were seen in *fla10-fa1* or *fla10-fa2* cultures at any timepoint.

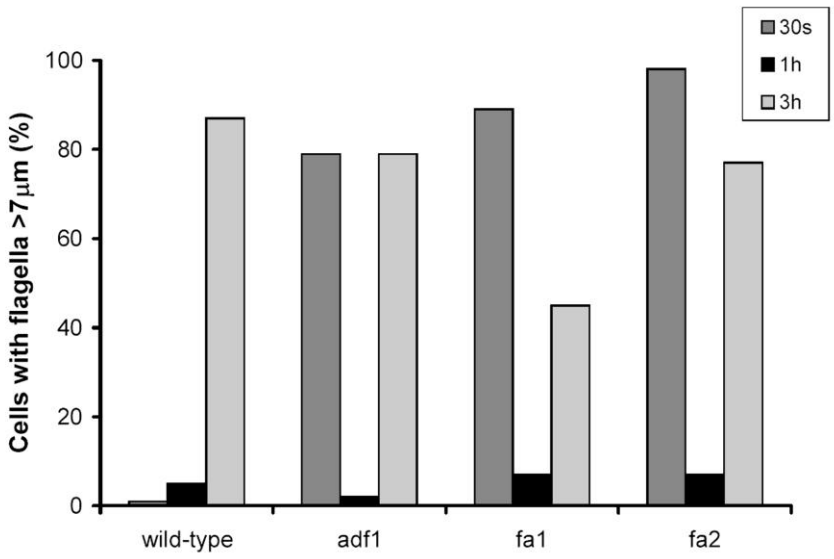

Figure 2-7. Acid shock causes resorption of mutants unable to deflagellate.

At the indicated times post-acid shock, flagellar length distributions were determined and percents of cells with long flagella (flagella longer than 7μm) were plotted.

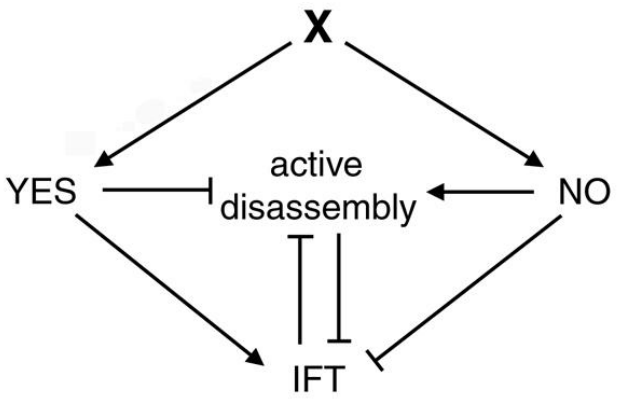

Figure 2-8. Flagella: to have or to have not.

Model for the co-regulation of flagellar assembly (mediated by IFT) and active flagellar disassembly by a common signal, X. Under conditions either permissive or nonpermissive for flagellar assembly, IFT and disassembly are proposed to be mutually antagonistic. Under conditions appropriate for flagellar assembly (Yes), the decision is made to activate IFT and block disassembly at the transition zone. Active IFT could provide a signal to inhibit active disassembly. When flagella are to be disassembled (No), IFT is inactivated. In the absence of IFT, an inhibitory signal would be removed, allowing disassembly to proceed. There may also be direct activation of disassembly.

2.8 References

1. Kozminski KG, Johnson KA, Forscher P, Rosenbaum JL: **A motility in the eukaryotic flagellum unrelated to flagellar beating.** *Proc Natl Acad Sci USA* 1993 **90:**5519-5523.

2. Cole DG, Diener DR, Himelblau AL, Beech PL, Fuster JC, Rosenbaum JL: ***Chlamydomonas* kinesin-II-dependent intraflagellar transport (IFT): IFT particles contain proteins required for ciliary assembly in *Caenorhabditis elegans* sensory neurons.** *J Cell Biol* 1998 **141:**993-1008.

3. Pazour GJ, Dickert BL, Vucica Y, Seeley ES, Rosenbaum JL, Witman GB, Cole DG: ***Chlamydomonas* IFT88 and its mouse homologue polycystic kidney disease gene tg737 are required for assembly of cilia and flagella.** *J Cell Biol* 2000, **151:**709-718.

4. Rosenbaum JL, Witman GB: **Intraflagellar transport.** *Nat Rev Mol Cell Biol* 2002 **3:**813-825.

5. Cole DG: **The intraflagellar transport machinery of *Chlamydomonas reinhardtii*.** *Traffic* 2003 **4:**435-442.

6. Matsuura K, Lefebvre PA, Kamiya R, Hirono M: **Kinesis-II is not essential for mitosis and cell growth in *Chlamydomonas*.** *Cell Motil Cytoskel* 2002 **52:**195-201.

7. Pazour GJ, Wilkerson CG, Witman GB: **A dynein light chain is essential for the retrograde particle movement of intraflagellar transport (IFT).** *J Cell Biol* 1998, **141:**979-992.

8. Marshall WF, Rosenbaum JL: **Intraflagellar transport balances continuous turnover of outer doublet microtubules: implications for flagellar length control.** *J Cell Biol* 2001 **155:**405-414.

9. Marshall WF: **Size control in dynamic organelles.** *Trends Cell Biol* 2002 **12:**414-419.

10. Berman SA, Wilson NF, Haas NA, Lefebvre, PA: **A novel MAP kinase regulates flagellar length in *Chlamydomonas*.** *Curr Biol* 2003 **13:**1145-1149.

11. Vashishtha M, Walther Z, Hall JL: **The kinesin-homologous protein encoded by the *Chlamydomonas* FLA10 gene is associated with basal bodies and centrioles.** *J Cell Biol* 1994, **126:**175-188.

12. Adams GMW, Huang B, Luck DJL: **Temperature-sensitive assembly-defective flagella mutants of *Chlamydomonas reinhardtii*.** *Genetics* 1982 **100:**579-586.

13. Vale RD: **The molecular motor toolbox for intracellular transport.** *Cell* 2003 **112:**467-480.

14. Huang B, Rifkin MR, Luck DJL: **Temperature-sensitive mutations affecting flagellar assembly and function in *Chlamydomonas reinhardtii*.** *J Cell Biol* 1977 **72:**67-85.

15. Piperno G, Siuda E, Henderson S, Segil M, Vaananen H, Sassaroli M: **Distinct mutants of retrograde intraflagellar transport (IFT) share similar morphological and molecular defects.** *J Cell Biol* 1998 **143:**1591-601.

16. Iomini C, Babaev-Khaimov V, Sassaroli M, Piperno G: **Protein particles in *Chlamydomonas* flagella undergo a transport cycle consisting of four phases.** *J Cell Biol* 2001 **153:**13-24.

17. Quarmby LM: **Cellular deflagellation.** *Int Rev Cytology* 2004 **233**:47-91

18. Quarmby LM: **Ca^{2+} influx activated by low pH in *Chlamydomonas*.** *J Gen Physiol* 1996 **108:**351-361

19. Lohret TA, McNally FJ, Quarmby LM: **A role for katanin-mediated axonemal severing during *Chlamydomonas* deflagellation.** *Mol Biol Cell* 1998 **9:**1195-1207.

20. Finst RJ, Kim PJ, Griffis ER, Quarmby LM: **Fa1p is a 171 kDa protein essential for axonemal microtubule severing in *Chlamydomonas*.** *J Cell Sci* 2000 **113:**1963-1971.

21. Mahjoub MR, Montpetit B, Zhao L, Finst RJ, Goh B, Kim AC, Quarmby LM: **The *FA2* gene of *Chlamydomonas* encodes a NIMA family kinase with roles in cell cycle progression and microtubule severing during deflagellation**. *J Cell Sci* 2002 **115:**1759-1768.

22. Lohret TA, Zhao L, Quarmby LM: **Cloning of the *Chlamydomonas* p60 katanin and localization to the site of outer doublet severing during deflagellation.** *Cell Motil Cytoskel* 1999 **43:**221-231.

23. Bloodgood RA: **Resorption of organelles containing microtubules.** *Cytobios* 1974 **9:**143-161.

24. Cavalier-Smith T: **Basal body and flagellar development during the vegetative cell cycle and the sexual cycle of *Chlamydomonas reinhardii*.** *J Cell Sci* 1974 **16:**529-556.

25. Rieder CL, Jensen CG, Jensen LCW: **The resorption of primary cilia during mitosis in a vertebrate (PtK_1) cell line.** *J Ultrastr Res* 1979 **68:** 173-185.

26. Tucker RW, Pardee AB: **Centriole ciliation is related to quiescence and DNA synthesis in 3T3 cells.** *Cell* 1979 **17:**527-535.

27. Pazour GJ, Witman GB: **The vertebrate primary cilium is a sensory organelle.** *Curr Opin Cell Biol* 2003 **15:**105-10.

28. Lewin RA, Lee KW: **Autotomy of algal flagella: electron microscope studies of Chlamydomonsa (Chlorophyceae) and Tetraselmis (Prasinophyceae).** *Phycologia* 1985 **24:**311-316.

29. Johnson UG, KR Porter: **Fine structure of cell division in *Chlamydomonas reinhardi* basal bodies and microtubules.** *J Cell Biol* 1968 **38:**403-425.

30. Harris EH: *The* Chlamydomonas *Sourcebook*. Berkeley: Academic Press; 1989.

31. Lux FG 3rd, Dutcher SK: **Genetic interactions at the *FLA10* locus: suppressors and synthetic phenotypes that affect the cell cycle and flagellar function in *Chlamydomonas reinhardtii.*** *Genetics* 1991 **128:**549-561.

32. Rosenbaum JL, Moulder JE, Ringo DL: **Flagellar elongation and shortening in *Chlamydomonas.*** *J Cell Biol* 1969 **41:**600-619.

33. Evans JH, Keller LR: **Receptor-mediated calcium influx in *Chlamydomonas reinhardtii*.** *J Euk Microbiol* 1997 **44:**237-245.

34. Kamiya R, Witman GB: **Submicromolar levels of calcium control the balance of beating between the two flagella in demembranated models of *Chlamydomonas*.** *J Cell Biol* **98:**97-107.

35. Stephens RE: **Synthesis and turnover of embryonic sea urchin ciliary proteins during selective inhibition of tubulin synthesis and assembly.** *Mol Biol Cell* 1997 **8:**2187-2198.

36. Stephens RE: **Preferential incorporation of tubulin into the junctional region of ciliary outer doublet microtubules: a model for treadmilling by lattice dislocation.** *Cell Motil Cytoskel* 2000 **47:**130-140.

37. Quarmby LM, Hartzell HC: **Two distinct calcium-mediated signal transduction pathways can trigger deflagellation in *Chlamydomonas reinhardtii*.** *J Cell Biol* 1994 **124:**807-15.

38. Finst RJ, Kim PJ, Quarmby LM: **Genetics of the deflagellation pathway in *Chlamydomonas.*** *Genetics* 1998 **149:**927-936.

39. Sanders MA, Salisbury JL: **Centrin plays an essential role in microtubule severing during flagellar excision in *Chlamydomonas reinhardtii*.** *J Cell Biol* 1994 **124:**795-805.

40. Pan J, Snell WJ: **Kinesin-II is required for flagellar sensory transduction during fertilization in *Chlamydomonas*.** *Mol Biol Cell* 2002 **13:**1417-26.

41. Kozminski KG, Beech PL, Rosenbaum JL: **The *Chlamydomonas* kinesin-like protein FLA10 is involved in motility associated with the flagellar membrane.** *J Cell Biol* 1995 **131:**1517-1527.

42. Lewin RA, Burrascano C: **Another new kind of *Chlamydomonas* mutant, with impaired flagellar autotomy.** *Experimentia* 1983 **39:**1397-1398.

CHAPTER 3
PHYLOGENETIC ANALYSIS OF THE NEKS REVEALS EARLY DIVERSIFICATION OF CILIARY-CELL CYCLE KINASES

The following chapter was published Oct. 24, 2007 in Public Library of Science ONE.

J.D.K. Parker*, B.A. Bradley*, A.O. Mooers and L.M. Quarmby
*equal contribution

Author Contributions: Conceived and designed the experiments: JP, BB. Performed the experiments: JP (assembled lists of kinase domains from BLAST results, did majority of Bayesian computer/cluster work), BB (performed BLAST analysis, did alignments, and set up constraint analyses). Analyzed the data: JP (researched species, determined clades), BB (assisted JP). Wrote the paper: JP. Other: Provided expertise for the design and analysis of the experiments: AM. Conceived the project: LQ. Contributed to data analysis: LQ. Contributed to writing of the paper: LQ.

3.1 Abstract

Background

NIMA-related kinases (Neks) have been studied in diverse eukaryotes, including the fungus *Aspergillus* and the ciliate *Tetrahymena*. In the former, a single Nek plays an essential role in cell cycle regulation; in the latter, which has more than 30 Neks in its genome, multiple Neks regulate ciliary length. Mammalian genomes encode an intermediate number of Neks, several of which are reported to play roles in cell cycle regulation and/or localize to centrosomes. Previously, we reported that organisms with cilia typically have more Neks than organisms without cilia, but were unable to establish the evolutionary history of the gene family.

Methodology/Principle Findings

We have performed a large-scale analysis of the Nek family using Bayesian techniques, including tests of alternate topologies. We find that the Nek family had already expanded in the last common ancestor of eukaryotes, a ciliated cell that likely expressed at least five Neks. We suggest that Neks played an important role in the common ancestor in regulating cilia, centrioles, and centrosomes with respect to mitotic entry, and that this role continues today in organisms with cilia. Organisms that lack cilia generally show a reduction in the number of Nek clades represented, sometimes associated with lineage specific expansion of a single clade, as occurred in the plants.

Conclusion/Significance

This is the first rigorous phylogenetic analysis of a kinase family across a broad array of phyla. Our findings provide a coherent framework for the study of Neks and their roles in coordinating cilia and cell cycle progression.

3.2 Introduction

The NIMA-related family of serine/threonine kinases (Neks) are widespread among eukaryotes. They are defined by similarity in their N-terminal catalytic domains to the founding member, Never In Mitosis A from the fungus *Aspergillus* [1,2]. NIMA, the sole Nek in the *Aspergillus* genome, plays multiple roles in cell cycle progression and localizes to the fungal equivalent of the centrosome, the spindle pole body [1,3]. There are 11 NIMA-related kinase (Nek) genes in the human genome. Those that have been studied appear to have cell cycle-related functions and some localize to centrosomes [4-11].

Centrosomes are typically located near the nucleus in the centre of the cell, where they serve as organizers of the microtubular cytoskeleton during both interphase and mitosis [12]. In addition to their well-established role as microtubule organizers, centrosomes serve as important scaffolds for the integration of multiple signaling pathways that coordinate cell cycle progression [13]. Of the centrosomal Neks, only for Nek2 has a function been clearly defined. Nek2 phosphorylates proteins which physically link centrioles, the microtubule-based structures at the core of centrosomes [14-16]. In mammalian cells, the elder centriole of the centrosomal pair often directly nucleates a cilium. Cilia have functions in both motility and sensory signaling [17]. The recent demonstration that flies without centrioles develop normally but then die due to multiple sensory defects [18] suggests that the most important function of centrioles may be to nucleate sensory cilia, at least in some lineages. An indication of the ciliary function of some Neks derives from their association with polycystic kidney diseases, which are caused by defective ciliary signaling [19]: The causative mutations in two mouse models of polycystic kidney diseases are in the mNek1 and mNek8 genes [20,21]. We have shown that Nek8 is ciliary [11] and mutations that affect ciliary localization are associated with a rare form of a cystic kidney disease that affects children, Nephronophthisis type 9 [22]. Although the functions of Neks in mammalian cilia are unknown, it has been established that Neks in *Chlamydomonas* and *Tetrahymena* regulate ciliary length and/or disassembly [23-26]. We have previously noted a correlation between the number of Neks a eukaryotic organism expresses, and the presence of ciliated cells which re-enter the cell cycle in that organism [2]. Together, these

observations have led us to propose that Neks evolved with centrosomes and serve to coordinate ciliary and cell cycle functions [2,27].

The breadth of organisms in which Neks are found and the lack of sequence conservation outside the kinase domains has meant no large-scale phylogenetic analysis has been possible via traditional methods. Many authors refer to NIMA as "ancestral" to the mammalian Neks, yet no eukaryotic phylogeny would ever place *Aspergillus* as an ancestor to mammals. The assumption by these authors is that the last common ancestor of Fungi and Metazoa had one Nek, similar to NIMA, and this gene underwent an expansion in Metazoa and especially in mammals. This conflicts with previously published phylogenies [26,28] which suggest that there are orthologies between mammalian Neks and Neks in both *Chlamydomonas* and *Tetrahymena*. However, these earlier Nek phylogenies had few taxa and poor support at many nodes. We set out to establish a more complete Nek family tree, from distantly-related phyla, and by using Bayesian methods, including hypothesis testing. To our knowledge, no similar analyses have been published for a eukaryotic kinase family. Our results suggest that the last common ancestor of the eukaryotes, which must have been a ciliated cell able to divide [29], had at least five Neks. This finding and new cell biological data further strengthen the three-way bond between Neks, cilia/centrosomes, and the cell cycle.

3.3 Materials and Methods

Species from a broad range of eukaryotic lineages, with publicly available sequenced genomes, were selected for analysis (Figure 3-1). We generated a dataset of Nek kinase domains from these species via the following methods: with the NIMA kinase domain as a query sequence, we used BLASTP analysis [30] to identify Neks from the predicted

proteomes, using their publicly-available genomes. Top scoring BLASTP hits from the predicted proteomes were reciprocally used as queries of the non-redundant NCBI GenBank database. Only those queries that produced Nek proteins as top scoring BLASTP hits were retained in the dataset. Only kinase domains, as predicted by the SMART HMMER search tool [31,32] were included in our phylogenetic analysis, leading us to exclude the predicted human Nek10 (GenBank id NP_001026911), amongst other weak hits from various other organisms. Multiple sequence alignments were produced using ClustalX software [33] and manually inspected. Any kinase domain sequences containing large insertions or truncated kinase domains, likely the result of incorrect protein prediction, were excluded from the dataset at this stage. Our master list of kinase domains is available as supplemental data.

In the course of our BLAST searching, we found some prokaryotic kinases that were reciprocal best hits with Neks. However, these sequences do not represent *bona fide* Neks, as they are outgroup to a clade containing multiple eukaryotic kinase families (not shown).

We used the Metropolis-coupled Markov chain Monte Carlo program MrBayes v. 3.1.2 [34,35] to infer phylogenies. We allowed the program to determine the most probable model of protein evolution (aamodel), and specified an inverse gamma distribution of variability in substitution rate. Each analysis was composed of two simultaneous runs of either four or eight MCMC chains run for at least $2x10^6$ generations, sampled every 100 generations, and run until the average standard deviation of split frequencies between the two runs remained below the 0.01 convergence threshold for at least 1×10^5 generations. Ninety percent of each run was burned in before the

parameters were analyzed. Human Cdk2 was used to root all trees in either Treeview [36] or HyperTree [37]. HsCdk2 was selected as the outgroup because on a tree including Cdk2, Mlk3, Aurora A, Plk1 and the mammalian Neks, Cdk2 was the kinase most closely related to the Neks (data not shown). See Table 3-2 for detailed tree statistics.

To test hypotheses on the unikonts plus *Chlamydomonas* dataset we first analyzed the unconstrained dataset and obtained a harmonic mean of the log likelihood values of the MCMC samples (Table 3-1). We then re-ran the analysis, constraining the topology to reflect various hypotheses (for example, constraining nodes or pairs of nodes, Table 3.1), and recorded the harmonic mean of log likelihood values. Twice the difference in mean harmonic likelihood (known as the Bayes Factor) can be used to determine relative support for alternative hypotheses; values for the Bayes Factors of >10 indicate strong support for the less constrained tree over the *a priori* imposed constraint (i.e. the hypothesis). [38,39]. Analyses were otherwise run as described above. Constraining the amino acid model did not affect either the topology or likelihood of the resulting tree (Table 3.1).

3.4 Results

We use the terminology of Cavalier-Smith [29] to refer to the major eukaryotic lineages: unikonts include Metazoa, Fungi, and Amoebozoa, while bikonts include all other organisms considered. We found Neks from a broad sampling of eukaryotic lineages (Figure 3-1), but we identified no Neks in the genomes of the diatom *Thalassiosira* or the green alga *Ostreococcus*.

Large numbers of Neks were found in the genomes of the kinetoplastids *Leishmania* and *Trypanosoma*, as well in the genome of *Giardia* (Figure 3-1). Inclusion

of sequences from either the kinetoplastids or *Giardia* in our analyses lead to failure of convergence, so we excluded these species from further analysis. We note that these species are parasitic, and recent analyses consider them to be highly derived, rather than basal, eukaryotes [40]. This, in combination with their large number of Nek sequences, accounts for the difficulty in resolving Nek trees including these organisms. However, our analysis indicates that most of the kinetoplastid Neks form a lineage-specific expansion in a clade with human Nek8 (data not shown). Our SMART analysis showed that with rare exceptions (all of which are in *Tetrahymena*) all sequences recognized as having a Nek-like kinase domain had that domain at the N-terminus of the predicted protein; when C-terminal domains were predicted by SMART, these were always protein-protein interaction domains. These results are consistent with the view that Neks have rapidly evolving C-terminal regulatory/interaction domains, allowing differential localization, regulation, or function in various lineages.

A dataset consisting of the unikont Neks plus the *Chlamydomonas* Neks was the largest dataset we could analyze in a reasonable time (~1 week on a desktop computer), while inclusion of the bikont Neks to produce the tree in Figure 3-3 required much more analysis time (~3 months) on a computer cluster using the equivalent of eighteen desktop processors. Due to these computational limitations, we performed stringent analyses by Bayesian testing of alternate topologies on the former dataset, represented in Figure 3-2 and Table 3-1 (see below).

The topology of the tree in Figure 3-2 is consistent with previous studies (e.g. [41]), but the inclusion of several additional species in our tree allows us to differentiate more clearly orthology and paralogy. For example, analysis of the unikont Neks (Figure

3-2) suggests that hNek2 is indeed the NIMA orthologue, based on the observations that the nodes connecting these taxa are strongly supported (posterior probability typically ~1), contain sequences from all the unikont taxa included, including distantly related taxa such as humans and yeast. Consequently, we refer to this group of sequences as the Nek2 clade. Similarly, we note that the human Neks are scattered among six *a posteriori*-defined clades, each of which contains representatives from most species tested and most of which have well-supported nodes (posterior probability >0.85, Figure 3-2). Importantly, the above statement is valid despite the inclusion of *Chlamydomonas*; that is, most *Chlamydomonas* Neks fall into the same well-supported clades as the Neks of the unikont species included in this analysis.

Four of the ten *Chlamydomonas* Neks are not members of any clades in Figure 3.2. In order to test whether this was a *bona fide* result, we tested various alternative hypotheses for the topology. We constrained Cnk1p and Cnk2p (node **5** in Figure 3-2) to be sister to the Nek2 clade (node **1** in Figure 3-2), and calculated the resulting Bayes Factor (Table 3.1, "node 5 + node 1"). The Bayes Factor of 42 strongly rejects a composite Cnk2/Nek2 clade in favour of the topology seen in Figure 3-2. As controls, we repeated this analysis to test alternate topologies for the *Chlamydomonas* sequences that fell within well-supported clades in Figure 3-2. Reassuringly, the topology reported in Figure 3-2 was not rejected for any of these hypotheses, including Cnk10p membership in the same clade as vertebrate Nek1 (Table 3-1). We repeated this experiment for less well-supported nodes, e.g., the Nek4 and Nek11 clades. Cnk5p and Cnk8p are sister to unikont Nek4's with a posterior probability of only 0.54, but could not be rejected as members of the Nek4 clade by Bayes Factor Analysis (BF = 7.04); a

similar result was obtained indicating that Cnk9p is a tentative member of the Nek11 clade.

In only three instances did Bayes Factor analysis reveal a lack of support for the tree reported in Figure 3-2: the *Dictyostelium* DDB0229345 sequence was rejected from the Fa2p/Cnk4p clade, the *C.elegans* sequence D1044.8 was rejected from the Nek2 clade, and the Cnk2p/Cnk1p and Fa2p/Cnk4p clades cannot be distinguished as independent clades (Table 3.1). In summary, the analyses presented in Figure 3-2 and Table 3-1 indicate at least five *bona fide* Nek clades with members from both the mammal *Homo* and the green alga *Chlamydomonas*, plus two additional clades, the *Chlamydomonas*-specific Fa2p/Cnk2p clade, and the unikont-specific Nek2 clade.

Addition of Nek sequences from other bikonts, as well as the (unikont) chytrid fungus *Batrachochytrium* to the data set used to generate Figure 3-2 did not significantly affect the topology of the tree (Figure 3-3). Several of the newly added sequences arise in the tree as polytomies, a result consistent with the difficulties inherent in constructing a multigene phylogeny across a broad sampling of eukaryotes. However, with the exception of the Nek1/3/5 clade, but including the Nek2 and Cnk2p/Fa2p clades, our previously defined clades now include sequences from distantly related species such as *Arabidopsis, Naegleria*, and *Tetrahymena* (Figures 3-4 to 3-7). The previously unikont-only Nek2 clade has members from *Tetrahymena*, while two apicocomplexan sequences (Cp cgd1 1490 and Pf Nek1) branch near the well-supported Nek2 clade (Figure 3-4). The Nek6/7 clade is well supported, and like the Nek2 clade, now contains sequences from *Tetrahymena* and *Batrachochytrium* (Figure 3-5). Satisfyingly, Cnk2p and Fa2p now form a clade with several *Tetrahymena* Neks (consistent with Wloga et al. [26]), as

well as a *Naegleria* Nek (Figure 3-5). Similarly, the Nek8/9 clade remains intact (Figure 3-6), and now contains *Naegleria* "Nek2", which has a similar C-terminal domain composition to its orthologue in *Chlamydomonas*, Cnk3p (not shown).

The Nek1/3/5 clade did not resolve with sequences from both unikonts and bikonts (Figure 3.6). However, a tree from a smaller dataset shows that *Chlamydomonas* Cnk10p, *Tetrahymena* Nrk29 and *Cryptosporidium* cgd7 3760 are members of a well-supported Nek1/3/5 clade (posterior probability of 0.94, data not shown). This suggests that some of the clades arising from the polytomy could be orthologous to members of the unikont Nek1/3/5 clade. Above, we provided additional evidence that Cnk10p is a Nek1/3/5 family member (Figure 3-2, Table 3-1, Figure 3-8, Figure 3-9). Unfortunately, tests of hypotheses on this larger dataset are not feasible with our current methods and available computational power.

Consistent with our previous results (Figure 3-2 and Table 3-1), the Nek4 and Nek11 clades are closely related to each other and thus difficult to resolve (Figure 3-7). We note that human Nek11 (a protein localized to the nucleolus [9]) and the higher plant Neks are all in the Nek11 clade, consistent with the hypothesis that a non-centrosomal Nek family expanded in a lineage which does not have centrosomes; however, these Neks still play roles in cell cycle regulation [42,43]. In contrast, we find *Tetrahymena* Nrk30p, which localizes to cilia [26], to be in the Nek4 clade (Figure 3-7). We therefore hypothesize that in contrast to the Nek11 clade, members of the Nek4 group may retain ciliary function.

Neks were found in nearly every genome sampled, and the numbers of Neks we identified roughly correlates with whether the organism has non-terminally differentiated

ciliated cells (Figure 3-1). We included both the raw number of Neks found in the organisms' genomes, and the minimal number of Nek subfamilies represented, to further clarify the Nek/cilia relationship. We define our Nek subfamilies as moderately well supported clades (posterior probability >0.85) with members from both unikont and bikont species. The Nek2, Nek6/7, Nek8/9, and Nek11 clades meet this definition (Figures 3-4 to 3-7). As discussed above, the Nek1/3/5 clade is well supported in Figure 3-9. Also, the Nek 11 clade in Figure 3-7 meets our definition, but the Nek4 clade does not; however, a composite Nek4/11 clade is well-supported in our smaller dataset (Figure 3.9). Thus, we define five Nek subfamilies, named after their human members: Nek1/3/5, Nek2, Nek4/11, Nek6/7, and Nek8/9. Our analysis thus allows identification of lineage-specific expansions, for example, the plant *Arabidopsis* has seven Neks in its genome, but all seven are part of an expansion in the same Nek subfamily (Figure 3-3). Conversely, *Batrachochytrium* has only four Neks, but these all belong to separate subfamilies. Thus a correlation is evident amongst the organisms sampled between the presence of ciliated cells which divide and the diversity of Neks (Figure 3-1).

3.5 Discussion

We draw two major conclusions from our phylogenetic analysis. First, tree reconciliation suggests that the last common ancestor (LCA) of unikonts and bikonts most likely had at least five Neks and variations in the numbers of Neks in different lineages was due to expansion or loss of multiple Neks; this is a novel finding and changes our view of this kinase family and the relationships of its members. Second, this work confirms and extends our previous suggestion that Neks are more abundant in the genomes of

organisms that must co-ordinate ciliary assembly and disassembly with respect to the cell cycle.

Currently, there is a paucity of functional data relevant to the cell biology of the Nek family. Consequently, there is insufficient data available to discern clear roles for particular Nek subfamilies from comparison of the Nek repertoires. However, the availability of the relationships between the various Neks will make future research on any particular Nek more relevant to the field at large. While most Neks that have been studied are associated with cilia/centrosomes/cell cycle, we do not propose that all Neks subserve this triumvirate. Indeed, expansion of the subfamilies was inevitably associated with both loss of function and acquisition of new roles [44], but analysis of which Neks have ancestral functions and which have derived functions requires the availability of phylogeny such as we present here. For example, Nek3, which is not centrosomal and has functions seemingly unrelated to microtubular-based structures [45,46], is now revealed to be a relatively recent innovation (Figure 3-2), which likely underwent neofunctionalization.

Although we cannot discern cellular roles for individual Nek subfamilies, it is clear that Neks are not required for the formation of centrioles or cilia. Diatoms, for example, make both of these organelles *de novo* when differentiating into gametes [47] but have no Neks. Nor are the Neks required for mitosis, as exemplified by the many species whose genomes do not encode Neks. Importantly, we have yet to find a species that does not encode any Neks but does have ciliated cells that divide. Conversely, the *Giardia* genome has >70 Neks; *Giardia* flagella undergo a complex maturation process which takes four cell cycles [48], which may represent an extreme case of requirement

for Neks during division in a flagellated cell. We predict that as functional studies progress, it will be revealed that many Neks participate in the important cellular role of coordinating the activities of centrioles as basal bodies during interphase and as spindle pole foci during mitosis.

Given our phylogenetic results, ciliary and centrosomal Nek functions are likely to be ancestral and thus may be retained in phylogenetically distant organisms. The wide distribution of the Neks from both unikonts and bikonts suggests strongly that the Neks had already expanded in the eukaryotic LCA. We suggest deviations of the topologies of the Nek subfamilies from our analysis from the species tree may represent different evolutionary constraints in the various lineages.

Our conclusion that the LCA, which must have been a non-terminally differentiated ciliated cell, had at least five Neks, should be interpreted in two ways: first, we are discerning the nature of the eukaryotic LCA, which is distinct from the first eukaryote; second, the presence of several Neks in the LCA conforms well with our idea that this kinase family is ancestrally correlated with the presence of ciliated cells which divide. The cell biology of the eukaryotic LCA can be partially inferred by applying the principal of parsimony to diverse extant eukaryotes: it is thus likely that the LCA was ciliated with a 9+2 axoneme and centrioles with triplet microtubules, and that the LCA could undergo both mitosis and meiosis [49]. The feature of extant eukaryotes most predictive for the number of retained Nek subfamilies appears to be the presence of ciliated cells which can re-enter the cell cycle (Figure 3-1 and [2]). Our data is consistent with a growing body of data which suggests that the eukaryotic last common ancestor had a sophisticated cellular organization and possessed many proteins required for

centriole/cilium assembly [50,51]. It is also consistent with the notion that early eukaryotes underwent a period of rapid evolution, especially of cytoskeletal elements [52]. We suggest that the Neks may have expanded during this time.

Although the relationship between cilia and the cell cycle is a long-standing problem in cell biology [53] which is receiving renewed interest [27,54], our understanding of the complex regulatory relationship that must exist remains rudimentary. Functional studies of the Nek family may provide new points of entry into this important but undoubtedly complex signaling network.

3.6 Acknowledgements

We thank Martin Seigert of the SFU High Performance Computing Facility for assistance. This work was supported by a Natural Sciences & Engineering Research Council of Canada (NSERC) Discovery Grant to LMQ. BAB was supported by fellowships from NSERC and the Michael Smith Foundation for Health Research.

3.7 Tables and Figures

Table 3-1 Bayes Factor analysis of topology constraints.

Results of hypothesis-testing for the unikonts + *Chlamydomonas* dataset (Figure 2-2). Using Bayes Factor analysis, values <10 suggest the constrained topology is a reasonable representation of the data [38,39]. Constrained nodes are indicated in Figure 2-2; "Node x + Node y" indicates all taxa arising from both nodes were constrained to branch from a single internal node.

Topology Constraint	Num. of Gens. ($x10^6$)	Avg. Std. Dev. of Split Freqs. Between Runs	Arithmetic Mean of log Likelihood Values	Harmonic Mean of log Likelihood Values	Bayes Factor
Unconstrained	3.00	0.008612	-22754.85	-22798.76	-
Node 4	5.53	0.005674	-22756.15	-22805.89	14.26
Node 10	5.51	0.006724	-22752.78	-22799.41	1.30
Node 9	4.34	0.006191	-22754.77	-22802.28	7.04
Node 7	3.90	0.004951	-22753.95	-22800.50	3.48
Node 6	2.58	0.008200	-22755.26	-22799.71	1.90
Node 3	3.47	0.007247	-22755.96	-22798.18	1.16
Node 4 + Node 2	2.67	0.007250	-22813.60	-22861.38	125.24
Node 5 + Node 2	2.33	0.008065	-22802.93	-22844.09	90.66
Ce D1044.8 + Node 1	3.59	0.006875	-22756.55	-22802.11	6.70
Node 8 + Node 7	4.01	0.006743	-22756.61	-22807.16	16.80
Node 5 + Node 1	3.03	0.006723	-22767.36	-22820.18	42.84
Node 4 + Node 1	5.18	0.007722	-22764.13	-22816.73	35.94
Node 4 + Node 5	4.49	0.006659	-22755.90	-22798.78	0.04

Table 3-2 Detailed MrBayes output for datasets analyzed in this study

Dataset	Number of taxa	Number of chains/run	Num. of Gens. ($x10^6$)	Avg. Std. Dev. of Split Freqs. Between Runs	Arithmetic Mean of log Likelihood Values	Harmonic Mean of log Likelihood Values
Figure 3-2	63	4	3.00	0.008612	-22754.85	-22798.76
Figure 3-3-3-7	128	8	16.39	0.009892	-45555.61	-45636.61
Figure S1	78	8	4.88	0.008434	-29007.99	-29053.90
Figure S2	101	8	7.21	0.009652	-31078.76	-31099.13

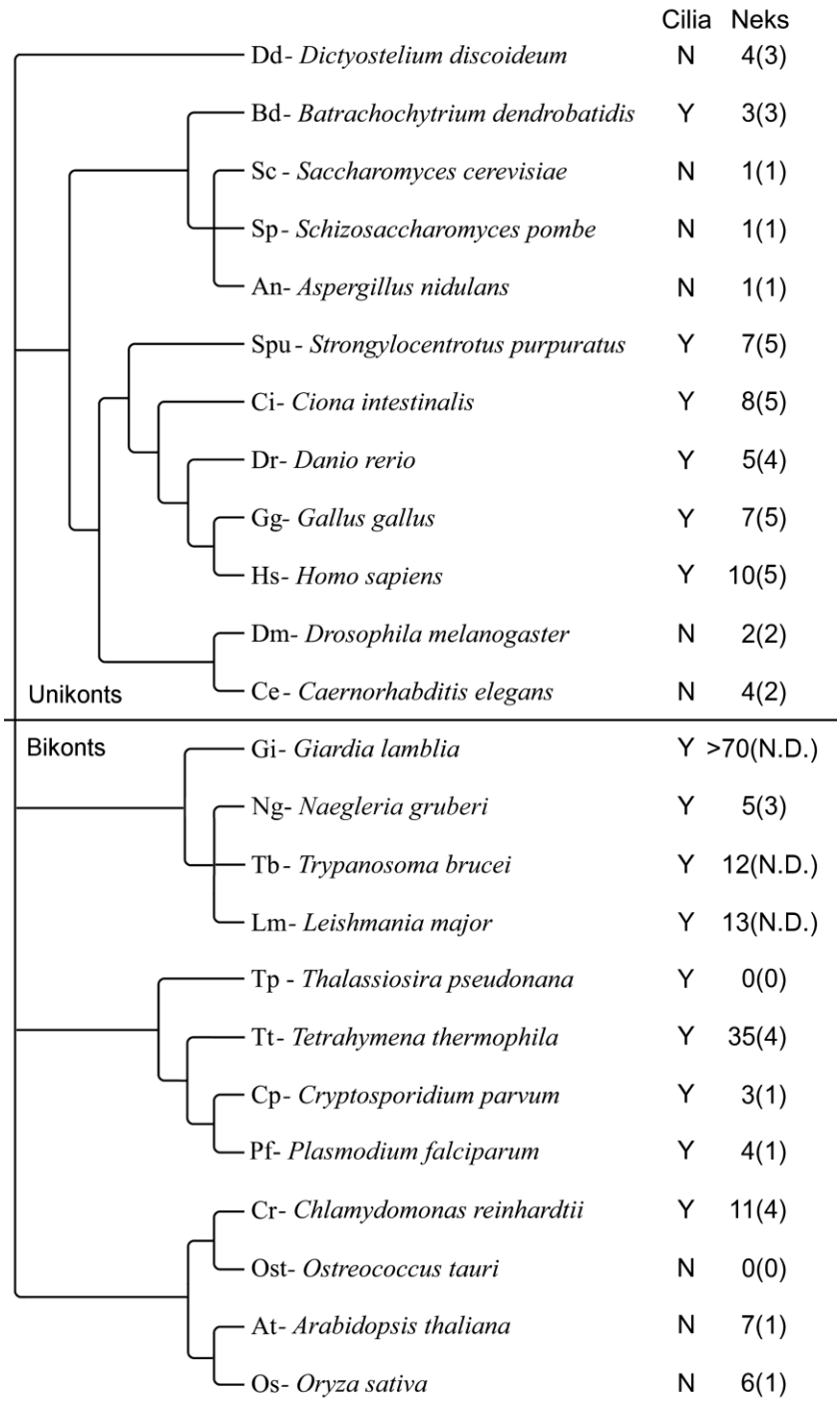

Figure 3-1. Cladogram of species included in our analysis.

Full legend on next page.

Figure 3-1. Cladogram of species included in our analysis.

Relationships among taxa based on [29,55]. The "Ciliated cells divide" column indicates presence (Y) or absence (N) of cells in the species which both bear cilia and re-enter the cell cycle: gametes and other terminally differentiated ciliated cells are excluded. The "Neks" column indicates both how many genes encoding Nek kinase domains were identified in the indicated species. The number in parentheses is a minimal estimate of how many Nek subfamilies are represented in the genome, as determined from our analysis (see text).

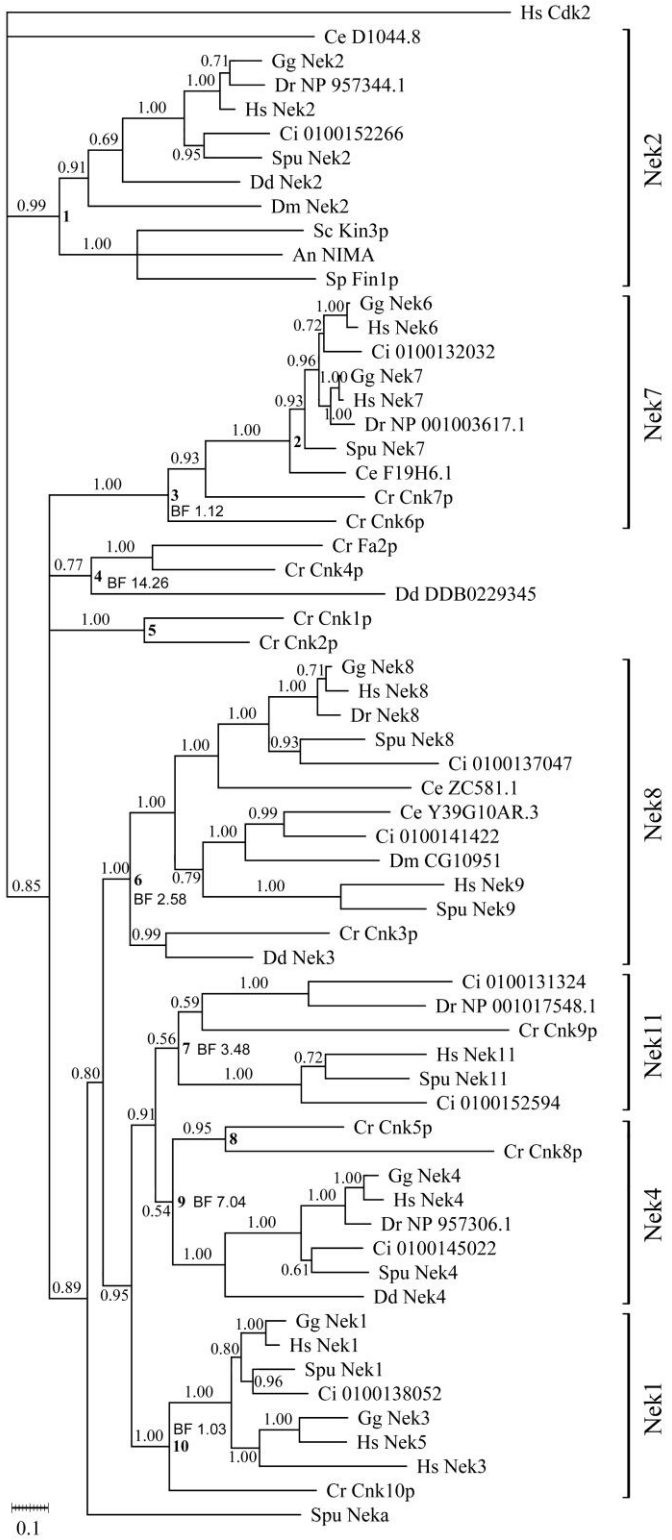

Figure 3-2. Phylogram of Nek kinase domains from unikonts + *Chlamydomonas*
Numbers at nodes are interpreted as *a posteriori* support values. Bold digits at some nodes indicate nodes used for hypothesis testing, and the Bayes Factor (BF) where indicated. Right brackets include sequences joined by well-supported internal nodes, which we propose to refer to as Nek subfamilies, named after the human member with the shortest branch length.

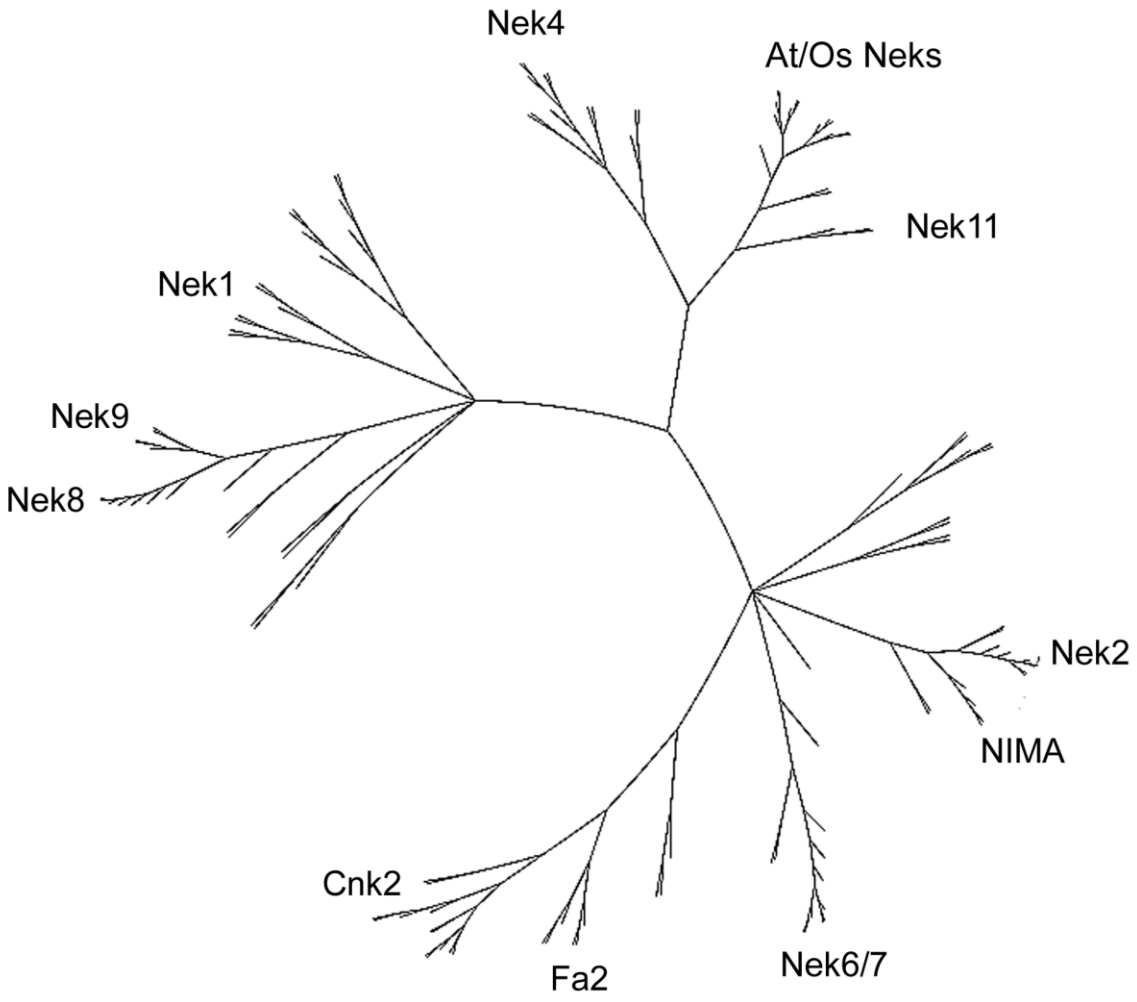

Figure 3-3. Phylogram of Nek kinase domains from a larger sampling of eukaryotes.

Neks from all species shown in Figure 3-1 having Neks in their genome were included in this dataset except for Leishmania, Trypanosoma, and Giardia. This represents an overview of the tree that is examined in detail in Figures 3-4 to 3-7.

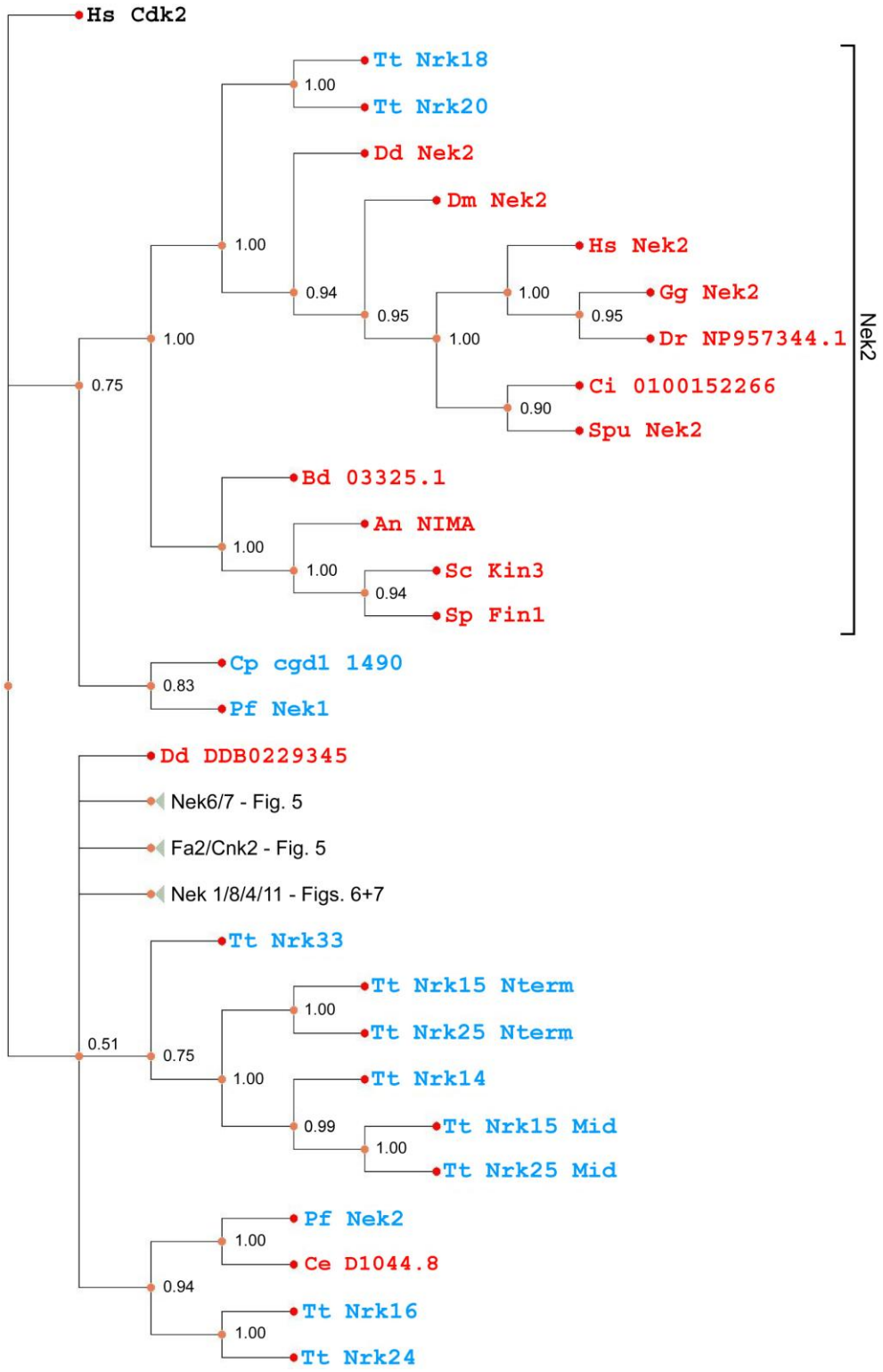

Figure 3-4. Phylogram of Nek kinase domains across eukaryotes, Nek2 clade shown expanded

Full Legend on next page.

Figure 3-4. Phylogram of Nek kinase domains across eukaryotes, Nek2 clade shown expanded. For ease of visualization, large nodes have been collapsed (triangles) and are shown expanded in subsequent figures (such that the node marked "5" is shown expanded in Figures 3-5, etc.) as indicated. In these Figures, sequences from bikont species are cyan, while sequences from unikont species are red. Right brackets include sequences joined by well-supported internal nodes, which we propose to refer to as Nek subfamilies, named after the human member with the shortest branch length where appropriate. The Nek4 clade is marked with an asterisk due to its poor support (see text).

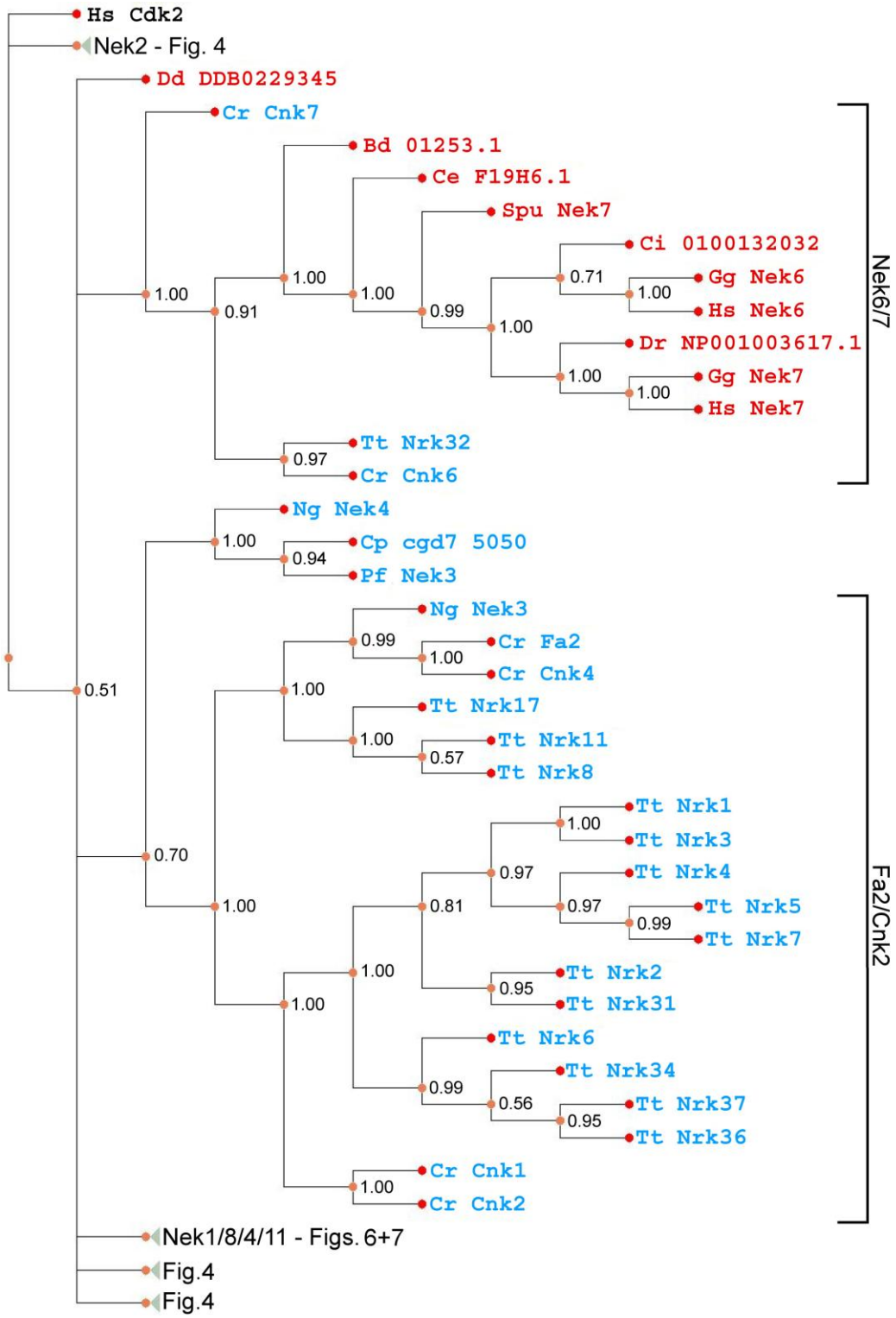

Figure 3-5. Phylogram of Nek kinase domains across eukaryotes, Nek 6/7 clade and Fa2/Cnk2 clade shown expanded.

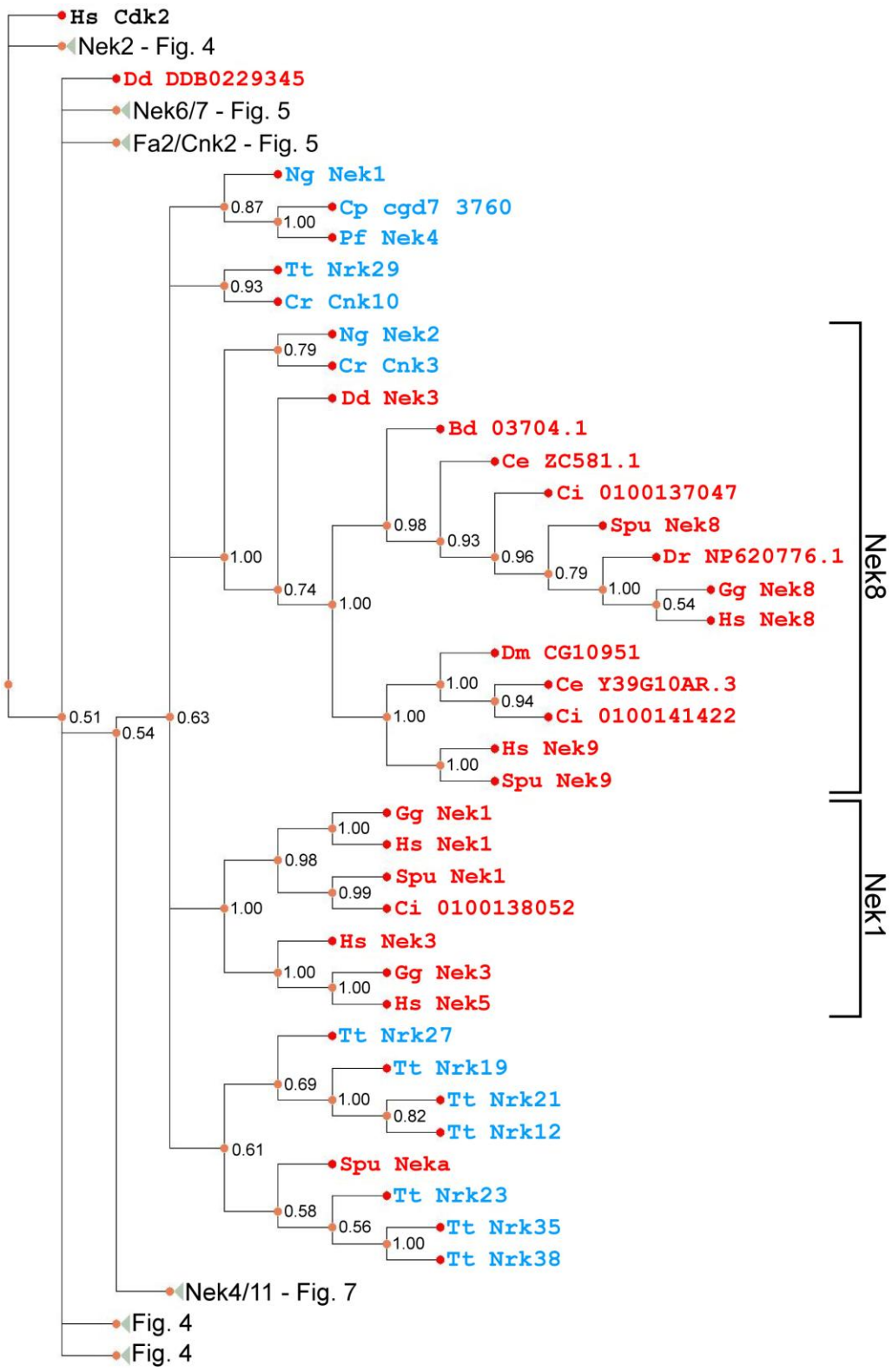

Figure 3-6. Phylogram of Nek kinase domains across eukaryotes, Nek8 and Nek1 clades shown expanded.

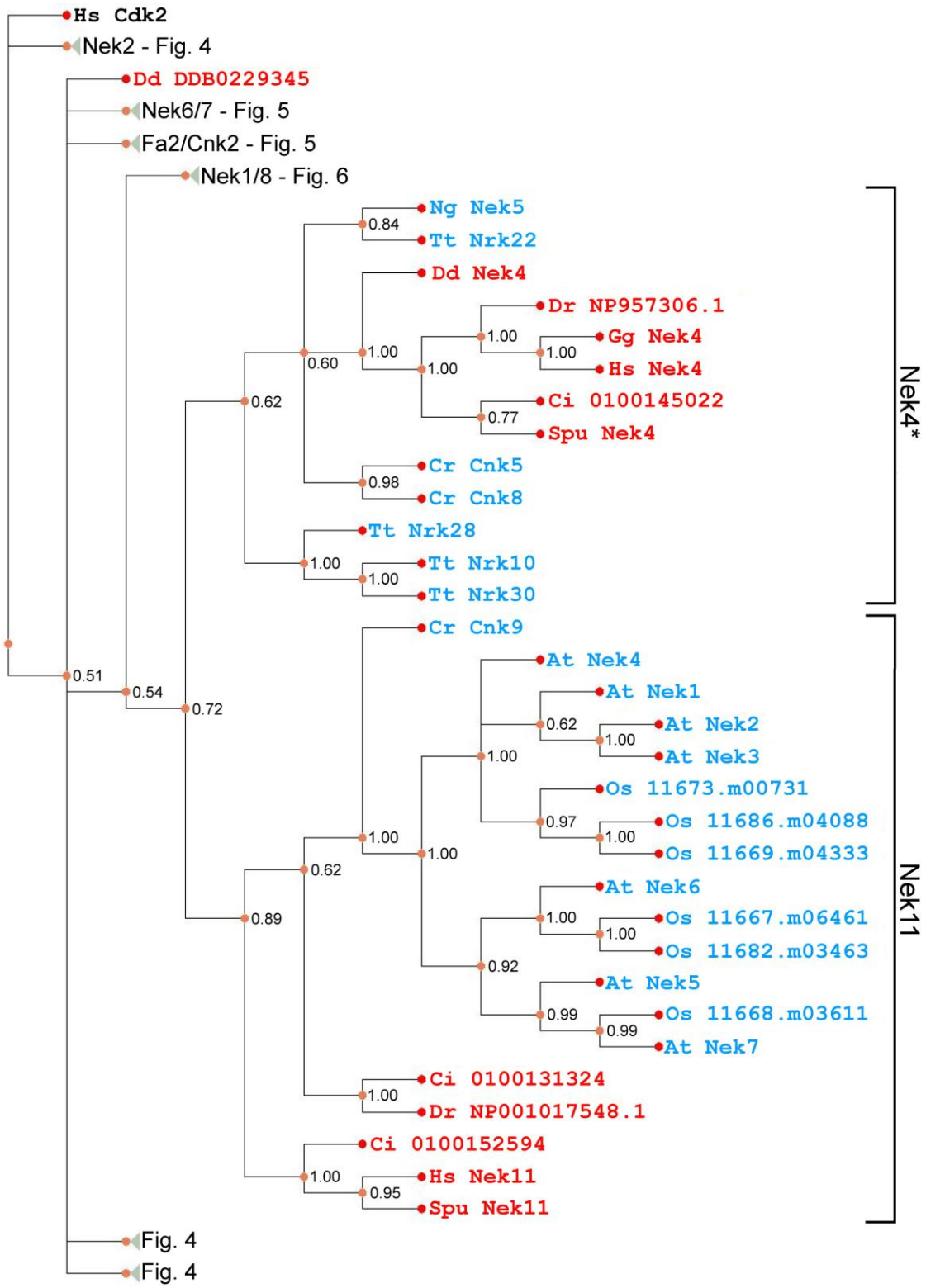

Figure 3-7. Phylogram of Nek kinase domains across eukaryotes, Nek4 and Nek11 clades shown expanded.

3.8 References

1. O'Connell MJ, Krien MJ, Hunter T (2003) Never say never. The NIMA related protein kinases in mitotic control. Trends Cell Biol 13: 221-228.

2. Quarmby LM, Mahjoub MR (2005) Caught Nek-ing: cilia and centrioles. J Cell Sci 118: 5161-5169.

3. Osmani AH, McGuire SL, Osmani SA (1991) Parallel activation of the NIMA and p34cdc2 cell cycle-regulated protein kinases is required to initiate mitosis in A. nidulans. Cell 67: 283-291.

4. Belham C, Roig J, Caldwell JA, Aoyama Y, Kemp BE, et al. (2003) A mitotic cascade of NIMA family kinases. Nercc1/Nek9 activates the Nek6 and Nek7 kinases. J Biol Chem 278: 34897-34909.

5. Feige E, Shalom O, Tsuriel S, Yissachar N, Motro B (2006) Nek1 shares structural and functional similarities with NIMA kinase. Biochim Biophys Acta 1763: 272-281.

6. Fry AM (2002) The Nek2 protein kinase: a novel regulator of centrosome structure. Oncogene 21: 6184-6194.

7. Tan BC, Lee SC (2004) Nek9, a novel FACT-associated protein, modulates interphase progression. J Biol Chem 279: 9321-9330.

8. Yissachar N, Salem H, Tennenbaum T, Motro B (2006) Nek7 kinase is enriched at the centrosome, and is required for proper spindle assembly and mitotic progression. FEBS Lett 580: 6489-6495.

9. Noguchi K, Fukazawa H, Murakami Y, Uehara Y (2004) Nucleolar Nek11 is a novel target of Nek2A in G1/S-arrested cells. J Biol Chem 279: 32716-32727.

10. Yin MJ, Shao L, Voehringer D, Smeal T, Jallal B (2003) The serine/threonine kinase Nek6 is required for cell cycle progression through mitosis. J Biol Chem 278: 52454-52460.

11. Mahjoub MR, Trapp ML, Quarmby LM (2005) NIMA-related kinases defective in murine models of polycystic kidney diseases localize to primary cilia and centrosomes. J Am Soc Nephrol 16: 3485-3489.

12. Doxsey S, McCollum D, Theurkauf W (2005) Centrosomes in cellular regulation. Annu Rev Cell Dev Biol 21: 411-434.

13. Doxsey S, Zimmerman W, Mikule K (2005) Centrosome control of the cell cycle. Trends Cell Biol 15: 303-311.

14. Bahe S, Stierhof YD, Wilkinson CJ, Leiss F, Nigg EA (2005) Rootletin forms centriole-associated filaments and functions in centrosome cohesion. J Cell Biol 171: 27-33.

15. Mayor T, Hacker U, Stierhof YD, Nigg EA (2002) The mechanism regulating the dissociation of the centrosomal protein C-Nap1 from mitotic spindle poles. J Cell Sci 115: 3275-3284.

16. Fry AM, Mayor T, Meraldi P, Stierhof YD, Tanaka K, et al. (1998) C-Nap1, a novel centrosomal coiled-coil protein and candidate substrate of the cell cycle-regulated protein kinase Nek2. J Cell Biol 141: 1563-1574.

17. Marshall WF, Nonaka S (2006) Cilia: tuning in to the cell's antenna. Curr Biol 16: R604-614.

18. Basto R, Lau J, Vinogradova T, Gardiol A, Woods CG, et al. (2006) Flies without centrioles. Cell 125: 1375-1386.

19. Pazour GJ (2004) Intraflagellar transport and cilia-dependent renal disease: the ciliary hypothesis of polycystic kidney disease. J Am Soc Nephrol 15: 2528-2536.

20. Upadhya P, Birkenmeier EH, Birkenmeier CS, Barker JE (2000) Mutations in a NIMA-related kinase gene, Nek1, cause pleiotropic effects including a progressive polycystic kidney disease in mice. Proc Natl Acad Sci U S A 97: 217-221.

21. Liu S, Lu W, Obara T, Kuida S, Lehoczky J, et al. (2002) A defect in a novel Nek-family kinase causes cystic kidney disease in the mouse and in zebrafish. Development 129: 5839-5846.

22. Otto, E.A., M.L. Trapp, U.T. Schultheiss, L.M. Quarmby, & F. Hildebrandt (2008). Mutations in NIMA-related kinase NEK8 causes nephronophthisis in humans and affects ciliary and centrosomal localization. *J. Am. Soc. Nephrology*. 2008 Mar;19(3):587-92.

23. Bradley BA, Quarmby LM (2005) A NIMA-related kinase, Cnk2p, regulates both flagellar length and cell size in *Chlamydomonas*. J Cell Sci 118: 3317-3326.

24. Mahjoub MR, Montpetit B, Zhao L, Finst RJ, Goh B, et al. (2002) The FA2 gene of *Chlamydomonas* encodes a NIMA family kinase with roles in cell cycle progression and microtubule severing during deflagellation. J Cell Sci 115: 1759-1768.

25. Mahjoub MR, Qasim Rasi M, Quarmby LM (2004) A NIMA-related kinase, Fa2p, localizes to a novel site in the proximal cilia of *Chlamydomonas* and mouse kidney cells. Mol Biol Cell 15: 5172-5186.

26. Wloga D, Camba A, Rogowski K, Manning G, Jerka-Dziadosz M, et al. (2006) Members of the NIMA-related kinase family promote disassembly of cilia by multiple mechanisms. Mol Biol Cell 17: 2799-2810.

27. Quarmby LM, Parker JD (2005) Cilia and the cell cycle? J Cell Biol 169: 707-710.

28. Bradley BA, Wagner JJ, Quarmby LM (2004) Identification and sequence analysis of six new members of the NIMA-related kinase family in *Chlamydomonas*. J Eukaryot Microbiol 51: 66-72.

29. Richards TA, Cavalier-Smith T (2005) Myosin domain evolution and the primary divergence of eukaryotes. Nature 436: 1113-1118.

30. Altschul SF, Gish W, Miller W, Myers EW, Lipman DJ (1990) Basic local alignment search tool. J Mol Biol 215: 403-410.

31. Letunic I, Copley RR, Pils B, Pinkert S, Schultz J, et al. (2006) SMART 5: domains in the context of genomes and networks. Nucleic Acids Res 34: D257-260.

32. Schultz J, Copley RR, Doerks T, Ponting CP, Bork P (2000) SMART: a web-based tool for the study of genetically mobile domains. Nucleic Acids Res 28: 231-234.

33. Thompson JD, Gibson TJ, Plewniak F, Jeanmougin F, Higgins DG (1997) The CLUSTAL_X windows interface: flexible strategies for multiple sequence alignment aided by quality analysis tools. Nucleic Acids Res 25: 4876-4882.

34. Huelsenbeck JP, Ronquist F (2001) MRBAYES: Bayesian inference of phylogenetic trees. Bioinformatics 17: 754-755.

35. Ronquist F, Huelsenbeck JP (2003) MrBayes 3: Bayesian phylogenetic inference under mixed models. Bioinformatics 19: 1572-1574.

36. Page RD (1996) TreeView: an application to display phylogenetic trees on personal computers. Comput Appl Biosci 12: 357-358.

37. Bingham J, Sudarsanam S (2000) Visualizing large hierarchical clusters in hyperbolic space. Bioinformatics 16: 660-661.

38. Kass R, Raftery A (1995) Bayes Factors. Journal of the American Statistical Association 90: 773-795.

39. Nylander JA, Ronquist F, Huelsenbeck JP, Nieves-Aldrey JL (2004) Bayesian phylogenetic analysis of combined data. Syst Biol 53: 47-67.

40. Simpson AG, Stevens JR, Lukes J (2006) The evolution and diversity of kinetoplastid flagellates. Trends Parasitol 22: 168-174.

41. Rellos P, Ivins FJ, Baxter JE, Pike A, Nott TJ, et al. (2007) Structure and regulation of the human Nek2 centrosomal kinase. J Biol Chem 282: 6833-6842.

42. Cloutier M, Vigneault F, Lachance D, Seguin A (2005) Characterization of a poplar NIMA-related kinase PNek1 and its potential role in meristematic activity. FEBS Lett 579: 4659-4665.

43. Zhang H, Scofield G, Fobert P, Doonan JH (1996) A nimA-like protein kinase transcript is highly expressed in meristems of *Antirrhinum majus*. J Microsc 181: 186-194.

44. Lynch M, Katju V (2004) The altered evolutionary trajectories of gene duplicates. Trends Genet 20: 544-549.

45. Miller SL, DeMaria JE, Freier DO, Riegel AM, Clevenger CV (2005) Novel association of Vav2 and Nek3 modulates signaling through the human prolactin receptor. Mol Endocrinol 19: 939-949.

46. Miller SL, Antico G, Raghunath PN, Tomaszewski JE, Clevenger CV (2007) Nek3 kinase regulates prolactin-mediated cytoskeletal reorganization and motility of breast cancer cells. Oncogene.

47. Chepurnov VA, Mann DG, Sabbe K, Vyverman W (2004) Experimental studies on sexual reproduction in diatoms. Int Rev Cytol 237: 91-154.

48. Nohynkova E, Tumova P, Kulda J (2006) Cell division of Giardia intestinalis: flagellar developmental cycle involves transformation and exchange of flagella between mastigonts of a diplomonad cell. Eukaryot Cell 5: 753-761.

49. Cavalier-Smith T (2002) The phagotrophic origin of eukaryotes and phylogenetic classification of Protozoa. Int J Syst Evol Microbiol 52: 297-354.

50. Inglis PN, Boroevich KA, Leroux MR (2006) Piecing together a ciliome. Trends Genet 22: 491-500.

51. Jekely G, Arendt D (2006) Evolution of intraflagellar transport from coated vesicles and autogenous origin of the eukaryotic cilium. Bioessays 28: 191-198.

52. Erickson HP (2007) Evolution of the cytoskeleton. Bioessays 29: 668-677.

53. Tucker RW, Pardee AB, Fujiwara K (1979) Centriole ciliation is related to quiescence and DNA synthesis in 3T3 cells. Cell 17: 527-535.

54. Qin H, Wang Z, Diener D, Rosenbaum J (2007) Intraflagellar transport protein 27 is a small G protein involved in cell-cycle control. Curr Biol 17: 193-202.

55. Keeling PJ, et al. (2005) The tree of eukaryotes. Trends Ecol Evol 20: 670-676.

CHAPTER 4
KATANIN KNOCKDOWN SUPPORTS A ROLE FOR MICROTUBULE SEVERING IN RELEASE OF BASAL BODIES PRIOR TO MITOSIS IN *CHLAMYDOMONAS*

This Chapter accepted for publication by Molecular Biology of the Cell, October 2008 as Manuscript Mol. Biol. Cell 10.1091/mbc.E07-10-1007, available at http://www.molbiolcell.org/cgi/content/abstract/E07-10-1007v1

M. Qasim Rasi[1], Jeremy D.K. Parker[1], Jessica L. Feldman[2], Wallace F. Marshall[2] and Lynne M. Quarmby[1]

[1]Department of Molecular Biology & Biochemistry, Simon Fraser University, Canada
[2]Department of Biochemistry & Biophysics, University of California San Francisco, USA

MQR and JDKP contributed equally to this work and are co-first authors.

Author Contributions:

MQR designed pEZ, assayed for katanin knock-down by various means, including screening colonies, mRNA determinations, antibody purification, and Western blotting.
JDKP assisted with the above experiments both intellectually and materially, backcrossed the original RNAi isolates, and performed the majority of cell cycle-related experiments, including synchrony and immunofluorescence; also co-wrote the manuscript.
JLF and WFM contributed conceptually to the idea of flagella remaining attached to cells during mitosis and provided Figure 4E.
LMQ contributed intellectually to all experiments and co-wrote the manuscript.

4.1 Abstract

Katanin is a microtubule-severing protein that participates in the regulation of cell cycle progression and in ciliary disassembly, but its precise role is not known for either activity. Our data suggest that in *Chlamydomonas*, katanin severs doublet microtubules at the proximal end of the flagellar transition zone, allowing disengagement of the basal body from the flagellum prior to mitosis. Using an RNAi approach we have discovered

that severe knock-down of the p60 subunit of katanin, KAT1, is achieved only in cells that also carry secondary mutations that disrupt ciliogenesis. Importantly, we observed that cells in the process of cell cycle-induced flagellar resorption sever the flagella from the basal bodies before resorption is complete and we find that this process is defective in KAT1 knock-down cells.

4.2 Introduction

Almost all eukaryotic cells are ciliated (note that in some cells, such as *Chlamydomonas*, cilia have historically been called flagella, but eukaryotic flagella are in fact cilia). Although cells with highly specialized cilia, such as respiratory or olfactory epithelial cells or sperm, do not re-enter the mitotic cell cycle, most ciliated cells do divide. With rare exception, there is a tightly orchestrated sequence involving loss of cilia prior to mitosis, and then, shortly after exit from mitosis, ciliogenesis occurs (Reider *et al.*, 1979). This coordination is thought to reflect the alternating roles of centrioles, as the basal bodies which nucleate cilia and as the organizing foci of mitotic spindle poles (Quarmby and Parker, 2005). The regulatory relationship between cilia and cell cycle progression has not been elucidated, but it has been proposed that one function of primary cilia is to sense environmental signals pertinent to cellular decisions about division, differentiation and apoptosis (Pan and Snell, 2007; Marshall and Nonaka, 2006).

There are two distinct ways that cells can lose their cilia: by deciliation or by resorption. Deciliation, also known as deflagellation, refers to the shedding of cilia into the environment (reviewed by Quarmby, 2004). Most (if not all) ciliated cells deciliate in response to chemical or physical stress. When cilia are resorbed in advance of mitosis, both axonemal and membrane components are retained by the cell. Although these two

processes appear to be distinct in both function and mechanism, we have previously shown that they share common aspects of regulation and that resorption likely involves activity at the base, in addition to the well-established disassembly which occurs at the ciliary tip (Marshall and Rosenbaum, 2001; Parker and Quarmby, 2003). We have previously proposed that elements of the deciliation machinery might play roles in resorption.

Deflagellation involves the precise severing of the axoneme at a specific site between the axoneme proper and the flagellar transition zone, known as the SOFA (Site of Flagellar Autotomy; Mahjoub *et al.*, 2004). The microtubule-severing ATPase, katanin, has been implicated as the protein responsible for the breakage of the outer doublet microtubules during deflagellation, but the evidence has been indirect (Lohret *et al.*, 1998; Lohret *et al.*, 1999). Purified sea urchin katanin is capable of breaking axonemes, antibodies against katanin inhibit calcium-activated axonemal severing in vitro, and immuno-gold labeling with an anti-katanin antibody places katanin at the site of action. However, a screen for deflagellation mutants in *Chlamydomonas* yielded multiple alleles of each of three genes, *FA1*, *FA2*, and *ADF1*, but not katanin (e.g. Finst *et al.*, 1998). The failure to isolate katanin mutants potentially indicated that either katanin plays no role in deflagellation or it plays an additional role that is essential for survival of the cell. Consistent with the latter possibility, it is well-established in other systems that katanin plays a role in cell cycle progression (Buster *et al.*, 2002; Toyo-Oka *et al.*, 2005; McNally *et al.*, 2006; Zhang *et al.*, 2007).

Based on the idea that cells with partial loss of katanin, but still retaining enough katanin to survive, might reveal hypomorphic phenotypes, we have taken an RNAi

approach to reduce levels of expression the catalytic p60 subunit of katanin in the haploid unicellular alga, *Chlamydomonas reinhardtii*. Katanin knock-down strains were recovered infrequently, and only in the context of additional mutations which affected flagellar assembly. We went on to show that there is a second site of axonemal severing proximal to the transition zone (the SOFA is distal) and that severing occurs at this site prior to complete pre-mitotic resorption of flagella. Experiments with a cell wall-less strain revealed that cells deficient in katanin fail to release resorbing flagella from the basal bodies. Taken together, our data suggest that one important role of katanin is separation of the basal body from ciliary remnants prior to functional reassignment of the basal bodies to the spindle poles.

4.3 Materials and Methods

Strains, culture conditions and nuclear transformations

Chlamydomonas strains 137c, *cw2*, *bld1*, and *ift88-1* were obtained from the *Chlamydomonas* Genetics Center (Durham, NC). *fa2-3* mutants were previously generated in our lab (Finst *et al.*, 1998). All cells were maintained on TAP (Tris-Acetate-Phosphate) medium plates (Harris, 1989) supplemented with 1.5% agar, under constant illumination at 22^{o}C. Nuclear transformation was by the glass bead method (Kindle *et al.*, 1989); recipient strains other than *cw2* were treated with gametic lytic enzyme (Harris, 1989) prior to transformation. All *par* and *ble* transformants were grown on 1.5% TAP plates supplemented with paromomycin (15µg/ml; Sigma-Aldrich, Oakville, ON) or Zeocin (30µg/ml; Invitrogen, Burlington, ON).

For experiments involving mitotic cells, partial cell cycle synchrony was achieved by growing cells ~2 days in liquid TAP, followed by starvation in minimal medium (MI)

in foil-wrapped flasks for 24-30 hours (Umen and Goodenough, 2001). Cells were then resuspended in fresh TAP in unwrapped flasks, and aliquots fixed at several timepoints starting 12 hours after the shift to light. The exact timing and degree of synchrony is dependent upon culture conditions, but typically at 12 hours ~50% of cells were in division (as judged by the presence of furrows, unhatched cells, or phospho-histone H3 immunofluorescence).

Molecular constructs

Nuclear transformation of *Chlamydomonas* is accomplished by non-homologous insertion of the exogenous DNA into the genome, a process that can frequently involve deletions of the transforming and genomic DNA. In order to maximize the frequency with which selected colonies are competent to express the transgene, we constructed transformation vectors with different selectable markers at each end (pEZ-KAT1-RNAi; see Figure 1A). Briefly, pEZ-KAT1-RNAi is derived from pGenD (Fischer and Rochaix, 2001), pSI103 (Sizova *et al.*, 2001) and pSP124S (Lumbreras *et al.*, 1998). The *aphVIII* gene, along with its promoter and 3'UTR (the "par cassette"), was amplified from pSI103 using primers Spe-par(+) and Spe-par(-) and cloned into the unique *Spe*I site in pGenD, while the *ble* cassette was removed from pSP124S by restriction digestion and ligated into a *Hin*dIII site in pGenD. The PsaD-derived promoter elements from pGenD drive expression of a cDNA hairpin such that transcription will result in double-stranded RNA. The hairpin was derived from the 5' end of the katanin cDNA (*KAT1*, *Chlamydomonas* gene c_80022; base pairs 114 to 800, then 114-552 in reverse orientation). This same hairpin targeting *KAT1* was also inserted into the pNI-537 vector (Rohr *et al.*, 2004; generously provided by H. Certutti). This region of the cDNA is outside of the coding

regions for the AAA domain, and has no significant similarity to the most similar genes in the *Chlamydomonas* genome (*KAT2*, C_620017, 46% identity to KAT1 and a predicted spastin-like protein, *Chlamydomonas* gene model e_gwW.1.632.1, 39% identity to *KAT1*). Primers used are in Table 1.

Assessment of mRNA levels

To assess relative transcript levels for our initial KAT1-RNAi experiments, we adopted a competitive PCR-based approach (Wang *et al.*, 1989). Experimental cDNA pools were normalized to equal concentrations, and then independently mixed with increasing concentrations of a competitor that differs in sequence and length from the target sequence, but which shares with the target the primer binding sites used for amplifying the target (or competitor) sequences. Primers K311A(+) and K1440-64R(-) give a product of 300 bp from the KAT1 cDNA. To make the competitor (pGEM-T-mimic), we performed low-stringency PCR using those same primers on *Chlamydomonas* genomic DNA to obtain a product of 400 bp, followed by a high-stringency second round of PCR using the same primers. The resulting product was cloned into pGEM-T Easy (Promega, Madison, WI). As a control, experimental cDNA pools were also assayed using the gene for ribosomal subunit RPS14 at the *CPH1* locus using the "CRY1" primers described by Kathir *et al.* (2003).

Total *Chlamydomonas* RNA, mRNA and cDNA were obtained as previously described (Mahjoub *et al.*, 2002). Varying concentrations of pGEM-T-mimic were mixed with the cDNA pool from pEZ-KAT1-RNAi cells as the substrate for PCR reactions. Quantification of PCR bands was performed with ImageQuant (GE Healthcare). For RT-PCR of genes putatively disrupted by insertion of pEZ-KAT1-RNAi, cDNA pools were

tested with control primers against centrin; primers specific to *IFT88* and *PKG2* are shown in Table 1.

Real Time Quantitative PCR

Chlamydomonas cDNA pools from wild-type (137c), KAT1-RNAi;*ift88-1* and KAT1-RNAi;*bld1-1* cells were prepared as described above. Primers specific to *KAT1* (Qcp60+/Qcp60-, Table 1) were initially used to PCR-amplify a 227 bp fragment from the 5' end of the *KAT1* cDNA cloned earlier into pEZ-KAT1-RNAi. Conditions that would yield a specific band corresponding to KAT1 were empirically determined. Next, Qcp60+/Qcp60- were used to quantitatively amplify target sequence in a 50 µl reaction mix containing 500 ng of cDNA pool (IQ SyberGreen Supermix; Bio-Rad, Mississauga, ON). The annealing and elongation steps of the amplification cycle were performed at 58^{o}C and 72^{o}C respectively. PCR was run for 44 cycles. Gene expression was standardized to the expression levels of ribosomal subunit RSP14. The MiniOpticon RT-PCR system (Bio-Rad) was used to monitor target sequence amplification and Opticon Monitor3 software (Bio-Rad) was used for data analysis. qPCR was carried out in triplicate and the average reading is represented as the final KAT1 transcript level.

Identification of the sites of insertion of the RNAi constructs

To determine the site of insertion of the RNAi constructs, we used the Vectorette PCR method (Riley *et al.*, 1990). Briefly, this method is based on annealed DNA adapters, that have large regions of mismatched nucleotides between the two DNA strands (the “bubble anchors”), to genomic DNA digested with blunt-cutting restriction endonucleases. Subsequent PCR, using one primer specific to one bubble anchor and the other primer

specific to the integrated construct, amplifies genomic DNA between the restriction enzyme cut site and the insertion. Primer sequences used are in Table 1.

Measurements of cell size

The length and width of at least 75 cells of each strain were measured by DIC microscopy and SoftWorx (v. 3.22) software package (Applied Precision, Issaquah, WA). Cell volumes were calculated using the formula $4/3\ \pi[L/2][W/2]^2$ (Umen and Goodenough, 2001), where L and W describe length and width of the cells, respectively.

Generation of Antibodies and Immunoblotting

KAT1 antibodies were raised against two synthetic peptides (Sigma-Aldrich), N-terminal (KGSAGEKAKKQY) and C-terminal (QVDGVHGSEKDK), conjugated to KLH and injected into four rabbits (Sigma-Aldrich). *KAT1* cDNA (KAT1 full length) and a derived construct lacking the sequence corresponding to the peptide epitopes (KAT1-Δ-epitope) were expressed using pET-DEST42 (Invitrogen) in BL21 *E.coli* (Novagen) and induced with 1mM IPTG (Invitrogen). Antisera from rabbit #8907 exhibited a reactive band of ~60 kDa, which is the predicted size of KAT1, from IPTG-induced cells expressing KAT1 full length but not cells expressing KAT1-Δ-epitope or uninduced cells (data not shown). Characterization of antisera recognizing PKG2 will be described in a future report. Protein levels in cell lysates were determined using QuickStart Bradford Reagent (Bio-Rad). Horseradish peroxidase-linked goat anti-rabbit IgG (1:10,000; Sigma-Aldrich) and ECL (GE Healthcare) were used for visualization of western blots. Densitometry was performed using Adobe Photoshop.

Immunofluorescence Microscropy

Indirect immunofluorescence was conducted as described (Mahjoub *et al.* 2004) using a DeltaVision imaging station (Applied Precision, Issaquah, WA). Primary antibodies used in this study were: mouse monoclonal anti-acetylated-tubulin Igγ2b (1:300; Sigma-Aldrich clone 6-11B-1), mouse monoclonal anti-α-tubulin (1:1000; Sigma-Aldrich clone DM1A) and anti-phosphohistone H3 (ser10, Cell Signalling). Secondary antibodies against mouse IgG2b, mouse IgG1, or rabbit were purchased conjugated to Alexa Fluor 488 or 594 (Invitrogen) and all were used at 1/500. Cells were also stained with DAPI.

For fixation of mitotic cells, a protocol graciously provided by Brian Piasecki and Carolyn Silflow (University of Minnesota, St. Paul, MN), and originally developed by M.A. Sanders, was modified. The fixative consists of 4% formaldehyde (added as formalin, Anachemia), 0.01% glutaraldehyde, 10 mM HEPES buffer pH 7.0, 1 mM EGTA, 1 mM $MgSO_4$ and 0.1% Igepal CA-630 (Sigma-Aldrich) and thus permeabilizes cells but also cross-links cyotological features. After incubation on ice, fixed cells were affixed to coverslips and methanol-extracted essentially as described previously (Mahjoub *et al.*, 2004), except coverslips were washed with ammonium chloride in addition to PBS.

For flagellar remnant determination, cells were counted as "mitotic" if either positive for phospho-histone H3, unhatched and in mother cell walls, or showing either clear reorganization of rootlet microtubules or separated centrosomes.

For the experiment shown in Figure 4E, cells were pre-stained with Lugol's iodine solution (Harris, 1989) and then fixed and permeabilized in MeOH (Cole *et al.*, 1998). Primary antibodies used were mouse anti-acetylated tubulin (Sigma), mouse anti-α tubulin (Sigma, clone DM 1A used at 1/300). Secondary antibodies (Jackson

ImmunoResearch, West Grove, PA) used were CY5-conjugated goat anti-mouse IgG, subclass I, FITC-conjugated goat anti-mouse IgG, subclass 2b (used at 1/100 dilution), and TRITC-conjugated goat anti-rabbit (1/300).

4.4 Results

Initial isolation of two KAT1 knock-down strains.

Currently, the most effective approach to RNA interference in *Chlamydomonas* involves the non-homologous insertion of a transgene which encodes the inhibitory RNA, into the nuclear genome (reviewed by Schroda, 2006). The insertion event is often associated with deletions of genomic sequence and part of the exogenous DNA (Gumpel *et al.*, 1994). Because our initial attempts using conventional methods did not yield katanin knock-down strains, we sought to increase the frequency of recovery of intact insertions. To do this we developed a vector wherein the inhibitory sequence (a hairpin loop corresponding to KAT1 sense and antisense sequence) is flanked by two different selectable markers (Figure 1A).

From fifteen independent transformation experiments, ~1500 colonies grew on plates containing both Zeocin and paromomycin. For initial characterization, we grew six of these isolates and assessed levels of KAT1 mRNA. Although all six had integrated the complete transgene, none of the colonies had reduced levels of KAT1 mRNA (data not shown). In *Chlamydomonas*, RNAi transgenes can be rapidly silenced or suppressed (especially those targeting genes involved in cell cycle progression; Schroda, 2006; Qin *et al.*, 2007) and we were concerned that in growing up sufficient quantities of cells for RNA analysis, suppressed strains would rapidly overtake the culture preventing us from observing authentic knockdowns. In order to narrow our search for KAT1 knock-down

isolates, we conducted a preliminary screen by phase-constrast microscopy. We examined live samples of the ~1500 isolates for gross defects in motility or for defects in deflagellation in response to weak acid (as described in Finst *et al.*, 1998). Fixed samples of each isolate were also examined by phase contrast microscopy for gross changes in ciliary length, number or position or for aberrant cell size (as a proxy for effects on cell cycle progression (Bradley and Quarmby, 2005).

Only two of the 1500 strains exhibited either flagellar or cell size defects, and both of these had the same phenotype: the cells were small relative to the cell wall-less parental strain (Figure 1B) and remained small after backcrossing into a wild-type (cell-walled) background (Figure 1C). In addition, both isolates also exhibited flagellar defects (Figure 1D). Katanin mRNA levels were dramatically reduced in both of these strains (Figure 1E). Although KAT1-RNAi#1 and #4 were clearly katanin knock-down strains, it was important to establish whether the phenotypes were due to the reduced levels of katanin. As described above, generation of transgenic strains in *Chlamydomonas* involves disruption of genomic DNA. We therefore set out to determine the sites of insertion of the RNAi transgenes in order to assess the possible role of these disruptions in affecting the observed phenotypes.

The two original KAT1 knock-down strains are also insertional mutants of flagellar assembly genes

We used a PCR-based approach to clone the DNA flanking the insertions (see Materials and Methods). This approach identified unique sites of insertion in each of the two back-crossed strains. We found that the KAT1-RNAi#4 transgene had inserted into the genomic sequence for the 3' UTR of the *IFT88* gene (C_500002 in version 3 of the *Chlamydomonas* genome), which encodes an intraflagellar transport protein that is

essential for ciliogenesis: *ift88* mutants are flagella-less (Pazour *et al.*, 2000). We confirmed that *IFT88* expression is lost in the KAT1-RNAi#4 strain by RT-PCR (Figure 1F). This result raised the important possibility that the flagella-less phenotype was not a bona fide KAT1-RNAi phenotype but rather was a consequence of the inadvertent knock-out of *IFT88*. It was thus imperative to determine the site of insertion of the transgene in the KAT1-RNAi#1 strain.

We determined that in the KAT1-RNAi#1 strain, the construct had inserted into the coding sequence of a predicted protein kinase G gene, which we will refer to as *PKG2* (C_740056). Primers specific to *PKG2* amplified cDNA from the *cw2* strain, but not from the KAT1-RNAi#1 strain (Figure 1F). We have subsequently determined that PKG2 plays an essential role in ciliogenesis, but does not affect cell size (Rasi *et al.*, unpublished observations.).

Is a defect in ciliogenesis permissive for knock-down of KAT1?

As described above, KAT1 knock-down strains were rare, and the only two that we identified were co-incident with mutations that disrupted ciliogenesis. These observations lead us to hypothesize that KAT1 might indeed be performing an essential function, but whatever this function might be, it is only essential in cells with normal flagella. In other words, we hypothesized that defects in flagellar assembly are permissive for knock-down of katanin. This hypothesis led us to predict that we would recover KAT1 knock-down strains at a much higher frequency if the recipient strain for the transformations was already defective in ciliogenesis.

In order to test this idea, we independently transformed two flagella-less strains, *ift88-1* and *bld1-1* (which is mutant for IFT52, Brazelton *et al.*, 2001; Deane *et al.*, 2001),

as well as wild-type cells, with the same KAT1-RNAi construct described in Figure 1A. In this experiment, we recovered only one isolate that was resistant to both selectable markers when the recipient strain was wild-type. In contrast, ten and eleven isolates were resistant to both Zeocin and paromomycin when the recipient strains were *ift88-1* and *bld1*, respectively. The single KAT1-RNAi isolate from a wild-type background that grew on double selection was not knocked down for *KAT1* mRNA (data not shown). In contrast, 9/10 and 8/11 double-selected isolates, from the transformations of *ift88-1* and *bld1* respectively, had significantly reduced levels of *KAT1* mRNA (Figure 2A and B; representative subset shown). Thus, seventeen new KAT1 knock-down strains were isolated. All of these strains lack flagella (as do the parental strains) and, distinct from the parental strains, all had substantially reduced cell size (see Figure 2C and D; representative subset shown).

In order to more directly assess levels of KAT1, we raised an antibody against two peptides of KAT1 (see Materials and Methods). Western blotting reveals a ~60 kDa band from wild-type *Chlamydomonas* cell lysates, not observed using preimmune serum from the same rabbit (Figure 3A). With this antibody in hand, we repeated the transformation of WT and *bld1* cells with the KAT1-RNAi construct.

In this experiment, 52 isolates grew on double selection when the recipient strain was flagellated (137c). None of these 52 isolates had severely reduced levels of KAT1, but in a few lines KAT1 protein levels were moderately reduced (Figure 3B shows the data for eight of these 52 isolates, including two with moderately reduced levels of KAT1 protein). In this same experiment 14 isolates grew on double selection when the recipient strain was *bld1*. In contrast to the flagellated cells transformed with the same construct,

most of these flagella-less isolates showed reduced levels of KAT1 protein and in some the reduction in KAT1 levels was severe. Of the seven isolates shown in Figure 3C, three show substantial reduction in KAT1 levels, three are moderately reduced and in the seventh KAT1 levels are unaffected.

In this experiment the severely knocked down strains showed distorted cell size profiles (Figure 3E), but unlike the experiment in Figure 2, reduction in cell volume did not correlate with the extent of knock-down of KAT1. It is interesting to note that the knock-down of KAT1 is transient, even in the *bld1* cells. Figure 3D shows that after an additional two weeks, levels of KAT1 are no longer severely reduced. Concomitantly, the cell size profiles become closer to WT (Figure 3E).

What are the cellular consequences of KAT1 knock-down?

In addition to their ciliogenesis defects, the two original KAT1 knock-down isolates had small cells (Figure 1B,C). The other genes disrupted in these strains, *IFT88* and *PKG2*, are essential for ciliogenesis (Pazour *et al.*, 2000; Rasi *et al.*, unpublished observations), but do not affect cell size (data not shown). Furthermore, the seventeen additional KAT1 knock-down strains generated in *ift88-1* and *bld1* backgrounds also had small cells (Figure 2C,D). However, this pattern was not as clear in a subsequent experiment (Figure 3E). Figures 3C and 3D reveal that isolate #29 has the most severe knock-down of KAT1, yet this isolate has unusually large cells (Figure 3E). Nevertheless, the data in Figure 3E also show that the cell size profiles approach wild-type as the levels of KAT1 return to normal. Taking all of these data together, we conclude that reduced levels of KAT1 can influence cell size, but the cell size phenotype is not consistent and appears to depend on some yet-to-be-defined differences in culture conditions.

Aberrant cell size is often an indication of defects in cell cycle progression. Unfortunately, none of the katanin knock-down strains remained phenotypically stable long enough for us to assess their cell cycle characteristics as we have previously done for other *Chlamydomonas* flagellar mutants with cell size defects (Mahjoub *et al.*, 2002; Bradley and Quarmby, 2005). We have attempted several approaches to obtaining conditional KAT1 knock-down strains, but so far none of these strategies has succeeded. Nevertheless, an independent line of study has led us to a possible ciliary-cell cycle role for KAT1. The experiments in the next section may provide the explanation for the difference in susceptibility to KAT1 knock-down of WT compared to *bld* cells.

Basal bodies are released by severing at the proximal transition zone prior to complete resorption of flagella

Taken together, our data thus far indicate that KAT1 plays an important role in *Chlamydomonas* and that this role is obviated in cells that do not have flagella. This suggests that katanin may play a role in coupling the cycle of flagellar resorption and regeneration with cell cycle progression. Our earlier work predicted that the machinery of deflagellation plays a part in pre-mitotic resorption of flagella. Indeed, we predicted that disassembly at the base of flagella might contribute to resorption (Parker and Quarmby, 2003).

The generally accepted model for pre-mitotic resorption of flagella is that disassembly continues down from the tip, through the transition zone of the flagella, until all that is left is the basal body (Cavalier-Smith, 1974). Contrary to this view, the images in Figure 4 reveal that flagella or their derivatives (visualized with indirect immunofluorescence using an antibody against acetylated tubulin) remain with the mother cell wall when cells enter mitosis. In Figure 4, panels A-D reveal pairs of

acetylated tubulin spots associated with the mother cell walls of dividing wild-type cells. The spots, or flagellar remnants, were observed in the mother cell walls of 226 out of 291 (78%) dividing cells. Flagellar remnants are not observed if gluteraldehyde, a cross-linking reagent, is omitted from the fixative, or in a cell wall-less mutant background, suggesting that the remnants are loosely associated with the cell walls (data not shown). Mitotic cells with more substantial incompletely-resorbed flagellar remnants, in some cases almost full-length flagella, were uncommon, but could be found (Figure 4E; also see Piasecki *et al.*, 2007). Importantly, in all of these cells it is clear that the basal bodies have separated from the residual flagella (Figure 4).

These data indicate that a severing event occurs between the basal bodies and the axoneme, releasing the basal bodies for service at the spindle poles. Severing of the axoneme is a well-established event in deflagellation (reviewed in Quarmby, 2004) and we wondered whether the release of basal bodies might be using the same pathway. In order to test this idea, we examined the *fa2* deflagellation-defective mutant. The *fa2-3* strain is null for FA2; the cells are completely defective in the axonemal severing associated with deflagellation and exhibit a G2/M delay in cell cycle progression (Mahjoub *et al.*, 2004). Figure 4F-H show examples of *fa2* cells clearly in mitosis, while retaining flagellar remnants. We examined 157 dividing *fa2-3* cells and observed that 144 (92%) retained flagella or flagellar remnants associated with the mother cell wall. Thus the production of flagellar remnants is at least as common in *fa2* cells as it is in wild-type. Severing in deflagellation occurs at the SOFA, which is distal to the transition zone and it is likely that the separation of basal bodies observed here is a consequence of severing at the proximal end of the transition zone (Figure 6). The proximal severing appears to be

intact in *fa2* mutants, consistent with the observation that the null mutation is not lethal. Taken together with the data of Mahjoub *et al.* (2004), our data indicates that FA2 plays a role in distal but not proximal severing. Katanin may play a role at both sites. Indeed, immuno-gold studies with an anti-katanin antibody revealed katanin at both sites (Lohret *et al.*, 1999).

Knock-down of KAT1 prevents pre-mitotic release of flagella from basal bodies.

We next asked whether the lethality of KAT1 knock-down in flagellated cells might be a consequence of failure to separate basal bodies from flagellar remnants. Our previous experiments indicated that flagellated recipient strains do not survive severe KAT1 knockdown, therefore we examined these colonies five days post-transformation. We used a *cw2* recipient strain in order to observe only flagella and flagellar remnants remaining attached to the basal bodies, without the complication of discarded flagellar remnants retained by association with the mother cell wall.

We examined sixty isolates that grew on paromomycin after transformation of cell wall-less (*cw2*) cells with the empty pNI-537 vector. We observed no flagella on cells with cytokinetic furrows (>20 presumptive dividing cells were examined in each colony; data not shown). These data support the idea that in cells with a normal allotment of katanin, release of the basal bodies from the flagella or flagellar remnants results in the shedding of the flagellar remnant from the cell. In the absence of cell walls, the flagellar remnants are washed away, whereas in walled cells remnants are observed because they are cross-linked to the mother cell wall (Figure 4). We next examined sixty isolates derived from pNI-537-KAT1-RNAi transformation of the same cell wall-less recipient strain. Dividing (furrowed) cells in 27/60 presumptive KAT1-RNAi colonies

had flagella attached to almost all of the furrowed cells observed. Because these cells are wall-less, flagella will only be retained if still anchored at the basal body. Figure 5 shows examples of *cw2* cells presumptively depleted for katanin. In addition, small malformed cells were common in these colonies (data not shown). These data suggest that depletion of KAT1 affects pre-mitotic loss of flagella and leads to gross cellular abnormalities. Most importantly, the presence of flagella on the KAT1-RNAi transformed wall-less cells with apparent cytokinetic furrows is consistent with a failure to separate basal bodies from flagella prior to mitosis.

4.5 Discussion

A phenomenological correlation between ciliary disassembly and entry into mitosis has been known for some time (Tucker *et al.*, 1979). More recently, several proteins have been implicated in coordinating ciliary resorption with cell cycle progression, including AurA, Hef1 and HDAC6 (Pugacheva *et al.*, 2007), and IFT27 (Qin *et al.*, 2007). The presumption has been that ciliary resorption is a consequence of down-regulation of anterograde intraflagellar transport (IFT) and possible upregulation of retrograde IFT, resulting in a net transport of disassembled ciliary components from the tip back to the cell body. While this is almost certainly the case based on the work of Qin et al (2004), our previous work with *Chlamydomonas* mutants revealed that events at the base of the cilium are also important (Parker and Quarmby, 2003). The most dramatic instance of ciliary deconstruction at the base is deflagellation (also known as deciliation; reviewed in Quarmby, 2004). Deflagellation, which usually occurs as a stress response, involves the activation of a signaling pathway that culminates in an increase in intracellular calcium concentration leading to activation of the severing machinery which breaks all nine outer

doublet microtubules at the SOFA. Although some elements of the signaling pathway have been established in *Chlamydomonas*, the actual machinery of severing has not been determined. Katanin has been implicated through biochemical and cell biological studies, but genetic evidence has been elusive. Because we were unable to sustain knock-down of katanin in flagellated cells, the current data do not allow us to test whether KAT1 or one of the other microtubule-severing proteins serves the stress-inducible deflagellation pathway.

Katanin is a conserved eukaryotic protein that has been implicated in the cell cycle since its original purification from M phase oocytes (McNally and Vale, 1993), but its specific role in cell cycle progression has been difficult to define. Evidence is accumulating that the microtubule-severing activity of katanin is required for rearrangement of the interphase microtubule cytoskeleton and concomitant spindle formation (Toyo-Oka et al, 2005), as well as spindle function and disassembly (Buster *et al.*, 2002; McNally *et al.*, 2006; Zhang *et al.*, 2007). Mitotic spindle formation involves multiple pathways, even in a single organism or cell type (Wadsworth and Khodjakov, 2004; O'Connell and Khodjakov, 2007). In flies, but not worms, multiple microtubule-severing enzymes, katanin, spastin, and fidgetin, all have different roles in contributing to mitotic spindle function (Zhang *et al.*, 2007; Srayko *et al.*, 2000). In mice, katanin p60 is recruited to splitting centrosomes by Ndel1 in an Aurora A-dependent manner (Toyo-Oka *et al.*, 2005; Mori *et al.*, 2007), but no obvious Ndel-like proteins are identifiable by tBLASTn in the *Chlamydomonas* genome (version 3.0, accessed July 2008). It is possible that the development of important roles for microtubule-severing in eukaryotic cell division preceded divergence of the microtubule severing proteins. This requires that, in

divergent lineages, different microtubule-severing proteins cooperate with diverse partner proteins to undertake the various specialized severing tasks.

Early evolutionary divergence could also serve to explain differences in subunit interactions. In animal cells katanin is usually isolated as a dimer, comprised of the p60 catalytic subunit and the p80 regulatory subunit (Hartman *et al.*, 1998). A human tumor suppressor, LAPSER, associates with the human p80 subunit and localizes preferentially to the mother centriole, which nucleates the primary cilium (Sudo and Maru, 2008). The *pf15* strain of *Chlamydomonas*, which carries a mutation in the sole katanin p80 subunit found in the genome, has defects in the formation and stability of the central pair of microtubules (Dymek *et al.*, 2004). Intriguingly, the central pair microtubules are nucleated close to the SOFA, where the p60 subunit is implicated in axonemal severing.

We observed that a substantial fraction of mitotic cells retain flagella or flagellar remnants, even though their basal bodies are no longer associated with the retained structures, indicating that the axonemes of these flagella have been successfully severed from their basal bodies. This is consistent with previous observations by electron microscopy of *Chlamydomonas* (Johnson and Porter, 1968) and *Chlorogonium* (Hoops and Witman, 1985) and immunofluorescence microscopy (Piasecki *et al.*, 2007). Based on these data, we propose that katanin-based severing of the axoneme proximal to the flagellar transition zone facilitates entry into mitosis (see Figure 6). We propose that severing proximal to the transition zone results in release of the basal bodies and abandonment of the transition zone at the mother cell wall. Consequently, *Chlamydomonas* cells without flagella do not require katanin.

To be more precise, our model predicts that transition zone-less cells will not depend upon katanin for the release of their basal bodies. In spite of this, we were able to knock-down KAT1 in *bld1* cells, which are capable of building transition zones (Brazelton *et al*., 2001; Deane *et al*., 2001). Our model suggests that the key event for mitosis is the release of basal bodies and that this it occurs by severing at the proximal end of the transition zone. In this case, why are flagella-less cells more tolerant of katanin knock-down than wild-type cells, even though both build transition zones? The higher frequency of recovery of knock-down strains might be indicative of a subpopulation of *bld1* cells that do not assemble transition zones, or transition zones that are less stable than wild-type. We think it more likely that there is an alternate mechanism to free basal bodies from transition zones, and in the absence of the need to disassemble flagella prior to mitosis, this alternate, albeit less efficient, pathway is taken.

It is interesting to note that in both *bld1* and wild-type cells, katanin may itself contribute to the process of RNAi-mediated knockdown. Recently, in the plant *Arabidopsis,* Argonaute-mediated translational suppression via the siRNA pathway was shown to be dependent on katanin (Broderson *et al.*, 2007) acting through an as yet unknown mechanism. If this is true in *Chlamydomonas,* then it is likely that katanin knockdown may be unsustainable, even in the absence of direct effects on cell cycle or growth.

We propose that severing at the proximal transition zone is an important activity of katanin in *Chlamydomonas* and possibly mammalian cells, but not necessarily all ciliated cells. For example, in *Tetrahymena,* another genetic model system for the study of cilia, misexpression of katanin affects ciliary length but does not result in a cell cycle

phenotype (Sharma *et al.*, 2007). However, in *Chlamydomonas* but not in *Tetrahymena,* ciliary basal bodies must be detached from their axonemes prior to mitosis, thus any proteins that affect this process in *Chlamydomonas* may cause a cell cycle phenotype, whereas such an effect would not be predicted in *Tetrahymena*.

Flagella-less cells can survive and divide without katanin, but in some of the isolates the cells are small (or large), and the KAT1 knock-down is quickly lost. To date, these cultures have not survived as KAT1 knock-down strains long enough for us to determine the reason for the cell size defects and our attempts to develop conditional strains have failed. It is possible that the cell size phenotype might not be related to severing of the proximal transition zone because katanin has been implicated in several other mitotic events (Buster *et al.*, 2002; Toyo-Oka *et al*., 2005; McNally *et al.*, 2006). In addition, microtubule severing by katanin regulates non-centrosomal microtubule arrays (Roll-Mecak and Vale, 2006) and in *Chlamydomonas*, a cortical array of non-centrosomal microtubles play important roles in cytokinesis (Ehler *et al.*, 1995). We speculate that katanin plays several fundamental roles essential to cell cycle progression in both *Chlamydomonas* and mammalian cells and that one of these roles is related to severing of the ciliary axoneme at the proximal transition zone prior to mitosis.

We have shown that *Chlamydomonas* cells free their basal bodies from flagella prior to mitosis. Katanin-mediated severing at the cell-proximal end of the transition zone is the likely mechanism for this disengagement, because of the relative ease with which katanin can be knocked down in flagella-less cells versus wild-type cells. This conclusion gains further support from our observation that presumptive KAT1 knockdown cells retain flagella during division. In retrospect, our initially perplexing observation that the

two original KAT1 knock-down isolates both coincidentally disrupted genes required for ciliogenesis is predictable.

4.6 Acknowledgements

We are grateful to Shazina Khan for her excellent technical support and persistent good cheer. We thank Brian Piasecki and John Glover for stimulating discussions and we further appreciate John Glover for valuable comments on the manuscript. We are deeply indebted to two persistent and thorough anonymous reviewers who guided us to substantial improvements in the quality of this work Laura Hilton and Marc Champigny are also thanked for comments that improved the quality of the final draft. We thank Heriberto Cerutti for providing pNI-537. We are deeply indebted to J. Salisbury (Mayo) for continuing to generously provide us with anti-centrin antibody. This work was supported primarily by an operating grant from the Canadian Institutes of Health Research to LMQ (MOP-37861) and in part by NIH grant # R01-GM077004 to WFM. JLF is supported by an NSF predoctoral fellowship and a UC Fletcher Jones fellowship.

4.7 Figures and Tables

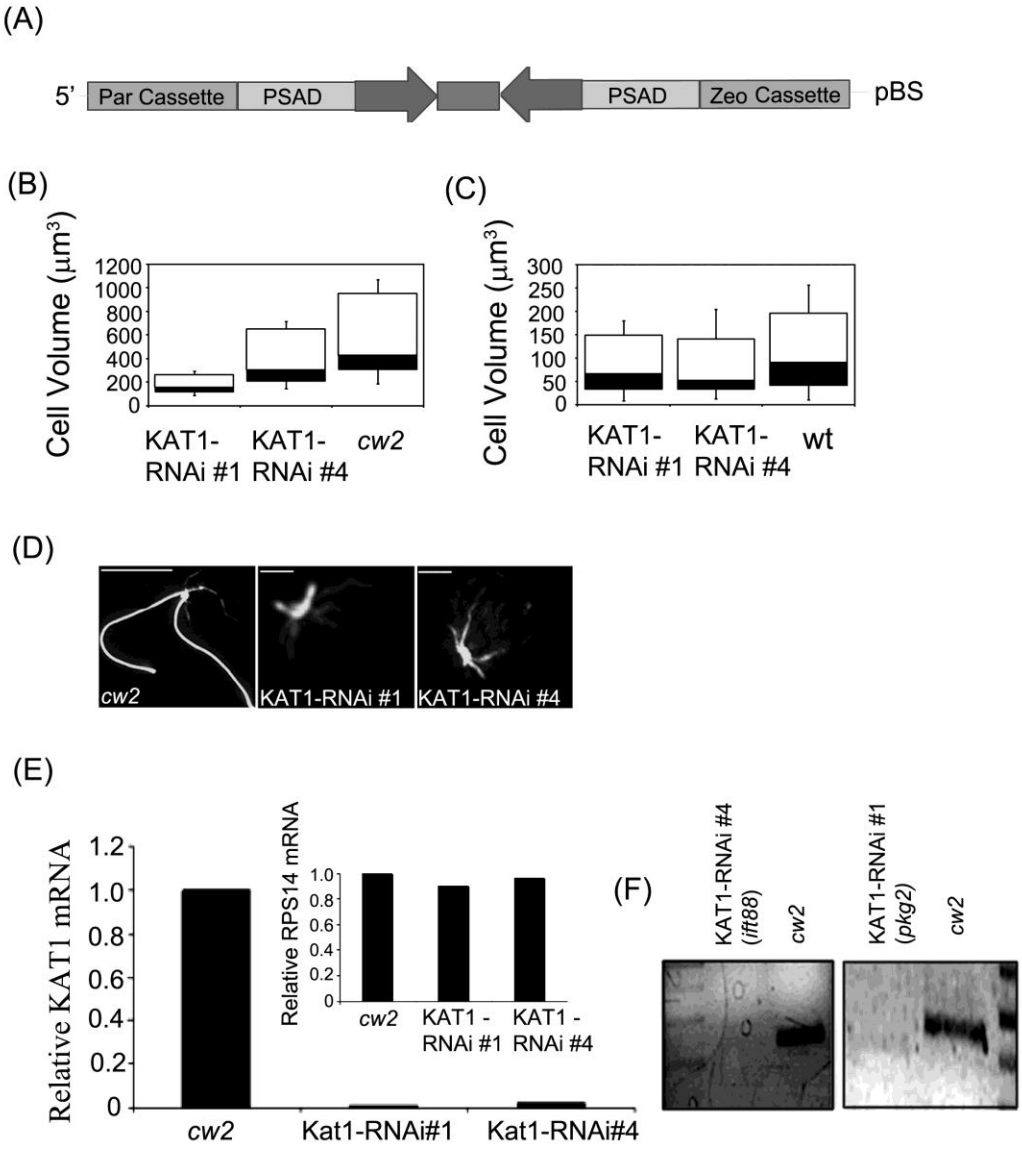

Figure 4-1. Isolation of two KAT1 knock-down strains.

(A). pEZ-KAT1-RNAi construct used to generate stable RNAi lines. Cells transformed with this construct were sequentially selected on plates containing paramomycin, then plates containing Zeocin, to confirm the presence of the PsaD-driven hairpin targeting KAT1 (large inward-pointing arrows).

Legend continued on next page.

Figure 4-1 Legend, continued.

(B). Box plots of cell volume distributions of two KAT1-RNAi isolates and the parental cw2 strain. Boxes encompass 50% of all data points (the interquartile range) and error bars encompass 90% of all data points. The boundary between the black and white boxes is the median cell volume.

(C). Box plots of cell volumes of both KAT1-RNAi isolates after backcross to a wild-type (cell walled) strain, as well as the wild-type cell volume. Boxes encompass the interquartile range and error bars encompass 90% of all data points.

(D). Anti-acetylated tubulin immunofluorescence visualization of typical cells from each isolate (right panels) shows lack of flagella in both KAT1-RNAi isolates. Scale bars, (cw2 panel) 7.5 μm, (KAT1-RNAi#1 and KAT1-RNAi#4, 2.5μm).

(E). Quantification of mRNA from *cw2* and the two KAT1-RNAi strains. Main graph shows relative KAT1 level (the amount of KAT1 mRNA in *cw2* cells is set at 1). The inset graph shows relative control transcript (RPS14) level.

(F). Agarose gel electrophoresis of reverse-transcriptase PCR products. Amplicons targeted putative genes disrupted by insertion of KAT1-RNAi constructs into strain KAT1-RNAi#4 (left panel) and KAT1-RNAi#1 (right panel). All cDNA pools showed accumulation of PCR products targeting a control gene (not shown).

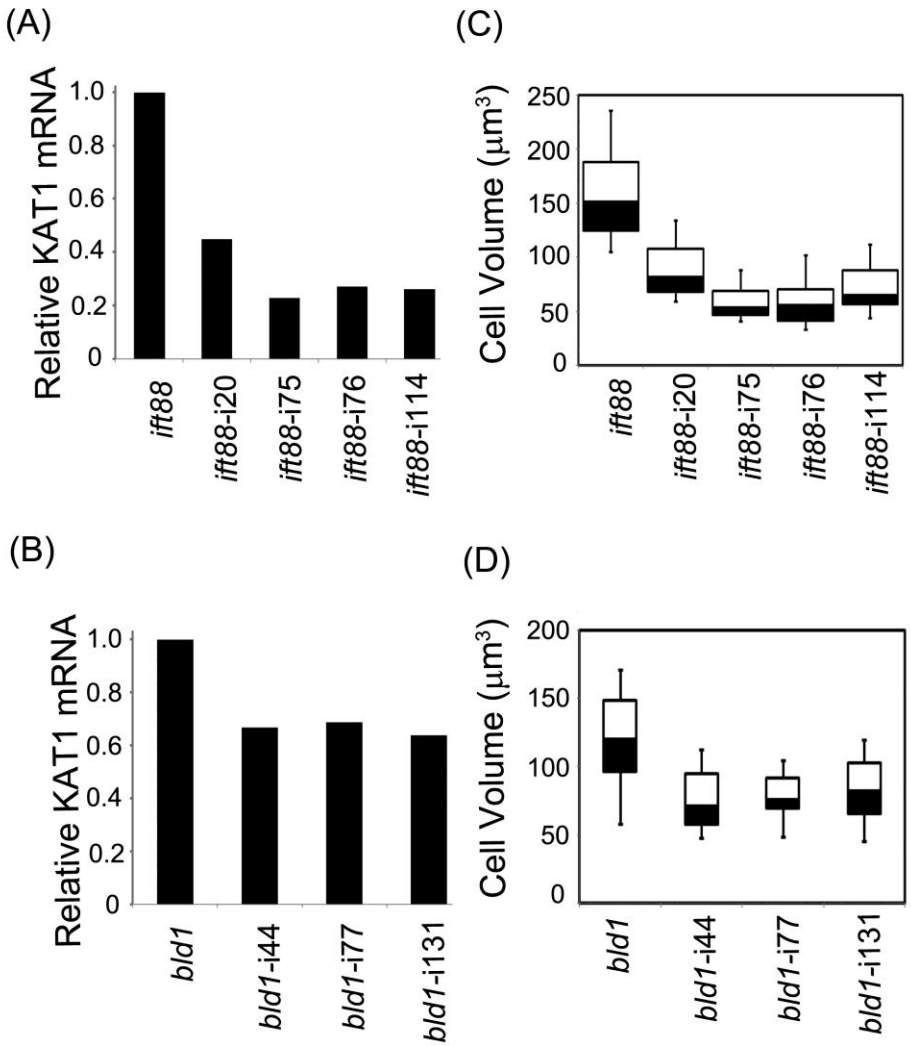

Figure 4-2. *KAT1* can be readily knocked down in flagella-less cells.

(A). Relative *KAT1* mRNA level, as determined by real-time PCR, from a representative subset of *ift88* strains transformed with, and selected for, pEZ-KAT1-RNAi.

(B). Relative *KAT1* mRNA level, as determined by real-time PCR, from a representative subset of *bld1* strains transformed with, and selected for, pEZ-KAT1-RNAi.

(C). Box plots of cell volume distribution of the same *ift88*-KAT1-RNAi isolates examined in (A). Error bars capture 90% of cells.

(D). Box plots of cell volume distribution of the same *bld1*-KAT1-RNAi isolates examined in (A). Error bars capture 90% of cells.

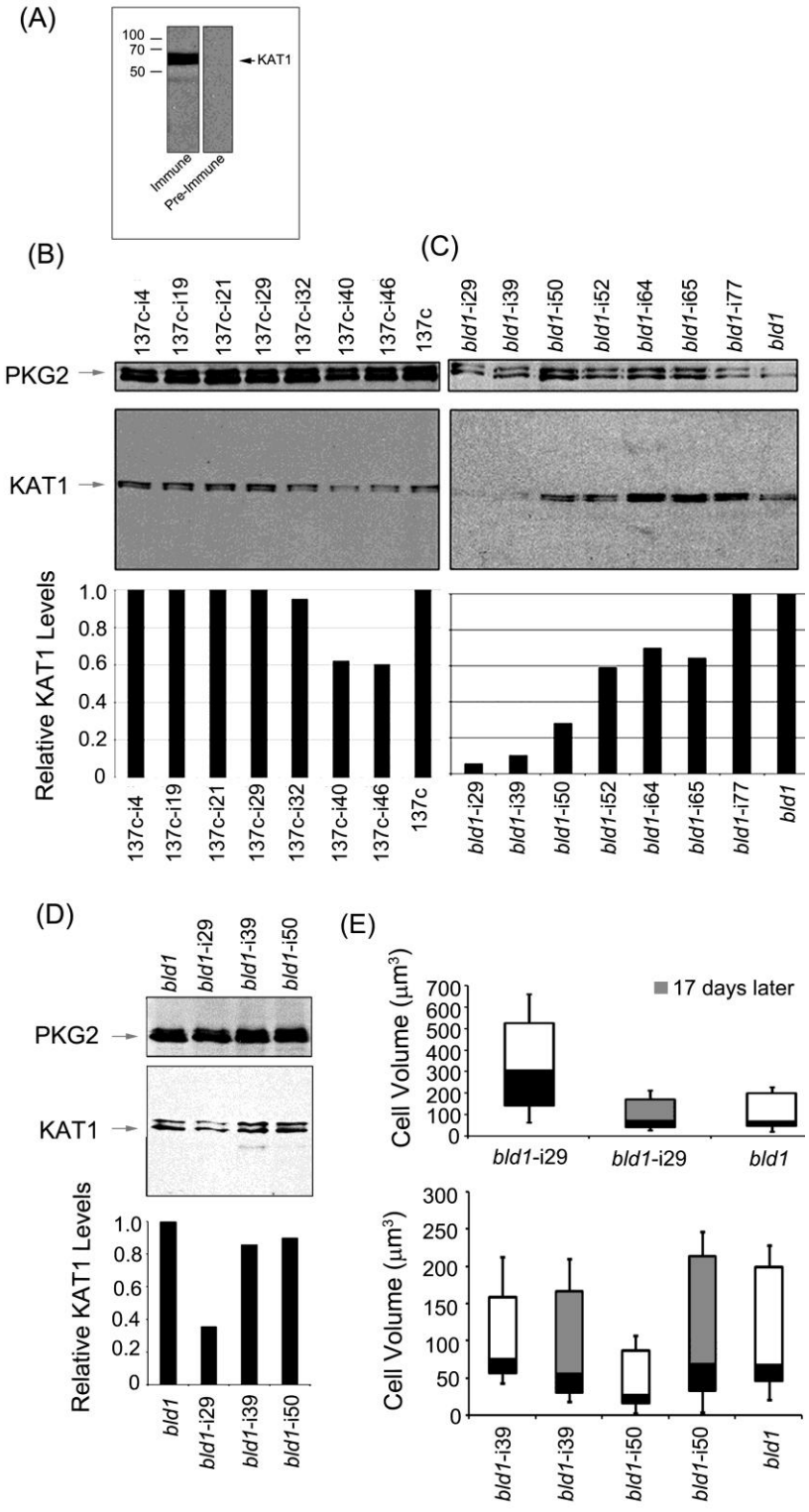

Figure 4-3. KAT1 protein can be readily knocked down in *bld1* mutants.

Full Legend on next page.

Figure 4-3. KAT1 protein can be readily knocked down in *bld1* mutants.

(A). Characterization of anti-KAT1 antiserum. Wild-type cell lysate was blotted in duplicate and probed with either immune antiserum (left panel) or pre-immune serum from the same rabbit (right panel). The expected molecular weight of KAT1 is 60kDa.

(B). Quantification of relative knock-down of KAT1 protein levels by anti-KAT1 western blot (middle panel) in seven random isolates recovered from transformation of wild-type cells with pEZ-KAT1-RNAi. Anti-PKG2 was used as a loading control by re-probing the same blot (top panel). Gel films were scanned and densitometric analysis (bottom panel) performed as described in Methods.

(C). Quantification of relative knock-down of KAT1 protein levels by anti-KAT1 western blot (middle panel) in seven random isolates recovered from transformation of *bld1* cells with pEZ-KAT1-RNAi. Anti-PKG2 was used as a loading control by re-probing the same blot (top panel). Gel films were scanned and densitometric analysis (bottom panel) performed as described in Methods.

(D). Quantification of relative knock-down of KAT1 protein levels in a subset of the same isolates examined in (C) after an additional two weeks of growth. Analysis as described for (C).

(E). Box plots showing cell volumes of the same *bld1*:KAT1-RNAi isolates examined in (B) and (C). White boxes show cell volume distribution data from the time of the experiment shown in (B) and grey boxes are data from the time of the experiment shown in (C). Boxes encompass the interquartile range and error bars encompass 90% of the total data points.

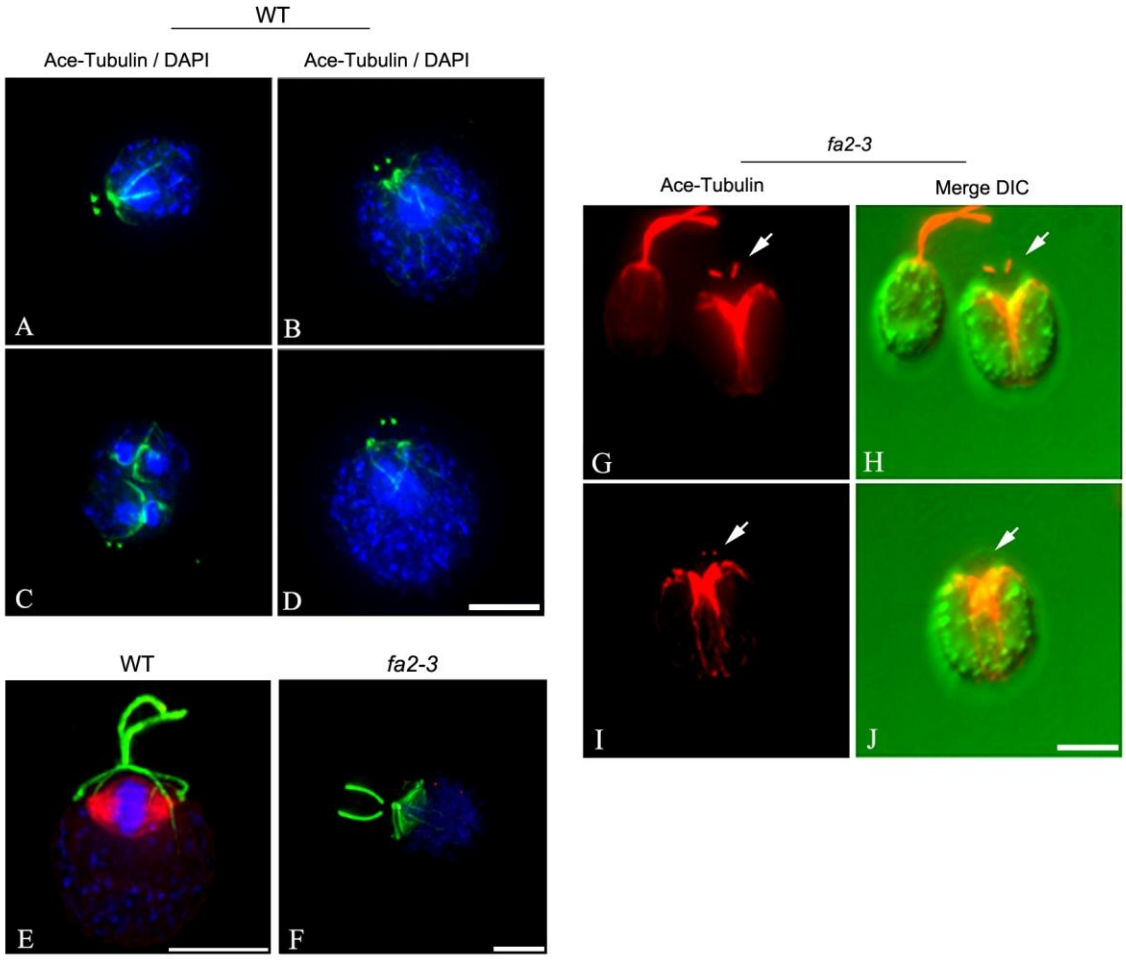

Figure 4-4. Basal bodies are freed from flagella by severing prior to mitosis.

(A-D). Representative images of flagellar remnants associated with representative wild-type mitotic cells. Remnants are visible as dots staining for acetylated-α-tubulin (green) and are found at the anterior end of the cell (A, B, D) or in a position consistent with the prior anterior of the mother cell, in cells that have completed at least one round of division (C). Blue is DAPI, which stains both nuclear and plastid DNA.

(E). Longer flagella (stained with anti-acetylated tubulin; green) are observed more rarely in wild-type mitotic cells. The spindle of this cell visualized with anti-α-tubulin (red).

(F-J). Remnants are found in mitotic *fa2* mutant cells. (F) a *fa2* cell early in cell division has relatively long flagella as stained by acetylated tubulin (green), counterstained with DAPI (blue). (G, I), *fa2* cells later on in cell division, as indicated by the presence of cleavage furrows, have flagellar remnants as visualized by acetylated-tubulin staining (red; the primary antibody for these cells was a mixture of anti-acetylated- and anti-α-tubulin) (H,J), overlay with corresponding DIC images.

Scale bars, 5 μm.

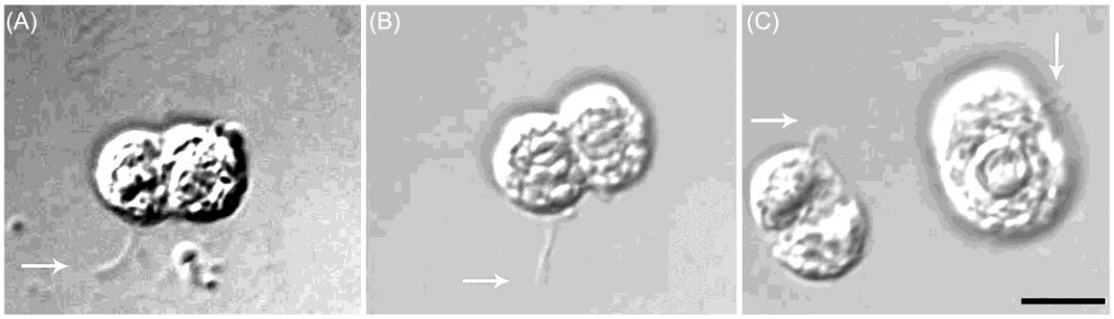

Figure 4-5. DIC images of presumptive *cw2*:KAT1-RNAi cells.

(A-C). Examples of presumptive KAT1 knock-down cells in a *cw2* (cell wall-less mutant) background. Note the presence of flagella on dividing cells. Similar cells were not seen in any control colonies. Scale bar, 5 µm.

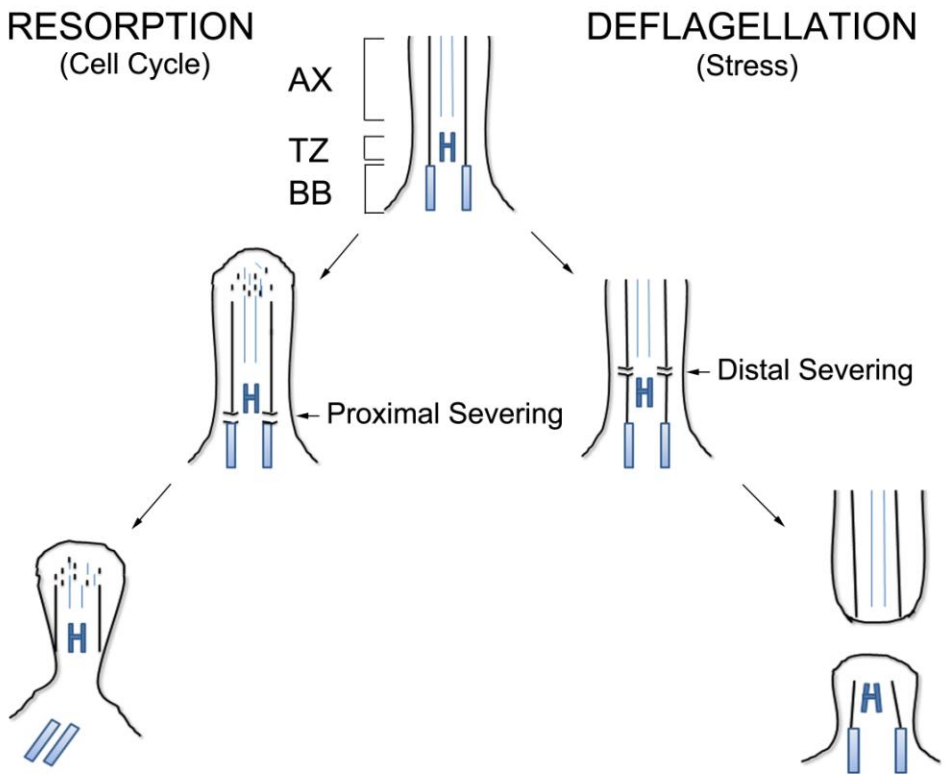

Figure 4-6. Severing may occur at either end of the flagellar transition zone.

Deflagellation in response to stress involves severing at the distal end of the transition zone (the SOFA), after which the flagellum is cast away from the cell while the transition zone remains associated with the basal body and can nucleate the assembly of a new flagellum.

Resorption before mitosis involves both shortening of the flagellum from its distal end and severing at the proximal transition zone. This proximal severing frees the basal body, leaving the transition zone. Any residual flagella, or flagellar remnants, remain associated with the cell wall.

Abbreviations: AX, axoneme; TZ, transition zone; BB, basal body

Table 4-1. Sequences of the oligonucleotides used in this work.

All sequences are listed in the 5'-3' direction. Plus and minus signs denote forward and reverse primer orientation respectively.

Primer Name	Sequence
Spe-par(+)	5' ATAACTAGTGAGCTCGCTGAGGCTTGA 3'
Spe-par(-)	5' ATAACTAGTGGTACCCGCTTCAAATAC 3'
Kat-EcoRI(+)	5'TAAGAATTCATCACTCGG TACGTCCGC 3'
Kat-Spacer(-)	5' TAAGGATCCCGCCGAGCCGGCGCGCCC 3'
Kat-IR(+)	5' ATATCTAGAGAATTCATCACTCGGTACGTCCGC 3'
Kat-IR(-)	5' ATTGGATCCCAGACCCGCAATGTCGTC 3'
K311A-1 (+)	5' CGGGACCGGCGCGACCATGCTCGCC 3'
KAT 1440-64 (-)	5' GGACCCGGCTCCTTGTCCTTTTCGC 3'
PKG-RT(+)	5' AACCAAGCTTTTTGTTGTGAGTGG 3'
PKG-RT(-)	5' CGGAAGACGTCGCGCTCCAGCA 3'
IFT88-RT(+)	5' ATAGTGATATCATTCAAGCCCTGTTCCTAC 3'
IFT88-RT(-)	5' GTGTGTGAATGTATGTGTGTGCTAGGTAAG 3'
Qcp60(+)	5' AACAGCTACCCCGAGATGAA 3'
Qcp60(-)	5' TTGTTGTTGTTAGCCCAGGA 3'
Bubble1	5'GAGAGGGAAGAGAGCAGGCAAGGAATGGAA-GCTGTCTGTCGCA GGAGGAAG 3'
Bubble2	5'GACTCTCCCTTCTCGAATCGTAACCGTTCGTAC-GAGAA TCGCTGTCCTCTCCTTC 3'
B-specific	5'CGAATCGTAACCGTTCGTACGAGAATCGCT 3'
Par-specific	5' TGGCGTTTTACCGGCTGTTGGACGAGTTC 3'

4.8 References

Bradley, B.A., and Quarmby, L.M. (2005). A NIMA-related kinase, Cnk2p, regulates both flagellar length and cell size in *Chlamydomonas*. J Cell Sci *118*, 3317-3326.

Brazelton, W.J., Amundsen, C.D., Silflow, C.D., Lefebvre, P.A. (2001). The bld1 mutation identifies the *Chlamydomonas* osm-6 homolog as a gene required for flagellar assembly. Curr Biol. 11(20):1591-4.

Brodersen, P., Sakvarelidze-Achard, L., Bruun-Rasmussen, M., Dunoyer, P., Yamamoto, Y.Y., Sieburth, L.,and Voinnet, O. (2008). Widespread translational inhibition by plant miRNAs and siRNAs. Science. *320*(5880):1185-90.

Buster, D., McNally, K., and McNally, F.J. (2002). Katanin inhibition prevents the redistribution of gamma-tubulin at mitosis. J Cell Sci *115*, 1083-1092.

Cavalier-Smith T. (1974). Basal body and flagellar development during the vegetative cell cycle and the sexual cycle of *Chlamydomonas reinhardii*. J Cell Sci. *16*, 529-56.

Cole, D.G., Diener, D.R., Himelblau, A.L., Beech, P.L., Fuster, J.C., and Rosenbaum, J.L. (1998). *Chlamydomonas* kinesin-II-dependent intraflagellar transport (IFT): IFT particles contain proteins required for ciliary assembly in *Caenorhabditis elegans* sensory neurons. J Cell Biol. *141*(4):993-1008.

Deane, J.A., Cole, D.G., Seeley, E.S., Diener, D.R., and Rosenbaum, J.L. (2001). Localization of intraflagellar transport protein IFT52 identifies basal body transitional fibers as the docking site for IFT particles. Curr Biol *11*, 1586-1590.

Dymek, E.E., Lefebvre, P.A., and Smith, E.F. (2004). PF15p is the *Chlamydomonas* homologue of the Katanin p80 subunit and is required for assembly of flagellar central microtubules. Eukaryotic Cell *3*, 870-879.

Ehler, L.L., Holmes, J.A., and Dutcher, S.K. (1995). Loss of spatial control of the mitotic spindle apparatus in a *Chlamydomonas reinhardtii* mutant strain lacking basal bodies. Genetics *141*, 945-960.

Feldman, J.L., Geimer, S., and Marshall, W.F. (2007). The mother centriole plays an instructive role in defining cell geometry. PLoS Biol *5*, e149.

Finst, R.J., Kim, P.J., and Quarmby, L.M. (1998). Genetics of the deflagellation pathway in *Chlamydomonas*. Genetics *149*, 927-936.

Fischer, N., and Rochaix, J.D. (2001). The flanking regions of PsaD drive efficient gene expression in the nucleus of the green alga *Chlamydomonas reinhardtii*. Mol Genet Genomics *265*, 888-894.

Gumpel, N.J., Rochaix, J.D., and Purton, S. (1994). Studies on homologous recombination in the green alga *Chlamydomonas reinhardtii*. Curr Genet *26*, 438-442.

Harris, E. (1989). The *Chlamydomonas* Sourcebook: A Comprehensive Guide to Biology and Laboratory Use. Academic Press: San Diego.

Hartman, J.J., Mahr, J., McNally, K., Okawa, K., Iwamatsu, A., Thomas, S., Cheesman, S., Heuser, J., Vale, R.D., and McNally, F.J. (1998). Katanin, a microtubule-severing protein, is a novel AAA ATPase that targets to the centrosome using a WD40-containing subunit. Cell *93*, 277-287.

Hoops, H.J., and Witman, G.B. (1985). Basal bodies and associated structures are not required for normal flagellar motion or phototaxis in the green alga Chlorogonium elongatum. J Cell Biol. *100*(1):297-309

Johnson, U.G., and Porter, K.R. (1968). Fine structure of cell division in *Chlamydomonas* reinhardi. Basal bodies and microtubules. J Cell Biol *38*, 403-425.

Kathir, P., LaVoie, M., Brazelton, W.J., Haas, N.A., Lefebvre, P.A., and Silflow, C.D. (2003). Molecular map of the *Chlamydomonas reinhardtii* nuclear genome. Eukaryot Cell *2*, 362-379.

Kindle, K.L., Schnell, R.A., Fernandez, E., and Lefebvre, P.A. (1989). Stable nuclear transformation of *Chlamydomonas* using the *Chlamydomonas* gene for nitrate reductase. J Cell Biol *109*, 2589-2601.

Lohret, T.A., McNally, F.J., and Quarmby, L.M. (1998). A role for katanin-mediated axonemal severing during *Chlamydomonas* deflagellation. Mol Biol Cell *9*, 1195-1207.

Lohret, T.A., Zhao, L., and Quarmby, L.M. (1999). Cloning of *Chlamydomonas* p60 katanin and localization to the site of outer doublet severing during deflagellation. Cell Motil Cytoskeleton *43*, 221-231.

Lumbreras, V.S., David R.; Purton, Saul. (1998). Efficient foreign gene expression in *Chlamydomonas reinhardtii* mediated by an endogenous intron. The Plant Journal, *14*, 441-447.

Mahjoub, M.R., Montpetit, B., Zhao, L., Finst, R.J., Goh, B., Kim, A.C., and Quarmby, L.M. (2002). The FA2 gene of *Chlamydomonas* encodes a NIMA family kinase with roles in cell cycle progression and microtubule severing during deflagellation. J Cell Sci *115*, 1759-1768.

Mahjoub, M.R., Qasim Rasi, M., and Quarmby, L.M. (2004). A NIMA-related kinase, Fa2p, localizes to a novel site in the proximal cilia of *Chlamydomonas* and mouse kidney cells. Mol Biol Cell *15*, 5172-5186.

Marshall, W.F., and Nonaka, S. (2006). Cilia: tuning in to the cell's antenna. Curr Biol *16*, R604-614.

Marshall, W.F., and Rosenbaum, J.L. (2001). Intraflagellar transport balances continuous turnover of outer doublet microtubules: implications for flagellar length control. J Cell Biol *155*, 405-414.

McNally, F.J. and Vale, R.D. (1993). Identification of katanin, an ATPase that severs and disassembles stable microtubules. Cell *75*(3):419-29.

McNally, K., Audhya, A., Oegema, K., and McNally, F.J. (2006). Katanin controls mitotic and meiotic spindle length. J Cell Biol *175*, 881-891.

Mori, D., Yano, Y., Toyo-oka, K., Yoshida, N., Yamada, M., Muramatsu, M., Zhang, D., Saya, H., Toyoshima, Y.Y., Kinoshita, K., Wynshaw-Boris, A., and Hirotsune, S. (2007). NDEL1 phosphorylation by Aurora-A kinase is essential for centrosomal maturation, separation, and TACC3 recruitment. Mol Cell Biol. *27*(1):352-67.

O'Connell, C.B. and Khodjakov, A.L. (2007). Cooperative mechanisms of mitotic spindle formation. J Cell Sci. *120*:1717-22

Pan, J., and Snell, W. (2007). The primary cilium: keeper of the key to cell division. Cell. *129*(7):1255-7.

Parker, J.D., and Quarmby, L.M. (2003). *Chlamydomonas* fla mutants reveal a link between deflagellation and intraflagellar transport. BMC Cell Biol *4*, 11.

Pazour, G.J., Dickert, B.L., Vucica, Y., Seeley, E.S., Rosenbaum, J.L., Witman, G.B., and Cole, D.G. (2000). *Chlamydomonas* IFT88 and its mouse homologue, polycystic kidney disease gene tg737, are required for assembly of cilia and flagella. J Cell Biol *151*, 709-718.

Piasecki, B.P., LaVoie, M, Tam, L-W., Lefebvre, P.A., and Silflow, C.D. (2007). The Uni2 Phosphoprotein is a Cell Cycle–regulated Component of the Basal Body Maturation Pathway in *Chlamydomonas reinhardtii*. Mol Biol Cell 19: 262-273.

Pugacheva, E.N., Jablonski, S.A., Hartman, T.R., Henske, E.P., and Golemis, E.A. (2007). HEF1-dependent Aurora A activation induces disassembly of the primary cilium. Cell *129*, 1351-1363.

Qin, H., Diener, D.R., Geimer, S., Cole, D.G., and Rosenbaum, J.L. (2004). Intraflagellar transport (IFT) cargo: IFT transports flagellar precursors to the tip and turnover products to the cell body. J Cell Biol. *164*(2):255-66.

Qin, H., Wang, Z., Diener, D., and Rosenbaum, J. (2007). Intraflagellar transport protein 27 is a small G protein involved in cell-cycle control. Curr Biol *17*, 193-202.

Quarmby, L.M. (2004). Cellular deflagellation. Int Rev Cytol *233*, 47-91.

Quarmby, L.M., and Parker, J.D. (2005). Cilia and the cell cycle? J Cell Biol *169*, 707-710.

Rieder, C.L., Jensen, C.G., and Jensen, L.C. (1979). The resorption of primary cilia during mitosis in a vertebrate (PtK1) cell line. J Ultrastruct Res. *68*(2):173-85.

Riley, J., Butler, R., Ogilvie, D., Finniear, R., Jenner, D., Powell, S., Anand, R., Smith, J.C., and Markham, A.F. (1990). A novel, rapid method for the isolation of terminal sequences from yeast artificial chromosome (YAC) clones. Nucleic Acids Res *18*, 2887-2890.

Rohr, J., Sarkar, N., Balenger, S., Jeong, B., and Cerutti H. (2004). Tandem inverted repeat system for selection of effective transgenic RNAi strains in *Chlamydomonas*. The Plant Journal 40 (4), 611–621

Roll-Mecak, A., and Vale, R.D. (2006). Making more microtubules by severing: a common theme of noncentrosomal microtubule arrays? J Cell Biol *175*, 849-851.

Schroda, M. (2006). RNA silencing in *Chlamydomonas*: mechanisms and tools. Curr Genet *49*, 69-84.

Sharma, N., Bryant, J., Wloga, D., Donaldson, R., Davis, R.C., Jerka-Dziadosz, M., and Gaertig, J. (2007). Katanin regulates dynamics of microtubules and biogenesis of motile cilia. J Cell Biol *178*, 1065-1079.

Sizova, I., Fuhrmann, M., and Hegemann, P. (2001). A Streptomyces rimosus aphVIII gene coding for a new type phosphotransferase provides stable antibiotic resistance to *Chlamydomonas reinhardtii*. Gene *277*, 221-229.

Srayko, M., Buster, D.W., Bazirgan, O.A., McNally, F.J., and Mains, P.E. (2000). MEI-1/MEI-2 katanin-like microtubule severing activity is required for *Caenorhabditis elegans* meiosis.Genes Dev. *14*(9):1072-84.

Sudo, H. and Maru, Y. (2008). LAPSER1/LZTS2: a pluripotent tumor suppressor linked to the inhibition of katanin-mediated microtubule severing. Hum Mol Genet. *17*(16), 2524-40

Toyo-Oka, K., Sasaki, S., Yano, Y., Mori, D., Kobayashi, T., Toyoshima, Y.Y., Tokuoka, S.M., Ishii, S., Shimizu, T., Muramatsu, M., Hiraiwa, N., Yoshiki, A., Wynshaw-Boris, A., and Hirotsune, S. (2005). Recruitment of katanin p60 by phosphorylated NDEL1, an LIS1 interacting protein, is essential for mitotic cell division and neuronal migration. Hum Mol Genet. *14*(21):3113-28.

Tucker, R.W., Pardee, A.B., and Fujiwara, K. (1979). Centriole ciliation is related to quiescence and DNA synthesis in 3T3 cells. Cell *17*(3):527-35.

Umen, J.G., and Goodenough, U.W. (2001). Control of cell division by a retinoblastoma protein homolog in *Chlamydomonas*. Genes Dev *15*, 1652-1661.

Wadsworth, P., and Khodjakov, A. (2004). E pluribus unum: towards a universal mechanism for spindle assembly. Trends Cell Biol. *14*(8):413-9.

Wang, A.M., Doyle, M.V., and Mark, D.F. (1989). Quantitation of mRNA by the polymerase chain reaction. Proc Natl Acad Sci U S A *86*, 9717-9721.

Zhang, D., Rogers, G.C., Buster, D.W., and Sharp, D.J. (2007). Three microtubule severing enzymes contribute to the "Pacman-flux" machinery that moves chromosomes. J Cell Biol. *177*(2):231-42.

CHAPTER 5
CONCLUSIONS AND FUTURE WORK.

5.1 IFT, Resorption, and Deflagellation

In Chapter 2, I examined *fla10* mutants, which are *Chlamydomonas* temperature-sensitive intraflagellar transport (IFT) mutants. These mutants were previously thought to gradually resorb their flagella at the restrictive temperature because of the absence of IFT-mediated assembly to balance constitutive flagellar disassembly [Marshall and Rosenbaum, 2001]. I made two significant observations that suggest otherwise. First, while *fla10* mutants do resorb at the restrictive temperature in the absence of calcium, they deflagellate instead if a physiologically-relevant concentration of calcium is present in the medium (Figure 2-1). Second, double mutants of *fla10* with mutants unable to deflagellate, *fa1* or *fa2*, resorb their flagella much more slowly than *fla10* single mutants (Figure 2-6). These data led me to propose the hypothesis that severing at the transition zone, such as occurs during deflagellation, might also be occurring during resorption.

If the resorption of *fla* mutants was due to only a lack of anterograde IFT, then it ought not to matter whether calcium is present in the medium and the resorption should take the same time in a deflagellation-mutant background. The lesion in the *fla10-1* allele, the allele I used, is a single amino acid change at a conserved lysine residue in the motor domain [Vashishtha et al., 1996], and in *fla10-1* mutants this mutation results in the depletion of the anterograde IFT motor from flagella at the restrictive temperature [Cole et al., 1998]. Since *fa;fla10* mutants retain flagella much longer than *fla10* mutants

at the restrictive temperature, then either the *fa* mutations are rescuing the mutant FLA10 protein function, and thus sustaining anterograde IFT, or the *fa* mutants must be instead preventing efficient disassembly of flagella. The latter possibility is much more likely, as the *fa* mutants were isolated in a screen for flagellar disassembly [Finst et al., 1998].

Resorbing flagella were thought to only disassemble from their distal ends [Cavalieri-Smith, 1974; Marshall and Rosenbaum, 2001]. However, both FA1 and FA2 localize to the opposite end of the flagellum, at the distal transition zone [Figure 5-1; Mahjoub et al., 2004]. The simplest explanation is therefore that the slow resorption phenotype of *fa;fla* double mutants be related to the deflagellation defect of *fa* mutants, and thus leads to the hypothesis that resorption involves severing at the transition zone. If axonemal components are indeed being removed at the transition zone in resorbing cells, then this could be tested by examining individual resorbing *fa;fla* cells from the restrictive temperature are motile upon shifting to the permissive temperature. Such cells would not be predicted to recover flagellar length, as new FLA10 protein must be made before anterograde IFT could begin (even FLA10 single mutants undergo a ~1 hour lag in assembly upon shift to the permissive temperature (data not shown)). The motility of resorbing cells is predicted to be impaired if subunits have been removed at the transition zone and there are no longer continuous microtubules between the basal bodies and the flagella (however, related algae are motile without having their flagella and basal bodies linked [Hoops and Witman, 1985]).

As for the identity of the hypothetical deflagellation signal in IFT-defective cells (Figure 2-8), there has been no follow-up on this aspect, so I will speculate. It is possible that calcium itself is the signal, and that resorption in *fla* mutants leads to leakiness in the

flagellar membrane and allows extracellular calcium to enter the cell and activate the severing machinery. This hypothesis would be technically very difficult to test. It would also not provide an explanation for deflagellation in terms of evolutionary adaptation: The best-characterized pathway leading to deflagellation is treatment with weak organic acids, and *Chlamydomonas* is rarely suddenly exposed to vinegar in its natural habitats, as it is during acid-shock experiments. That being said, it is interesting that *chronic* exposure to low pH, such that could occur in soils, leads *Chlamydomonas* to differentiate into a palmelloid state, in which the cells become large, aflagellate, and surrounded by a mucilage-like material [Visiviki and Santikul, 2000].

Thus, I still favour the idea of a signal that leads to deflagellation. Such a signal could be inhibitory, so that normal IFT blocks deflagellation, or instructive, such that a defect in IFT actively signals deflagellation. I hypothesize that deflagellation due to defective IFT could be an evolutionary adaptation because *Chlamydomonas* cells can rapidly regenerate their flagella after deflagellation, and this could potentially restore motility more quickly than repairing a damaged flagellum in which IFT is blocked. From an adaptive viewpoint, an inhibitory signal seems more suitable as it is more conservative: a cell would require all its IFT particles to be defective (due to mechanical disruption, as possibly in the case of predation, in which *Chlamydomonas* flagella may be physically constrained) before taking the drastic step of deflagellating. In the case of predation, this deflagellation could potentially allow the cell to escape and re-grow new flagella [Pickett-Heaps and Pickett-Heaps, 1995]. A paradigm for this would be the mitotic Mad2-based system in which anaphase is inhibited until all chromosomes are properly attached to kinetochore microtubules [Nasmyth, 2005]. But for

IFT/deflagellation, how could functional IFT be sensed? Wemmer and Marshall [2007] have suggested that cells may monitor IFT in a simple manner. In this model, each IFT particle is confined to an individual outer doublet microtubule, and each flagellum would have nine IFT "elevator cars" travelling from the transition zone to the flagellar tip complex and back [Wemmer and Marshall, 2007]. A (still-theoretical) monitor at the transition zone would then sense the lack of an IFT particle on a particular doublet, and thus either allow a new IFT particle to enter via the (still-theoretical) flagellar pore complex, or in different circumstances, signal to the deflagellation apparatus.

It should also be noted that my "signal" hypothesis is consistent with the long-zero regeneration seen by Rosenbaum [Rosenbaum et al., 1969; Coyne and Rosenbaum, 1970]. In terms of the balance point model, deflagellation of one flagellum leads to resorption of the other, because the proposed mechanism for maintaining flagella of constant length is dependent on IFT-mediated assembly [Marshall and Rosenbaum, 2001]. My interpretation of these experiments is that the insult causing deflagellation of one flagellum is interpreted as an attenuated deflagellation signal by the other flagellum, akin to the acid shock signal that causes *fa* mutants to resorb (Figure 2-7). This more readily accounts for "undershoots", in which the resorbing flagellum may entirely resorb even while the previously missing flagellum has partially regenerated, than a strict mass action-based model. This can be addressed by future studies, perhaps using an *adf1-6* strain that typically loses one flagellum per cell upon acid shock (J. Kirschner, personal communication).

Our original interest in the *fla2* mutant was because it was the only *fla* mutant reported to deflagellate rather than resorb at the restrictive temperature (originally *fla2*

was called *dd-fragile-1* [Huang et al., 1977]). *fla2*, but not other *fla* mutants, is also able to regenerate its cilia at the restrictive temperature [Huang et al., 1977]. My discovery that several other *fla* mutants, including the canonical *fla*/IFT mutant, *fla10-1*, also deflagellate, makes it less likely that *fla2* encodes a novel component of the deflagellation machinery. I confirmed *fla2* to be recessive by construction of a stable diploid heterozyous *fla2*/*FLA2* strain (data not shown); this argues against a gain-of-function mutation and suggests that FLA2 may, like FLA10 [Kozminski et al., 1995] or FLA3 [Mueller et al., 2005], be another IFT component. Consistent with this, *fla2* mutants are defective in retrograde IFT; retrograde particles move at only half the rate in *fla2* mutants at the permissive temperature as in wild-type cells [Iomini et al., 2001]. Alternatively, the *FLA2* gene could encode a redox-sensitive flagellar component, as modifiers of redox state have been reported to induce deflagellation [Wakabayashi and King, 2006]. The study in Chapter 2 also informed us about another deflagellation mutant, the deflagellation-defective *adf1*. Both *fla2;adf1* and *fla10;adf1* double mutants deflagellate at the restrictive temperature even though the double mutants are, like the *adf1* single mutant alleles used, fully resistant to acid deflagellation (data not shown). This suggests that at least two independent pathways can initiate deflagellation: an ADF1-sensitive pathway, which acts via intracellular acidification and calcium release, and an ADF1-insensitive pathway, which is activated by defective or absent IFT.

Since publication of our study, several other groups have released studies on flagellar disassembly in *Chlamydomonas*. Prominent among these was the implication of an aurora-like kinase in flagellar disassembly [Pan et al., 2004]. This group identified ALK1 (then called CALK) as a protein that undergoes changes in its phosphorylation

state coincident with flagellar status. When cells are deflagellated, ALK1 is phosphorylated; furthermore, addition of the kinase inhibitor staurosporine blocked both ALK1 phosphorylation and deflagellation [Pan et al., 2004]. RNAi against *ALK1* produced a strain unable to undergo normal acid deflagellation [Pan et al., 2004]. While these data imply that ALK1 is a candidate to be a component of the "flagellation switch" we proposed (Figure 2-8), additional work is required to verify that 1) *ALK1* RNAi was not affecting other Aurora-like kinases (*Chlamydomonas* encodes five potential Aurora homologues, as annotated in JGI release 3.0, and the RNAi construct used was targeting the conserved kinase domain), 2) the phenotype of the one *ALK1* RNAi strain studied was not due to insertional mutagenesis, 3) the cellular target of staurosporine was ALK1 and not another kinase (for example, FA2), and 4) that the effect of staurosporine was not due to nonspecific effects on calcium homeostasis.

Direct evidence for IFT particles in mediating transport of axonemal components was lacking at the time of publication of Chapter 2, thus models of resorption involving IFT discussed there were solely based on theory. The first clear data in support of a role for IFT in resorption came from Qin et al. in 2004, who showed that a radial spoke complex is partially assembled at the base of flagella, then transported via anterograde IFT and assembled into a larger complex [Qin et al., 2004]. The larger complex accumulates in the matrix fraction of resorbing *fla10-1* flagella, but not in the flagella of cells induced with IBMX to resorb [Qin et al., 2004]. The authors attribute this phenotype to a lack of functional IFT in the *fla10-1* cells meaning that, unlike in the IBMX-treated cells, old flagellar components are not returned to the cell body in the *fla10-1* mutant.

The results discussed above suggest that resorption can occur by more than one mechanism. EM studies of premitotic or premeiotic resorption showed that the distal flagellum is often disorganized [Johnson and Porter, 1968; Cavalier-Smith, 1974; Gaffal, 1988]. I therefore hypothesize that premitotic resorption is mechanistically more similar to the temperature-sensitive resorption of *fla10-1* mutants than it is to IBMX-induced resorption.

5.2 The Nek8/9 Family in Cilia and the Cell Cycle

Chapter 3 describes my work on the evolutionary history of the Neks, and describes a correlation between Neks and ciliated organisms. Overall, there are few Neks in species lacking cilia or lacking basal body/centriole duality, and many Neks in organisms having this duality. Furthermore, Neks have expanded in at least two lineages having either many cilia (*Tetrahymena*) or very complex ciliary cycles (*Giardia*) [Figure 3-1]. The two major cilia-less groups of eukaryotes, Fungi and Plants, each retained a separate Nek clade. In Fungi, which typically have a closed mitosis, Nek2 orthologues were kept, and Fungal Neks play roles in mitotic events such as nuclear envelope regulation [Fry, 2007]. In plants, the Nek4/11 clade has expanded [Figure 3-7] and members play roles in development [Motose et al., 2008; Sakai et al., 2008]. Spindle orientation is critical for plant cells, especially during development [reviewed by Kost et al., 1999], thus this role for plant Neks is not inconsistent with their roles/proposed roles in regulating mitotic entry in ciliated organisms. In ciliated organisms, we predict Neks to have roles in regulating cilia assembly/disassembly, and therefore perhaps length control, as well as regulating centrosome splitting, mitotic entry, spindle assembly, spindle orientation, kinetochore-microtubule attachment, and other microtubule/cell cycle connections

[Chapter 3-1; Quarmby and Mahjoub, 2005]. In this section I discuss my thoughts and recent data on the evolution of one specific clade, the Nek8/9 sub-family.

NEK 9 has been reported to localize to the cytoplasm and nucleus [Pelka et al., 2007], or centrosomes and spindle poles [Roig et al., 2002; 2005] and also has been reported to associate with several important proteins. These include the transcription factor c-Myc [Koch et al., 2007], the dynein-associated protein Bicaudal D2 [Holland et al., 2002], the chromatin-modifying FACT complex [Tan and Lee, 2004], the small GTPase RAN [Roig et al., 2002], and another centrosomal Nek, NEK6 [Roig et al., 2002; Belham et al., 2003]. Thus, NEK9 is either an extremely important protein and/or it is promiscuous in its interactions. At least it seems that NEK9 may be safely referred to as a mitotic kinase. Unfortunately, this protein has not yet been studied with regard to cilia, but it is possible that some apparently conflicting data (ie, the subcellular localization) would be resolved if a well-controlled study of Nek9 were carried out in a ciliated cell line. Perhaps NEK9 localizes to cilia in cells that have cilia, and is localized in different ways in different cell lines. Flies and worms both have a Nek9 gene, called *niki* and *nekl-1* respectively, but these, while annotated, have not been characterized.

Human NEK8 is a disease gene for the ciliopathy, nephronophthisis [Otto et al., 2008]. Mice with a specific point mutation in *Nek8*, *jck* mice, are an important model for anther ciliopathy, autosomal dominant polycystic kidney disease (ADPKD). Mouse NEK8 localizes to cilia in cultured kidney epithelial cells (IMCD-3 cells)[Mahjoub et al., 2005] and the *jck* mutation leads to reduced NEK8 in cilia both in kidneys and in IMCD-3 cells [Trapp et al., 2008]. NEK8 has been found to interact with the two ADPKD gene products, the proposed ciliary mechnosensory/signalling protein Polycystin-1 and the

calcium channel Polycystin-2 (PC-2), and leads to increased ciliary localization of both [Natoli et al., 2008; Sohara et al., 2008]. Epidermal growth factor receptor (EGFR) is mislocalized in *jck* cysts [Smith et al., 2006], and there is evidence that PC-2 is activated by EGFR signalling [Ma et al., 2005], suggesting that a consequence of altered EGFR localization could be reduced signalling through PC-2. Since PC-2 loss-of-function leads to ADPKD, this means that if altered EGFR localization is a consequence of mutations in *NEK8* rather than a consequence of kidney cysts (due to other changes in other pathways), then the ADPKD-like phenotype of *jck* mice could be due to reduced PC-2 function. Interestingly, in worms, the Nek8-like gene is called *nekl-2* and RNAi against this gene is able to suppress vulval development phenotypes that are also suppressed by canonical EGF pathway genes, although a functional role remains to be established [Lehner et al., 2006]. Also in worms, RNAi against *nekl-2* also results in a shortened lifespan, about half that of wild-type worms [Kell et al., 2007]. The transcription factor SKN-1 is phosphorylated by NEKL-2 [Kell et al., 2007] and SKN-1 is inhibited by signalling from the insulin growth factor pathway [Tullet et al., 2008], which in worms requires normal sensory cilia [Apfield and Kenyon, 1999]. Together, these data suggest that metazoan Nek8 proteins play roles in the development and maintenance of multiple tissues, and may do so by integrating signalling from cilia with other intracellular signalling pathways, including possibly the EGFR/RAS/MAPK pathway.

Our phylogenetic analysis identified *CNK3* as the *Chlamydomonas* gene co-orthologous to human *NEK8* and *NEK9*. Our tree (Figure 3-6) reveals that unikont Nek8/9 members have RCC1-like domains in their C-termini, while bikont members such as CNK3 have coiled-coil domains. I hypothesize that CNK3 represents the ancestral

form of this protein family. The finding that the Nek8/9 clade derived from the Nek2 and Nek1 clades [Figures 3-2, 3-6], supports this, and since only unikont Nek8/9 proteins have RCC1 domains, the most parsimonious interpretation is that the primordial Nek had a coiled-coil domain. Thus, only the unikont Nek8/9 lineage acquired an RCC1 domain. The practical implications of this are that while the physiological substrates of CNK3 and NEK8 or NEK9 may be related, the regulation or targeting (localization) of the proteins may be different. I propose that a hybrid protein of the CNK3 kinase domain fused to the C-terminus of NEK8 (or 9) could rescue a NEK8 (or 9) mutant, but that a full-length CNK3 could not. However, reduction of CNK3 protein levels via RNAi gives a flagellar phenotype in *Chlamydomonas*: the cells have short flagella (data not shown). Thus while mammalian NEK9 plays cell-cycle roles, and NEK8 is a cilia-related disease gene, their closest *Chlamydomonas* homologue has a ciliary role, consistent with our hypothesis that Neks generally help regulate cilia and the cell cycle.

5.3 Premitotic Resorption in *Chlamydomonas*

In *Chlamydomonas*, katanin p60 (KAT1) can be easily knocked down in aflagellate mutants but not wild-type cells [Chapter 4]. It is possible that complete loss (as opposed to knock-down) of katanin could be lethal in any background, as its microtubule severing activity plays a role in spindle formation in mammalian cell lines [Buster et al., 2002]. Also in mammals, katanin p60 is recruited to splitting centrosomes by Ndel1 in an Aurora A-dependent manner [Toyo-Oka et al, 2005; Mori et al., 2007], but no obvious Nde-like proteins are identifiable by tBLASTn in the *Chlamydomonas* genome (version 3.0, accessed July 2008). Regardless, the relative ease of knocking down KAT1 in aflagellate mutants (Figure 4-2) suggests that this background is permissive because

KAT1 plays an important role in flagella. We present additional data demonstrating that flagellar severing occurs prior to mitosis in wild-type cells (Figure 4-5), and KAT1 is thus likely to mediate this severing. In short, we propose that the essential role played by KAT1 in the *Chlamydomonas* cell cycle is due to its flagella-severing function. KAT1 may also sever the axoneme at the SOFA, but conclusive proof is lacking due to the lethality of KAT1-RNAi in wild-type cells. *Chlamydomonas* also has a second katanin p60 gene, KAT2, which is 46% identical along its length to KAT1, as well as a homologue of a related microtubule-severing protein, spastin. Either KAT2 or spastin could potentially be responsible for deflagellation at the SOFA. The presence of these genes also could account for the non-lethality of KAT1 knock-down in aflagellate cells, as they could perform any other essential microtubule-severing roles such as remodelling the cytoplasmic microtubules to help form the mitotic spindle.

In Chapter 4, we suggest that flagellar remnants observed by immunofluorescence are transition zones. This is supported by EM, courtesy of our collaborators, Drs. Dennis Deiner and Joel Rosenbaum (Figure 5-2). These data indicate that transition zones are not disassembled during resorption but instead, perhaps due to their unique composition, are instead abandoned prior to mitosis. "Remnants" as such have not been previously reported, but we used synchronized cells to obtain a high proportion of mitotic/unhatched cells, and used a fixation protocol that preserves both the cell wall and the attached remnants. Using a similar fixation protocol and a synchronized cell population, Piasecki et al. [2007] also reported seeing both remnants and flagella, but did not quantify the frequency of their observations. Once one knows what they are looking for, however, flagellar remnants are seen in 80% of wild-type unhatched mother cell walls, suggesting

that this is a common phenomenon, but one that is not often observed, for several reasons. First, it is likely that freed flagella are loosely associated with cell walls, and longer flagella especially would be subject to torque during sample handling that could cause the flagella to be lost entirely from the cell. Second, as mentioned above, the fixative is important: glutaraldehyde must be present in the fixative or else flagella/remnants are not seen. Third, many fixation/staining protocols call for treatment to remove cell walls prior to staining, and this would remove any associated remnants. Remnants are not observed in cell wall-less mutants, supporting the hypothesis that remnants are only associated with cells via the mother cell wall, as seen in Figure 5-2.

If KAT1 indeed mediates severing at the proximal transition zone, the key consequence of lack of severing would be failure to free the parental basal bodies from the flagella. In addition to being required for flagellar assembly, basal bodies are required for organization of the flagellar rootlet microtubules, which are in turn required for cleavage furrow placement [reviewed by Dutcher, 2003]. Thus mutations affecting basal body function or positioning could manifest as defective cytokinesis as well as defective mitotic spindle function. However, *Chlamydomonas* mutants lacking basal bodies are viable [Dutcher et al., 2002; Matsuura et al., 2004]. Mutants having too many/misplaced basal bodies are also viable [Adams et al., 1985; Marshall et al., 2001; Feldman et al., 2007]. Therefore, I hypothesize that failure of basal bodies to detach from flagellar transition zones leads to a dominant negative effect on spindle assembly. Spindle assembly can occur in the absence of centrioles in multiple systems, including naturally in plants [reviewed by Marshall, 2007]. However, centrioles may have a dominant effect in spindle formation, due to their ability to nucleate spindle poles: too many centrioles

will lead to too many spindle poles, which may lead to multipolar spindles and aneuploidy [Sluder and Nordberg, 2004]. It is not uncommon in such circumstances for the multipolar spindles to resolve into bipolar spindles, with more than one centriole at a spindle pole [Quintyne et al., 2005; Basto et al., 2008]. Thus, it is possible that centrioles "trapped" because they have not been disengaged from their transition zones attempt to form spindle poles, but cannot form proper ones due to their confined position. The abnormal spindle at the basal bodies may, interfere with the acentriolar spindle assembly pathway, and thus have a "dominant-negative" effect on spindle assembly.

Testing this hypothesis will require examination of the cellular effects of knocking down katanin in flagellated cells. If the basal bodies of KAT1-RNAi cells are found to remain attached to flagella at the apical end of the cells before mitosis, this would satisfy part of my hypothesis. Since this phenotype would also be lethal to the cells, a strain conditional either for expression of KAT-RNAi or for flagellar assembly could be used. Our attempts to obtain conditional KAT1-RNAi strains by transforming the RNAi construct into *fla10-1* cells failed. In theory, these cells would be permissive for katanin knock-down at 33^{o}C (the nonpermissive temperature for *fla10-1*) and nonpermissive for katanin knock-down at 21^{o}C (because there will be functional FLA10 protein and therefore flagella). However, strains that appeared to have less KAT1 protein at 33^{o}C appeared to be wild-type biflagellate cells at 21^{o}C, and had wild-type levels of KAT1 (not shown). Alternatively, RNAi against katanin could be attempted in *mut9* mutants, which are defective in silencing transgenes [Casas-Mollano et al., 2008] or microRNAs targeting KAT1 could be used instead, as these are less prone to transgene silencing than hairpin RNAi [A. Molnar and D. Baulcombe, personal communication].

Regardless of the role played by katanin, it is well-established that most cells resorb their cilia/flagella prior to mitosis. This has lead to the idea that the presence of the cilium might be inhibitory to entering cell division. In support of this idea, others in the Quarmby lab proposed that *fa2* mutants might have a cell cycle delay because mitotic entry was delayed while the flagellum was slowly disassembled [Mahjoub et al., 2002]. To test this, I first examined *fa1* single mutants, because *fa1;fla10* mutants have a similar resorption defect as *fa2;fla10* mutants (Figure 2-6), and confirmed that *fa1* mutants have no cell size defect (data not shown and M. Mahjoub, personal communication). *lf4* mutant cells have flagella 2-3 times the length of wild-type cells [Berman et al., 2003], so if resorption were rate-limiting for mitotic entry, these cells should be larger than wild-type, but they are not [data not shown; Bradley and Quarmby, 2005]. Furthermore, cultures of *lf4* cells often have numerous free flagella, as do wild-type cultures much more rarely (unpublished observations). The free flagella in *lf4* cultures could be due to "spontaneous" deflagellation upon flagellar damage (which would be much more probable with such long flagella) or due to premitotic severing. If the latter is true, then this could be experimentally shown by EM of the free flagella, or even simply immunofluorescence to look at a known transition zone protein (ie, FA1 or FA2). I have also examined *fa2;lf4* double mutants, and found them to have no delay in mitotic entry, and, like *fa2* single mutants, these cells can sever their flagella at the proximal transition zone and leave behind remnants (not shown). Since *fa* mutants are able to sever their flagella at the proximal transition zone, then perhaps a complex similar to the deflagellation complex at the SOFA helps mediate katanin-based severing at this region. CNK4 is a candidate for a FA2-like role here, as it is a paralogue of FA2 (Figure 3-5).

Several FA1-like proteins (large proteins of low sequence complexity) are predicted in the *Chlamydomonas* genome and could perform a scaffolding role such as proposed for FA1.

The timing of cell division in *Chlamydomonas* is variable, and likely controlled by several factors, some of which may involve flagellar signalling. *Chlamydomonas* has a complex circadian clock system [Mittag et al., 2005], a pRB/E2F pathway [Umen 2007], and a TOR pathway [Díaz-Troya et al., 2007]; all these systems play roles in cell growth or timing of cell division. Additionally, the photoreceptor phototropin, which partially localizes to flagella, may also affect the timing of cell division [Münzner and Voigt, 1992; Huang et al., 2004]. I have found that cell density contributes to the timing of cell division; if cells are synchronized together (by starvation in the dark), and then released into the light under the same conditions except for cell density, the most dense culture will divide first. Indeed, cultures that are too dilute not only will not divide, they will not even grow (data not shown). This happens in other unicellular eukaryotes: *Tetrahymena*, for example, dies at low culture densities but can be rescued by addition of insulin, and expresses a ciliary insulin receptor-like tyrosine kinase [Christensen et al., 2003]. *Chlamydomonas* does not have an obvious homologue of this Tetrahymena protein, but does encode 28 putative tyrosine kinases, some of which have transmembrane domains [Wheeler et al., 2008]. I propose several simple experiments to test whether *Chlamydomonas* cells communicate their presence to each other via flagella, and whether this influences timing of cell division. A single culture of wild-type cells can be starved, then the cells released into light at different concentrations. If flagella and not cells per se are required for affecting the timing of division, then concomitant addition of *bld2*

mutants to the wild-type cells, in order to keep the overall cell densities equal, should still lead to difference in timing of mitosis in the wild-type cells (the two strains could be differentiated from each other by marking one with a GFP marker). For a second experiment, dilute synchronized cultures could be grown in media previously occupied by dense synchronized cultures; the media could be filtered/sterilized/denatured as need be and possibly concentrated and subject to mass spectrometry analysis in order to determine the molecular nature of the signalling molecule(s). Third, *bld* mutants should show no density dependence on division if my hypothesis is correct. If this proposed relationship between flagella and cell division holds, then it will be of great interest to re-examine CNK2 over- and under-expressing cells. CNK2 over-expressing cells have slightly long flagella, and divide later than wild-type cells, while CNK2-RNAi cells have slightly short flagella and divide sooner than wild-type cells [Bradley and Quarmby, 2005].

It is clear that *Chlamydomonas* cells can sever their flagella at the proximal transition zone and therefore free their basal bodies, without waiting for a whole flagellum to resorb [Chapter 4; Piasecki et al., 2007]. This could be adaptive, as it allows flexibility in when cells enter mitosis, or it could be an evolutionary relic, as some related algal species detach their basal bodies from flagella at the proximal transition zone and even remain motile during mitosis [Hoops and Witman, 1985; Bloodgood, 1977]. The flagella attached to dividing cells observed by Piasecki and colleagues [Piasecki et al., 2007] are probably similar to those observed in EM studies [Johnson and Porter, 1968; reproduced in Figure 1-2]. In these flagella, the transition zone still appears to be attached while the distal end of the flagellum is disorganized. This indicates that resorption from

the tip is likely already underway in these flagella before severing at the proximal transition zone. We observed just transition zones themselves, as flagellar remnants (Figure 5-2), more often than intact or short flagella (Chapter 4). One possible explanation for this observation is that resorption from the tip can continue after severing at the proximal transition zone; since these flagella are not likely to have functional IFT, they may be similar to resorbing *fla10-1* flagella. Alternatively, severed flagella may no longer shorten and whether one observes remnants or recognizable flagella may depend entirely upon the timing of severing. I propose that severing at the proximal transition zone marks the G2/M boundary in *Chlamydomonas*. Cells are committed to divide at a point during G1 [Spudich and Sager, 1980], and *Chlamydomonas* has little to no G2 phase. Perhaps G2 in *Chlamydomonas* is the phase in which flagella are resorbing, and entry into M can be either cell autonomous, in which case the severing happens after resorption is complete (down to the transition zone) or non-autonomous, in which case my hypothetical flagellar signal will induce severing while the flagellum is still mostly intact.

5.4 Conclusions

Most of my work was performed using *Chlamydomonas* because this remains the premiere model organism for studies of ciliary assembly, disassembly, and length regulation. Human primary cilia are difficult to image without fluorescent techniques and cannot be easily experimentally removed and allowed to regenerate. Since loss of cilia or failure to assemble cilia leads to so many disease phenotypes arise in humans, understanding how cilia are built and maintained in any organism is valuable, especially given how structurally similar cilia are. Some human cilia can undergo stress-induced deflagellation [reviewed by Quarmby, 2004], but the mechanism of premitotic ciliary disassembly in humans is not at all understood. I suggest that the basic mechanisms of resorption may be conserved between humans and *Chlamydomonas*, but that the proteins carrying out the functions may not necessarily be orthologous. For example, FA2 is required for deflagellation in *Chlamydomonas* and localizes to the SOFA [Mahjoub et al., 2002; 2004], but none of the mammalian Neks are orthologous to FA2. However, Nek4 does localize to the base of the primary cilium in tissue culture cells [Figure 5-3]. Similarly, a homologue of FA1 in anything other than the closely-related algae *Volvox* cannot be identified by current bioinformatics methods, but I predict that a protein with a similar function will be found at the mammalian SOFA. However, due to its crucial function in microtubule severing during resorption, katanin should be exceptional, and my work predicts that mammalian katanin p60 is required for severing of cilia at the transition zone, in mammalian cells entering mitosis.

5.5 Figures

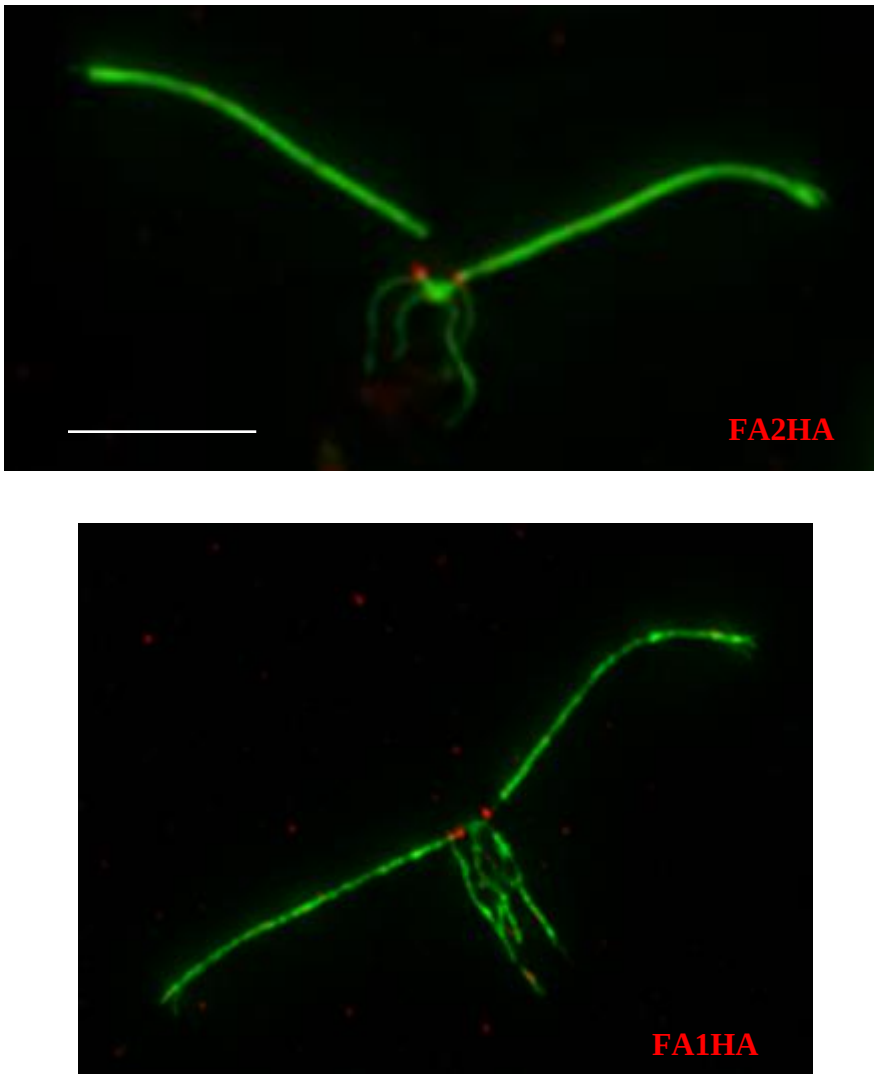

Figure 5-1. FA1HA localizes to the same site as FA2HA.

Anti-HA is in red and anti-acetylated tubulin is in green. Cells expressing FA2HA (top panel) or FA1HA (bottom panel) were treated with gametic lytic enzyme, affixed to coverslips, and lysed with two 30 second washes of 0.2% NP-40 to remove cell membranes, nuclei, and chloroplasts. Calcium (1mM) was then added for 30 seconds to induce deflagellation. Coverslips were then fixed in cold methanol before incubation with anti-acetylated alpha tubulin and anti-HA epitope primary antibodies, followed by incubation with fluorescent secondary antibodies. Control staining (using the same protocol on wild-type cells expressing no HA-tagged protein) gave no signal (not shown). A detailed immunofluorescence protocol is found in the Appendix. Both images are the same scale; scale bar in top panel, 5 micrometers.

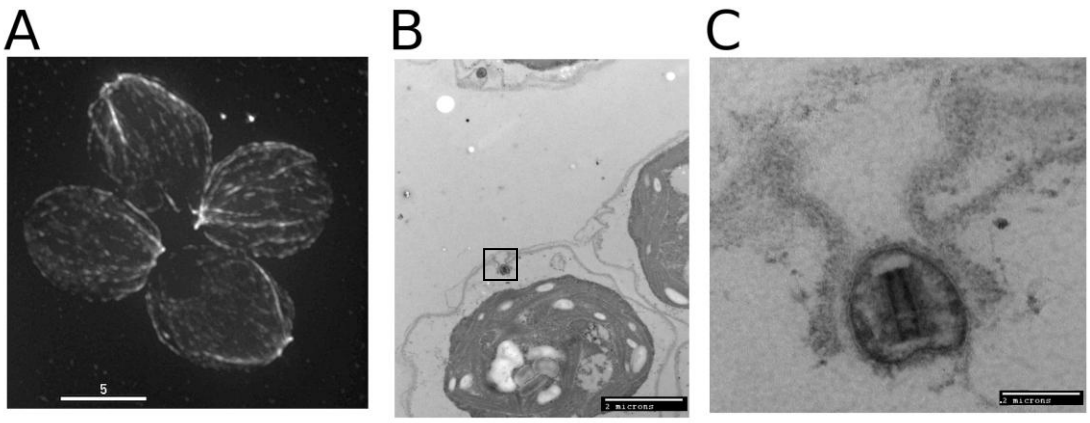

Figure 5-2. Flagellar remnants as viewed by immunofluorescence correspond to transition zones as viewed by electron microscopy.

Wild-type cells were synchronized and fixed in duplicate with either IF fixation buffer or 2.5% glutaraldehyde. Cells fixed in IF buffer were stained for anti-acetylated tubulin primary antibody and a fluorescent secondary antibody (Panel A). Cells fixed in glutaraldehyde were shipped cross-continent and then processed for TEM by Dr. Dennis Diener as described in Qin et al., 2004 (Panels B,C). 80% of unhatched cells had two acetylated-tubulin dots in the mother cell wall, as shown in panel A. Panel B, two neighboring cells have electron-dense material left in the mother cell wall. Panel C, magnified view of the lower remnant from Panel B (boxed in B) shows what appears to be a flagellar transition zone encapsulated in membrane. Scale bars: A, 5 µm; B, 2 µm, C, 0.2 µm.

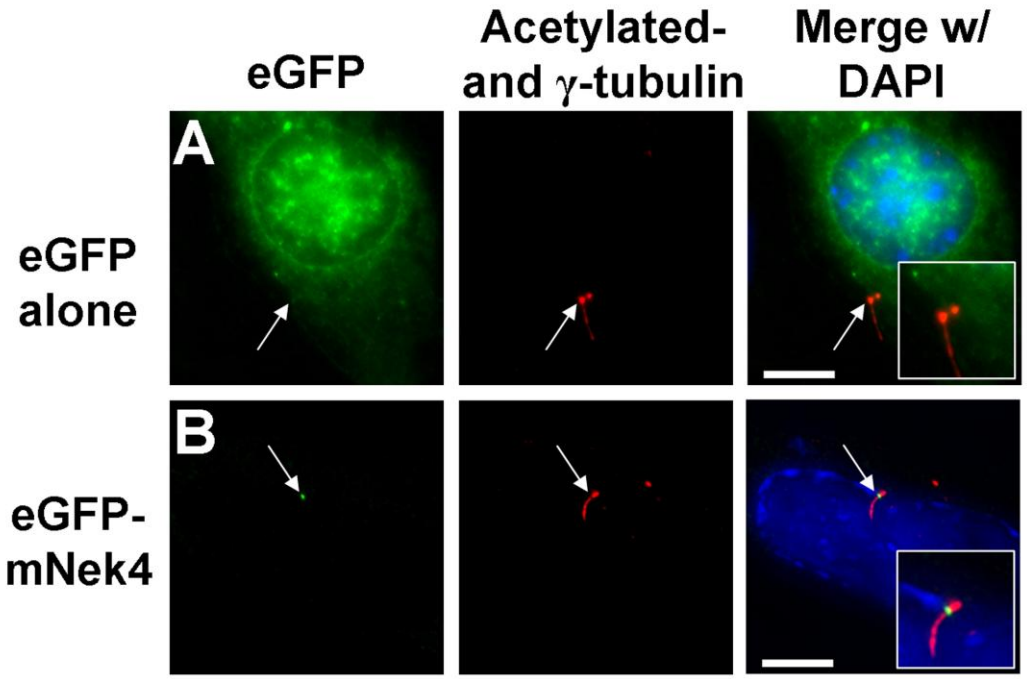

Figure 5-3. Mouse Nek4 localizes to a SOFA-like site in IMCD-3 cells.

EGFP-Nek4 or EGFP was transiently transfected into IMCD-3 cells and immunofluorescence performed as described [White and Quarmby, 2008]. Figure provided by Mark White.

5.6 References

Adams GM, Wright RL, Jarvik JW. Defective temporal and spatial control of flagellar assembly in a mutant of *Chlamydomonas reinhardtii* with variable flagellar number. J Cell Biol. 1985 Mar;100(3):955-64.

Apfeld J, Kenyon C. Regulation of lifespan by sensory perception in *Caenorhabditis elegans*. Nature. 1999 Dec 16;402(6763):804-9.

Basto R, Brunk K, Vinadogrova T, Peel N, Franz A, Khodjakov A, Raff JW. Centrosome amplification can initiate tumorigenesis in flies. Cell. 2008 Jun 13;133(6):1032-42.

Belham C, Roig J, Caldwell JA, Aoyama Y, Kemp BE, Comb M, Avruch J. A mitotic cascade of NIMA family kinases. Nercc1/Nek9 activates the Nek6 and Nek7 kinases. J Biol Chem. 2003 Sep 12;278(37):34897-909.

Berman SA, Wilson NF, Haas NA, Lefebvre PA. A novel MAP kinase regulates flagellar length in *Chlamydomonas*. Curr Biol. 2003 Jul 1;13(13):1145-9.

Bloodgood RA. Resorption of organelles containing microtubules. Cytobios. 1974 Mar-Apr;9(35):142-61.

Bradley BA, Quarmby LM. A NIMA-related kinase, Cnk2p, regulates both flagellar length and cell size in *Chlamydomonas*. J Cell Sci. 2005 Aug 1;118(Pt 15):3317-26.

Buster D, McNally K, McNally FJ. Katanin inhibition prevents the redistribution of gamma-tubulin at mitosis. J Cell Sci. 2002 Mar 1;115(Pt 5):1083-92.

Casas-Mollano JA, Jeong BR, Xu J, Moriyama H, Cerutti H. The MUT9p kinase phosphorylates histone H3 threonine 3 and is necessary for heritable epigenetic silencing in *Chlamydomonas*. Proc Natl Acad Sci U S A. 2008 Apr 29;105(17):6486-91.

Cavalier-Smith T. Basal body and flagellar development during the vegetative cell cycle and the sexual cycle of *Chlamydomonas reinhardtii*. J Cell Sci. 1974 Dec;16(3):529-56.

Christensen ST, Guerra CF, Awan A, Wheatley DN, Satir P. Insulin receptor-like proteins in Tetrahymena thermophila ciliary membranes. Curr Biol. 2003 Jan 21;13(2):R50-2.

Cole DG, Diener DR, Himelblau AL, Beech PL, Fuster JC, Rosenbaum JL. *Chlamydomonas* kinesin-II-dependent intraflagellar transport (IFT): IFT particles contain proteins required for ciliary assembly in *Caenorhabditis elegans* sensory neurons. J Cell Biol. 1998 May 18;141(4):993-1008.

Coyne B, Rosenbaum JL. Flagellar elongation and shortening in *Chlamydomonas*. II. Re-utilization of flagellar proteins. J Cell Biol. 1970 Dec;47(3):777-81

Dentler W. Intraflagellar transport (IFT) during assembly and disassembly of *Chlamydomonas* flagella. J Cell Biol. 2005 Aug 15;170(4):649-59.

Díaz-Troya S, Florencio FJ, Crespo JL. Target of rapamycin and LST8 proteins associate with membranes from the endoplasmic reticulum in the unicellular green alga *Chlamydomonas reinhardtii*. Eukaryot Cell. 2008 Feb;7(2):212-22.

Dutcher SK. Elucidation of basal body and centriole functions in *Chlamydomonas reinhardtii*. Traffic. 2003 Jul;4(7):443-51.

Dutcher SK, Morrissette NS, Preble AM, Rackley C, Stanga J. Epsilon-tubulin is an essential component of the centriole. Mol Biol Cell. 2002 Nov;13(11):3859-69.

Ehler LL, Dutcher SK. Pharmacological and genetic evidence for a role of rootlet and phycoplast microtubules in the positioning and assembly of cleavage furrows in *Chlamydomonas reinhardtii*. Cell Motil Cytoskeleton. 1998;40(2):193-207.

Fang SC, de los Reyes C, Umen JG. Cell size checkpoint control by the retinoblastoma tumor suppressor pathway. PLoS Genet. 2006 Oct 13;2(10):e167.

Feldman JL, Geimer S, Marshall WF. The mother centriole plays an instructive role in defining cell geometry. PLoS Biol. 2007 Jun;5(6):e149.

Gaffal KP The basal body-root complex of *Chlamydomonas reinhardtii* during mitosis. Protoplasma 1988 143(2):118-29.

Hildebrandt F, Zhou W. Nephronophthisis-associated ciliopathies. J Am Soc Nephrol. 2007 Jun;18(6):1855-71.

Holland PM, Milne A, Garka K, Johnson RS, Willis C, Sims JE, Rauch CT, Bird TA, Virca GD. Purification, cloning, and characterization of Nek8, a novel NIMA-related kinase, and its candidate substrate Bicd2. J Biol Chem. 2002 May 3;277(18):16229-40.

Hoops HJ, Witman GB. Basal bodies and associated structures are not required for normal flagellar motion or phototaxis in the green alga Chlorogonium elongatum. J Cell Biol. 1985 Jan;100(1):297-309.

Huang B, Rifkin MR, Luck DJ. Temperature-sensitive mutations affecting flagellar assembly and function in *Chlamydomonas reinhardtii*. J Cell Biol. 1977 Jan;72(1):67-85.

Huang K, Kunkel T, Beck CF. Localization of the blue-light receptor phototropin to the flagella of the green alga *Chlamydomonas reinhardtii*. Mol Biol Cell. 2004 Aug;15(8):3605-14.

Johnson UG, Porter KR. Fine structure of cell division in *Chlamydomonas reinhardi*. Basal bodies and microtubules. J Cell Biol. 1968 Aug;38(2):403-25.

Johnson KA, Rosenbaum JL. Polarity of flagellar assembly in *Chlamydomonas*. J Cell Biol. 1992 Dec;119(6):1605-11.

Kell A, Ventura N, Kahn N, Johnson TE. Activation of SKN-1 by novel kinases in *Caenorhabditis elegans*. Free Radic Biol Med. 2007 Dec 1;43(11):1560-6

Koch HB, Zhang R, Verdoodt B, Bailey A, Zhang CD, Yates JR 3rd, Menssen A, Hermeking H. Large-scale identification of c-MYC-associated proteins using a combined TAP/MudPIT approach. Cell Cycle. 2007 Jan 15;6(2):205-17.

Kost B, Mathur J, Chua NH. Cytoskeleton in plant development. Curr Opin Plant Biol. 1999 Dec;2(6):462-70.

Kozminski KG, Beech PL, Rosenbaum JL. The *Chlamydomonas* kinesin-like protein FLA10 is involved in motility associated with the flagellar membrane. J Cell Biol. 1995 Dec;131(6 Pt 1):1517-27.

Lehner B, Crombie C, Tischler J, Fortunato A, Fraser AG. Systematic mapping of genetic interactions in *Caenorhabditis elegans* identifies common modifiers of diverse signaling pathways. Nat Genet. 2006 Aug;38(8):896-903.

Liu S, Lu W, Obara T, Kuida S, Lehoczky J, Dewar K, Drummond IA, Beier DR. A defect in a novel Nek-family kinase causes cystic kidney disease in the mouse and in zebrafish. Development. 2002 Dec;129(24):5839-46.

Ma R, Li WP, Rundle D, Kong J, Akbarali HI, Tsiokas L. PKD2 functions as an epidermal growth factor-activated plasma membrane channel. Mol Cell Biol. 2005 Sep;25(18):8285-98.

Mahjoub MR, Montpetit B, Zhao L, Finst RJ, Goh B, Kim AC, Quarmby LM. The FA2 gene of *Chlamydomonas* encodes a NIMA family kinase with roles in cell cycle progression and microtubule severing during deflagellation. J Cell Sci. 2002 Apr 15;115(Pt 8):1759-68

Mahjoub MR, Qasim Rasi M, Quarmby LM. A NIMA-related kinase, Fa2p, localizes to a novel site in the proximal cilia of *Chlamydomonas* and mouse kidney cells. Mol Biol Cell. 2004 Nov;15(11):5172-86.

Mahjoub MR, Trapp ML, Quarmby LM. NIMA-related kinases defective in murine models of polycystic kidney diseases localize to primary cilia and centrosomes. J Am Soc Nephrol. 2005 Dec;16(12):3485-9.

Marshall WF, Rosenbaum JL. Intraflagellar transport balances continuous turnover of outer doublet microtubules: implications for flagellar length control. J Cell Biol. 2001 Oct 29;155(3):405-14.

Marshall WF, Vucica Y, Rosenbaum JL. Kinetics and regulation of de novo centriole assembly. Implications for the mechanism of centriole duplication. Curr Biol. 2001 Mar 6;11(5):308-17.

Marshall WF. What is the function of centrioles? J Cell Biochem. 2007 Mar 1;100(4):916-22.

Matsuura K, Lefebvre PA, Kamiya R, Hirono M. Bld10p, a novel protein essential for basal body assembly in *Chlamydomonas*: localization to the cartwheel, the first ninefold symmetrical structure appearing during assembly. J Cell Biol. 2004 Jun 7;165(5):663-71.

Mittag M, Kiaulehn S, Johnson CH. The circadian clock in *Chlamydomonas reinhardtii*. What is it for? What is it similar to? Plant Physiol. 2005 Feb;137(2):399-409.

Mori D, Yano Y, Toyo-oka K, Yoshida N, Yamada M, Muramatsu M, Zhang D, Saya H, Toyoshima YY, Kinoshita K, Wynshaw-Boris A, Hirotsune S. NDEL1 phosphorylation by Aurora-A kinase is essential for centrosomal maturation, separation, and TACC3 recruitment. Mol Cell Biol. 2007 Jan;27(1):352-67.

Motose H, Tominaga R, Wada T, Sugiyama M, Watanabe Y. A NIMA-related protein kinase suppresses ectopic outgrowth of epidermal cells through its kinase activity and the association with microtubules. Plant J. 2008 Jun;54(5):829-44.

Mueller J, Perrone CA, Bower R, Cole DG, Porter ME. The FLA3 KAP subunit is required for localization of kinesin-2 to the site of flagellar assembly and processive anterograde intraflagellar transport. Mol Biol Cell. 2005 Mar;16(3):1341-54

Münzner P, Voigt J.Blue Light Regulation of Cell Division in *Chlamydomonas reinhardtii*. Plant Physiol. 1992 Aug;99(4):1370-1375.

Nasmyth K. How do so few control so many? Cell. 2005 Mar 25;120(6):739-46.

Natoli TA, Gareski TC, Dackowski WR, Smith L, Bukanov NO, Russo RJ, Husson H, Matthews D, Piepenhagen P, Ibraghimov-Beskrovnaya O. Pkd1 and Nek8 mutations affect cell-cell adhesion and cilia in cysts formed in kidney organ cultures. Am J Physiol Renal Physiol. 2008 Jan;294(1):F73-83.

O'regan L, Blot J, Fry AM. Mitotic regulation by NIMA-related kinases. Cell Div. 2007 Aug 29;2:25.

Otto EA, Trapp ML, Schultheiss UT, Helou J, Quarmby LM, Hildebrandt F. NEK8 mutations affect ciliary and centrosomal localization and may cause nephronophthisis. J Am Soc Nephrol. 2008 Mar;19(3):587-92.

Pan J, Wang Q, Snell WJ. An aurora kinase is essential for flagellar disassembly in *Chlamydomonas*. Dev Cell. 2004 Mar;6(3):445-51.

Pelka P, Scimè A, Mandalfino C, Joch M, Abdulla P, Whyte P. Adenovirus E1A proteins direct subcellular redistribution of Nek9, a NimA-related kinase. J Cell Physiol. 2007 Jul;212(1):13-25.

Piasecki BP, Lavoie M, Tam LW, Lefebvre PA, Silflow CD. The Uni2 Phosphoprotein is a Cell Cycle regulated Component of the Basal Body Maturation Pathway in *Chlamydomonas reinhardtii*. Mol Biol Cell. 2008 Jan;19(1):262-73.

Pickett-Heaps, J, and Pickett-Heaps, J. CELLULAR EVOLUTION in the Green Algae". 12" CAV, 2 sides, 32 mins./side. Cytographics, Ascot Vale, Australia; 1995.

Quarmby LM, Mahjoub MR. Caught Nek-ing: cilia and centrioles. J Cell Sci. 2005 Nov 15;118(Pt 22):5161-9.

Qin H, Diener DR, Geimer S, Cole DG, Rosenbaum JL. Intraflagellar transport (IFT) cargo: IFT transports flagellar precursors to the tip and turnover products to the cell body. J Cell Biol. 2004 Jan 19;164(2):255-66.

Quintyne NJ, Reing JE, Hoffelder DR, Gollin SM, Saunders WS. Spindle multipolarity is prevented by centrosomal clustering. Science. 2005 Jan 7;307(5706):127-9.

Roig J, Groen A, Caldwell J, Avruch J. Active Nercc1 protein kinase concentrates at centrosomes early in mitosis and is necessary for proper spindle assembly. Mol Biol Cell. 2005 Oct;16(10):4827-40.

Roig J, Mikhailov A, Belham C, Avruch J. Nercc1, a mammalian NIMA-family kinase, binds the Ran GTPase and regulates mitotic progression. Genes Dev. 2002 Jul 1;16(13):1640-58.

Rosenbaum JL, Moulder JE, Ringo DL. Flagellar elongation and shortening in *Chlamydomonas*. The use of cycloheximide and colchicine to study the synthesis and assembly of flagellar proteins. J Cell Biol. 1969 May;41(2):600-19.

Sakai T, Honing H, Nishioka M, Uehara Y, Takahashi M, Fujisawa N, Saji K, Seki M, Shinozaki K, Jones MA, Smirnoff N, Okada K, Wasteneys GO. Armadillo repeat-containing kinesins and a NIMA-related kinase are required for epidermal-cell morphogenesis in Arabidopsis. Plant J. 2008 Jan;53(1):157-71.

Sluder G, Nordberg JJ. The good, the bad and the ugly: the practical consequences of centrosome amplification. Curr Opin Cell Biol. 2004 Feb;16(1):49-54.

Smith LA, Bukanov NO, Husson H, Russo RJ, Barry TC, Taylor AL, Beier DR, Ibraghimov-Beskrovnaya O. Development of polycystic kidney disease in juvenile cystic kidney mice: insights into pathogenesis, ciliary abnormalities, and common features with human disease. J Am Soc Nephrol. 2006 Oct;17(10):2821-31.

Sohara E, Luo Y, Zhang J, Manning DK, Beier DR, Zhou J. Nek8 regulates the expression and localization of polycystin-1 and polycystin-2. J Am Soc Nephrol. 2008 Mar;19(3):469-76.

Spudich JL, Sager R. Regulation of the *Chlamydomonas* cell cycle by light and dark. J Cell Biol. 1980 Apr;85(1):136-45.

Tan BC, Lee SC. Nek9, a novel FACT-associated protein, modulates interphase progression. J Biol Chem. 2004 Mar 5;279(10):9321-30.

Toyo-Oka K, Sasaki S, Yano Y, Mori D, Kobayashi T, Toyoshima YY, Tokuoka SM, Ishii S, Shimizu T, Muramatsu M, Hiraiwa N, Yoshiki A, Wynshaw-Boris A, Hirotsune S. Recruitment of katanin p60 by phosphorylated NDEL1, an LIS1 interacting protein, is essential for mitotic cell division and neuronal migration. Hum Mol Genet. 2005 Nov 1;14(21):3113-28.

Trapp ML, Galtseva A, Manning DK, Beier DR, Rosenblum ND, Quarmby LM. Defects in ciliary localization of Nek8 is associated with cystogenesis. Pediatr Nephrol. 2008 Mar;23(3):377-87.

Tullet JM, Hertweck M, An JH, Baker J, Hwang JY, Liu S, Oliveira RP, Baumeister R, Blackwell TK. Direct inhibition of the longevity-promoting factor SKN-1 by insulin-like signaling in C. *elegans*. Cell. 2008 Mar 21;132(6):1025-38.

Vashishtha M, Walther Z, Hall JL. The kinesin-homologous protein encoded by the *Chlamydomonas* FLA10 gene is associated with basal bodies and centrioles. J Cell Sci. 1996 Mar;109 (Pt 3):541-9.

Visviki I, Santikul D. The pH tolerance of *Chlamydomonas applanata* (Volvocales, Chlorophyta). Arch. Env. Cont. Tox., 2000 38(2):147-151.

Wakabayashi K, King SM. Modulation of *Chlamydomonas reinhardtii* flagellar motility by redox poise. J Cell Biol. 2006 Jun 5;173(5):743-54.

Wemmer KA, Marshall WF. Flagellar length control in *Chlamydomonas*--paradigm for organelle size regulation. Int Rev Cytol. 2007;260:175-212.

Wheeler GL, Miranda-Saavedra D, Barton GJ. Genome analysis of the unicellular green alga *Chlamydomonas reinhardtii* Indicates an ancient evolutionary origin for key pattern recognition and cell-signaling protein families. Genetics. 2008 May;179(1):193-7.

White MC, Quarmby LM. The NIMA-family kinase, Nek1 affects the stability of centrosomes and ciliogenesis. BMC Cell Biol. 2008 Jun 4;9:29.

APPENDIX: PROTOCOLS

Protocol 1. Mating Chlamy

- 1. If cells have not been recently (<2 weeks) replated, replate on regular TAP and grow 2-5 days to make them happy.

  2. Plate on low-N TAP. Use more cells than usual (~1/2-3/4 of a TAP plate, rather than <1/4 for regular replating).

  3. Grow 3-7 days, until mostly (but not entirely) yellow.

  4. Flood low-N plates with M-N or mating buffer. Scrape cells off into empty petri dish. Pipette to de-clump.

  5. After ~1-2 hours, mix mt+ and mt- cells in the same dish/well/flask. Can also leave overnight etc.

  6. plate on 4% TAP: less is more, ~400µL per plate max. Leave overnight in light, then wrap in foil and put at 18^{o}C for at least 5d.

- Variation 1: mating type assay

  Use a tiny amount of cells to be tested, along with a tiny amount of control strains, in 100µL mating buffer in well of 96 well plate. Well contents should be very pale green (translucent) for best results. Incubate 4-24 hours under light. You can spot out the contents of the well on agar and proceed with genetics if so desired.

- Variation 2: GLE preparation

  As steps 1-5, except usually replate multiple times on TAP (especially if doing a large-scale prep, many plates will be needed). Scrape cells from flooded low-N into wide-bottom or large flasks, and shake 1-2 hours before mixing the two mating types. Let cells mate 15-30 minutes before centrifuging out cells (2000g); pour supernatant in 20- or 5-mL aliquots into Falcon tubes and freeze with liquid nitrogen, store at -80.

Protocol 2. Mapping: *dd-l-108* case study

- Used random progeny from ~20 tetrads of mutant crossed to polymorphic strain S1D2.
- Did quick genomic preps and scanned PCRs for linkage groups (as per http://www.chlamy.org/mapkit/markers.html). Got 17:3 to tua2 on LGIV.
- Chose additional molecular markers *BLD1* and *COX3* and phenotypic markers *pf20* and *pyr1*. Crossed *dd* to both *pf20* and *pyr1*.
- At the time it was necessary to manually assemble v1 scaffolds into larger scaffolds, and contiguous sequence was not available between bld1, or bld1 and COX3, or COX3 and CAH1. Life was tough.
- Cloned *pyr1* to the *THI4* gene in silico by comparison with known fungal pyrithiamine-resistant mutants. This allowed identification of a v1 scaffold in between *PYR1* and *bld1*. This was still better than eg, making a BAC contig by end-walking to cover the whole linkage group, but not by much. Did I mention life was tough?
- Results of crosses with zygotes popped at 3am suggested mutant locus is between *pyr1* and *pf20*, closer to *pyr1*. Crossed *pyr1,dd-l-108* double mutant to S1D2 and popped zygotes on pyrithiamine-containing plates, incubated at 33^{oC} (thus only *pyr1* single mutant recombinants survive, validated with pyr-less test plates so I knew the pyr doesn't affect popping %).
- Also screened progeny from cross of *pf20;dd-l-108* to S1D2 and screened 33^{o}C survivors for motility. By now v3 is available, only one gap between scaffold containing *PYR1* and scaffold containing *BLD1, CAH1, COX3, PF20*.
- Chose 5 markers between *PYR1* and *PF20*, did PCR with recombinant progeny, lather, rinse, repeat. Highly recommend using markers in this order: Stern STS primers, Stern InDel primers, then make your own with Primer3 (preferably with primers in exons, target sequence in intron) and test-digest with wacky GC-righ 4-cutters (MspI, HaeIII, HhaI, etc).

- NB: no point in using map unit conversions due to various factors: variability across genome (although own data will inform this), temperature/mating-to-mating variability, ease of just increasing N and refining physical maps.
- NB2: no point in using complete tetrads (NPDs very rare at tightly-linked loci, so mostly dealing with PDs and tetratypes. By not assaying all four members of tetrad (or worse, all 8 of octet), you will miss half of recombinants, but so much time is saved by picking more tetrads, not separating all four members of tetrad (or worse, octet), plus irrelevant whether tetrad/octet/worse (just pick two)
- NB3: if you want to half your interval, you'll probably need twice the zygotes.
- Once interval is down to <500kb, it's time to consider BAC rescues and look for fabulous candidate genes. Life may be easier if you can subclone interesting genes from BAC minipreps directly into psi103 or psp124S, this depends on the size of the gene and your cloning skills.

Protocol 3. Immunofluorescence Staining of Chlamy

- I. Fixation for mitotic cells (adapted from Dutcher/etc via Brian Piasecki & Carolyn Silflow)
- Solutions: MTSB (from 10x stock: 100mM HEPES pH7, 10mM EGTA, 10mM MgSO4), formalin (ie, 37% formaldehyde in methanol), 4% glutaraldehyde, 10% NP-40, MT buffer, cold methanol, cold methanol/acetone, PBS, PBS/MeOH, Glut blocker! (50mM NH4Cl in HEPES or PBS).
- Make 1x MTSB+0.01% glute fresh from stocks on day of use. Aliquot 1 mL on ice in eppy tubes. Add 250µL cells to cold buffer, let fix on ice at least 30 minutes then pellet gently (if needed) or proceed directly to affixing cells to coverslips.
- Notes: if using cw strains, omit any NP-40; otherwise add 0.1% final. Unless you want to stain isolated spindles, in which case adding NP-40 to mitotic cw cells will let you obtain isolated spindles (hmmm...).
- II. Methanol fixation
- 1. Get a (preferably used) 6-well plate. Put 18x18, 1 1/2 coverslips in wells. Wash coverslips/wells 3x with dH_2O, then pour off.
- 2. Make polyethylenimine solution: using a cut yellow tip, transfer ~25µL into 50mL dH_2O in Falcon tube, invert to solubilize, then pour over coverslips. Let sit ~30 seconds. 50mL of the solution is enough for ~18 wells if you're careful.
- 3. Pour off polyethylenimine and rinse wells with dH_2O. Put 6-well plate on its side and aspirate off excess water. Centre coverslip in well and let it air dry ~10 minutes (or less in fumehood). Make sure coverslip is not sitting on any liquid, and make sure there's no puddles on/near coverslip before adding cells. Note: I have prepared coverslips this way then stored them (lidded) in fridge for 4 hours with no ill effects, this is useful for timecourses.
- 4. GLE-treat cells if desired or simply gently pellet (800g) and resuspend in MT buffer. NB: MT buffer is necessary to chelate Ca2+ which will otherwise cause many cells to deflagellate. If you forget this, you may end up with a coverslip of flagella without cell bodies (not always a bad thing).

- 5. Add 100-200µL of resuspended cells to coverslip. NB: the concentration of cells is dependent upon what you're doing; sometimes it's useful to have a dense lawn (>1x10^7) of cells (e.g. for counting mitotic cells) but if you just want a pretty picture, dilute (~5x10^6) would be better. NB2: agg strains (e.g. 137 mt-) will immediately stick themselves "headfirst" to the coverslip unless you add them in low light and put them in the dark during adherence to the coverslip.
- 6. Optional FBBC prep: add MT+0.2% NP-40 (made fresh), ~2mL per well, to cw or GLE-treated cells on coverslip. Rock gently (by hand is good), pour off after 15-30 seconds. Repeat if desired (will ensure more FBBCs, but one treatment is sufficient to get a really nice mixture of cells, really well permeabilized cells, and FBBCs. You should see cell lysis (as indicated by loss of green from the coverslip).
- 7. Optional deflagellation: to FBBCs or cells, add MT+1mM CaCl2 (made by adding 67mM CaCl2 to MT buffer due to the EGTA). Let sit 30 seconds, then gently add MeOH to fix (this is to fix cell bodies/basal apparati near flagella).
- 8. After ~5-10 minutes, fix with methanol directly by adding ~5mL of -20^{o}C MeOH to each well (do not skimp on the methanol - your staining will not work as well with only enough to cover the coverslip). Incubate 10 minutes at -20^{o}C. You should see cell lysis (as seen by loss of green from the coverslip) unless using FBBCs.
- 9. Pour off MeOH and add 5mL of -20^{o}C 1:1 MeOH:acetone. Incubate another 10 minutes at -20^{o}C. Notes: I don't know if the acetone really helps, but it doesn't seem to hurt anything! It should help solubilize more chlorophyll than MeOH alone. Can also use acetone neat, but not in plastic plate; need to use little glass petri dish!
- 10. Pour off MeOH/acetone and add 5mL of room temp 1:1 MeOH:PBS. Let sit on bench for 10-30 minutes.
- 11. Wash 3x with PBS.
- 12. If you used glutaraldehyde, you must quench any unreacted potential cross-links with glut block! solution. Two washes is good, then PBS again.

- 13. If desired/necessary for your antibody prep, block. In my experience this is not necessary for most antibodies I've used, but it'll probably help for home-made rabbit polyclonals etc.
- 14. Prepare primary antibody solution(s). I usually use 40µL per coverslip but have used 25µL with no ill effects. Cut parafilm to right size to fit into lid of 24-well plate, and make it stick in the plate/keep the chamber humid by squirting some water into the lid first. Label 6 spots corresponding to your wells/coverslips and add antibody. Pick coverslips out of 6-well plate with fine forceps, blot edge of coverslip on a Kimwipe, and INVERT onto the antibody solution so the cell side is down.
- 15. Stack another lid onto your lid (the Sarstedt 24-well-plate lids lock nice and tightly). Incubate in primary 2 hours at room temp or overnight at 4^{o}C.
- 16. Wash coverslips 3x 10 minutes in PBS at room temp, back in 6-well plate, with coverslips cell sides up again.
- 17. Prepare secondary antibody: as for primary, but keep solution out of direct light. I usually add DAPI at 1ug/mL along with secondaries. Once coverslips are on antibody solution, keep in dark. Again, 1-2 hours at room temp or longer at 4^{o}C both work.
- 18. Wash coverslips again 3x 10 minutes in PBS at room temp, keeping in dark chamber.
- 19. Mount in Mowiol. Label slides (one slide can hold 2 coverslips comfortably) with DATE and useful information such as coverslip # etc, depending upon how you cross-reference things to your notebook. Get a little beaker of dH_2O and thaw the mowiol (use a new aliquot every month). Pick the coverslip out of the PBS, dip it in the beaker of water (this removes the salt from the coverslip), blot the edge of the coverslip on a Kimwipe, and place cell side down on 9µL of mowiol. Let dry on a level surface, in the dark, overnight.

Protocol 4. Synchronizing cells

- Simple method: inoculate TAP liquid, let grow ~2 days. If doing more than one strain, or if comparing strains, ensure cells are equal density. Spin down and resuspend 50mL cells from TAP into 50mL M liquid. Put into flask, and keep flask in dark (box or foil) for 24-30 hours. Spin down, resuspend in TAP (again ensuring equal cell densities if required) and put into light. After ~10 hours, start taking hourly aliquots to find mitotic peak(s). Cell density greatly affects the timing of the mitotic peak: cells that are too dilute will not show any peak, while dense cultures will divide sooner.

Protocol 5. Cloning/Construct Making Tips

- General tips: for any straightforward cut 'n' paste operation, start with 5µL of your recipient plasmid and 15µL of your insert plasmid. Cut with 0.5µL enzyme(s) in 20µL final volume. Heat-kill enzyme in recipient plasmid and treat with CIP or antarctic phosphatase. Run out on gel (may not need to run out recipient vector if only one cut site or two sites close (<40 bp) together) and extract piece of interest and purify using Qiagen columns - elute both recipient and insert pieces in 30µL (this gives you a 3:1 ratio for your ligation). In general, ligate with 1µL each piece in 10µL total volume with 0.5µL ligase (NB: keep ligase in freezer until last second, and do not re-use same tube of ligase buffer, instead aliquot into 20µL one-shot tubes). Ligate at room temp for 2h or overnight at 16^{o}C.
- For blunt ends, add 2x the insert and incubate ligation at 37^{o}C for one hour.
- If insert is small (<200bp) it might help to digest more plasmid at the start, just to help you see the small piece of DNA more easily when you run it out on a gel. Adjust the volume you add to your ligations accordingly.
- If designing something, plan ahead! Plan for the right number of restriction sites: too many or too few and you won't be able to modify your product easily. Control the number of sites in your final product by using enzymes which give compatible ends but when ligated together are not re-cuttable by either starting enzyme (e.g. most blunt cutters, BamHI/BglII, SpeI/NheI/XbaI/AvrII, etc.).
- If rich, just buy everything synthetically-made. You might not be able to, due to Chlamy’s high GC%. Give it a few more years.